PHYSICAL REVIEW
LETTERS

VOLUME 2 APRIL 1, 1959 NUMBER 7

## SOFT X-RAYS FROM A MAGNETICALLY COMPRESSED PLASMA IN SCYLLA*

K. Boyer, E. M. Little, W. E. Quinn,
G. A. Sawyer, and T. F. Stratton
Los Alamos Scientific Laboratory,
University of California,
Los Alamos, New Mexico
(Received March 12, 1959)

The Scylla plasma experiment[1] employs a rapidly rising magnetic field in cylindrical mirror geometry to heat a deuterium plasma. A proposed mechanism consists of Joule and shock heating in the early stages of the discharge followed by an adiabatic compression to produce a hot plasma centered in the discharge tube. Emission of neutrons from the plasma has been observed and earlier measurements[2] of the neutron energy spectrum suggest that a plasma ion temperature of about 1 kev is achieved at the time of peak magnetic compression in a region about 1.5 cm in diameter and 3 cm long. In such a plasma bremsstrahlung radiation should be emitted as the fast-moving electrons are deflected in the Coulomb fields of the ions. Soft x-ray emission is observed from the central plasma region of the discharge.

The x-rays were detected with a plastic scintillator and photomultiplier. A system of collimating slits inserted along the axis of the discharge tube allowed only radiation from the central 2 cm of the discharge volume to fall on the scintillator. Thin metal foils shielded the scintillation counter from visible light. Soft x-rays were emitted mainly on the second half cycle of current although some x-rays were observed on subsequent half-cycles. Neither soft x-rays nor neutrons were emitted on the first half-cycle. Figure 1 shows the time history of x-ray and neutron emission together with the magnetic field in the discharge tube. Careful time correlation of the soft x-ray yield with neutron emission showed that the start of emission of neutrons and the start of x-ray emission coincided exactly. Both x-ray emission and neutron emission had a bell-shaped time distribution with full-width at half maximum of 0.8 $\mu$sec, centered exactly with

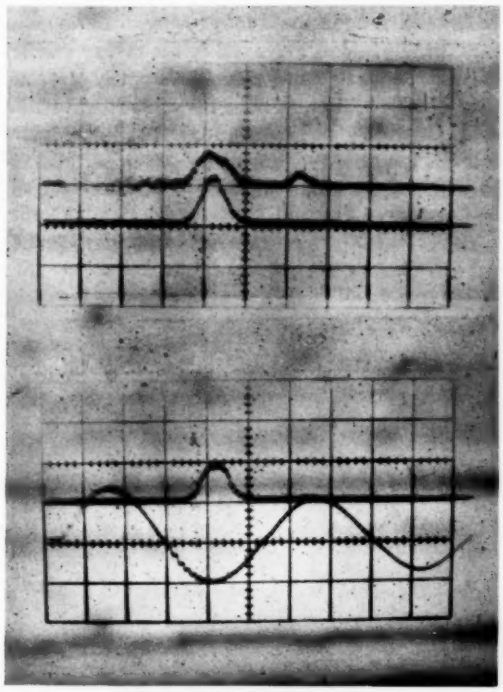

FIG. 1. Oscilloscope records of x-rays (top trace), neutrons (second and third traces), and magnetic field (bottom trace), showing that both neutrons and x-rays are emitted at the time of peak magnetic field in the second half-cycle. The time scale is 2 $\mu$sec per division.

the peak compression of the current cycle.

It was possible to obtain a photograph of the x-ray-emitting region with a pin-hole camera looking along the discharge axis. A pin-hole 1 mm in diameter accurately positioned on the coil axis and x-ray film protected from visible light by 1.46 mg/cm$^2$ aluminum foil produced the self-photograph shown in Fig. 2. The diameter of the x-ray-emitting region as determined from the photograph was 1.5 cm. It should be remarked that the diameter of the x-ray source established by the self-photograph agreed with the diameter of the neutron source as determined by an earlier collimated neutron experiment.

The energy of the x-rays emitted at the time of neutron emission was estimated by absorption measurements in thin foils of Be, Al, and Ni. The absorption coefficients deduced from the slopes of the transmission curves near the maximum transmission region indicated 0.9 kev from Be, 1.1 kev from Al, and 1.4 kev from Ni. In addition, the plot for Be, for which there were the best data over the widest range of absorber thickness, yielded 1.4 kev for the x-ray energy if the slope was drawn near the region of minimum transmission. From the curvature of the Be absorption plot it was clear that there was a distribution of x-ray energies which peaked in the neighborhood of 1 kev.

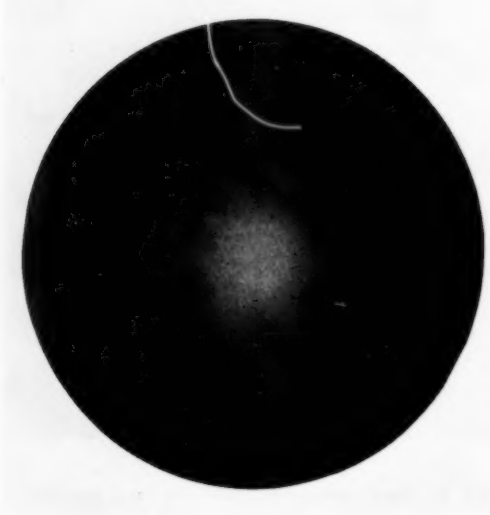

FIG. 2. Pin-hole photograph of the x-rays emitted from the compressed plasma in Scylla taken along the axis of the discharge tube. The circular boundary of the dark region corresponds to the tube wall.

The absolute intensity of the x-rays was determined from the integrated x-ray pulse height in a NaI(Tl) scintillation counter used in good geometry with an accurately positioned defining slit. The counter was calibrated with 300-kev and 1-Mev $\gamma$-ray sources. The pulse height vs energy characteristic of NaI(Tl) is known to be nonlinear at low quantum energy[3] but good data are not available at 1 kev quantum energy; the characteristic was assumed to be linear for these measurements. The x-ray yield measured in this way during the second compression cycle was $1.6\times10^6$ ergs. Correction for neutrons detected in the counter was less than 1%.

Calculation of the total free-free bremsstrahlung radiation from a plasma depends upon the temperature, density, and volume according to the relation[4]

$$Y = 0.54\times10^{-30} n_i n_e Z^2 g T^{1/2} V,$$

where $T$ is in kev and $Y$ is in watts. The best estimates for the particle density and reaction volume at peak compression are $n_i = n_e = 10^{17}$ cm$^{-3}$, $V = 6$ cm$^{-3}$. For a plasma of this density and volume with a temperature of 1 kev, the calculated total radiation is $3\times10^5$ ergs for a pulse corresponding to the observed x-ray pulse shape and length. The calculated bremsstrahlung yield is a factor 5 lower than the observed x-ray yield, but this is considered fair agreement considering the assumptions involved in the calculation.

The region of x-ray emission and the time history support the concept of a centrally located hot plasma created by magnetic compression. The x-ray yields and spectral distribution are consistent with bremsstrahlung from a plasma at an electron temperature of 1 kev.

We wish to acknowledge the helpful advice and support of James L. Tuck.

---

*Work performed under the auspices of the U. S. Atomic Energy Commission.

[1]Elmore, Little, and Quinn, Phys. Rev. Lett. 1, 32 (1958).

[2]Boyer, Elmore, Little, and Quinn, Proceedings of the Second International Conference on the Peaceful Uses of Atomic Energy, Geneva, 1958 (United Nations, Geneva, to be published); Boyer, Elmore, Little, and Quinn, The Edited Proceedings of the Second International Conference on the Peaceful Uses of Atomic Energy, Geneva, 1958 (Pergamon Press, London and New York, to be published).

[3]D. Engelkemeier, Rev. Sci. Instr. 27, 589 (1956).

[4]R. F. Post, Revs. Modern Phys. 28, 338 (1956).

# BREMSSTRAHLUNG FROM DENSE PLASMAS*

H. R. Griem
University of Maryland,
College Park, Maryland, and
United States Naval Research Laboratory,
Washington, D. C.

and

A. C. Kolb and W. R. Faust
United States Naval Research Laboratory,
Washington, D. C.

(Received March 13, 1959)

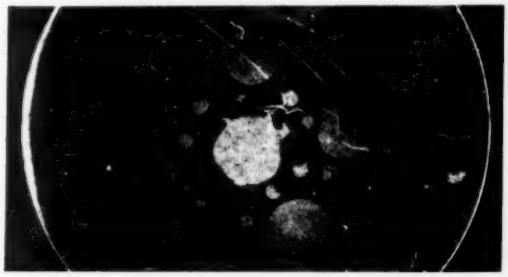

FIG. 1. X-ray photograph of a compressed deuterium plasma: $H = 200\,000$ gauss, $N_e = 7 \times 10^{16}$ cm$^{-3}$, $T_e = 8 \times 10^5$ °K.

Bremsstrahlung radiation in the optical and x-ray regions of the spectrum has been observed during the magnetic compression of a shock-preheated deuterium plasma in a magnetic mirror geometry. In earlier experiments,[1] streak camera observations of the shock velocities during the initial stages of the discharge and the subsequent adiabatic compression together with measurements of the field strength led to the conclusion that electron temperatures of about $8 \times 10^5$ °K and densities of the order $10^{17}$ cm$^{-3}$ might be expected during the first half-cycle of the discharge for field strengths of about 100 000 gauss. Under such conditions the thermal bremsstrahlung radiation in the soft x-ray region should be sufficiently strong to be detected photographically. Since the x-ray flux depends exponentially on the electron temperature, such measurements should yield reasonably good estimates of the temperatures. Because the bremsstrahlung intensity also depends on the square of the density it is necessary to observe two regions of the spectrum to determine both $N_e$ and $T_e$. The density is best determined from the intensity in the optical portion of the spectrum because this only varies with $T_e^{-1/2}$ since the factor $\exp(-h\nu/kT_e)$ in the bremsstrahlung spectral distribution is essentially unity.

The x-rays were detected by photographing the plasma through a 5-mil beryllium window which effectively transmits radiation with an energy above 1.6 kev. The tube was viewed axially through one of the magnetic mirrors and the solid angle was limited by a constriction in the quartz tube so that x-rays which might be generated by electrons striking the tube wall would not reach the central region of the film. The film was also partially shielded by a thick perforated foil used to support the thin beryllium window. In Fig. 1 it is seen that the central hole which views the axis of the plasma cylinder has the highest exposure and the film density falls off radially. The observed film density corresponds to $E = 0.3$ erg/cm$^2$ of incident x-ray energy at the film[2] which was placed 30 cm from one of the magnetic mirrors.

The continuous intensity in the visible region was measured with an $f/3$ streak camera with known transmission characteristics and exposure time, and also with a monochromator at 3800 A using a calibrated photomultiplier. A streak spectrograph with a time resolution of $10^{-7}$ second showed a continuum with a flat spectral distribution and no spectral lines of either deuterium or impurities during the compression cycle.

These experiments were performed under two different conditions in which the maximum field between the magnetic mirrors was 125 000 gauss and 200 000 gauss, respectively. The field was varied by varying the capacitance at constant voltage (15 kv). The other experimental parameters were: capacitance, 400 $\mu$f and 940 $\mu$f; maximum current, $2 \times 10^6$ amp and $3.2 \times 10^6$ amp; ambient pressure, 300 microns $D_2$; tube length, 20 cm; tube diameter, 2 cm i.d.; coil (steel) diameter, 3.5 cm; mirror ratio 2/1; and the final diameter of the plasma as determined with the streak camera was 2-3 mm. The plasma was first preionized by a $10^9$-watt, 6-Mc/sec, 20-kv discharge producing a magnetic field with an amplitude of 10 000 gauss. A low-inductance, 0.8-$\mu$f auxiliary bank of seven capacitors was used for this purpose. For the case of the highest field only one discharge of the main condenser bank was required to x-ray photograph the plasma and at the lower field, ~20 discharges were necessary. The electron temperature during the

early stages is determined by shock processes which are independent of the capacitance and maximum field strength but depend on the geometry, initial voltage, and ambient pressure, which were held constant. This serves to indicate that the x-ray emission is associated with the high final field and plasma pressure and not with the starting voltage.

The mean value of the electron density from the photographic and photoelectric measurements are $N_e = 7\times10^{16}$ cm$^{-3}$ and $4\times10^{16}$ cm$^{-3}$ for the two field strengths using a Gaunt factor[3] of 3.35 in the visible region. The electron temperatures were $8\times10^{6}$ °$K$ and $5.5\times10^{6}$ °$K$, respectively, using a Gaunt factor of 0.6 for the x-ray region. Any uncertainty in the temperature is mainly due to errors in the film sensitivity. Since $T_e$ depends on log$E$, these errors are not large. The relative values of $N_e$ for the two field strengths were obtained from the optical measurements and the relative values of $T_e$ were obtained from the number of x-ray exposures needed for the lower field experiment.

The electron-electron relaxation times calculated in the usual way are $\sim10^{-8}$ second for the above conditions, which is short compared to the compression time ($\sim5$ $\mu$sec). The observed final density and volume show that about 5% of the initial plasma was contained and heated. The measured confinement time and particle loss also agree quite well with the theoretical expectations for the magnetic mirror geometry. These observations imply that the ratio $\beta$ of the plasma pressure to the pressure associated with the maximum field is $\beta\sim0.1$. No x-rays were observed through an aluminum window which transmits x-rays above 8 kev, as expected if the radiation is of thermal origin.

*Jointly supported by the U. S. Atomic Energy Commission and the Office of Naval Research.

[1]A. C. Kolb, Proceedings of the Second United Nations International Conference on the Peaceful Uses of Atomic Energy, Geneva, 1958 (United Nations, Geneva, to be published), 31 $P$/345; Bull. Am. Phys. Soc. Ser. II, 4, 118 (1959).

[2]The spectral sensitivity of the DuPont Type 502 x-ray film was estimated from the data given in H. S. Seeman, Rev. Sci. Instr. 21, 314 (1949) and from the spectral response curves provided by DuPont.

[3]W. J. Karzas and R. Latter, Rand Report RM-2010-AEC, ASTIA Document No. AD-156046, 1958 (unpublished).

## HEATING AND CONFINEMENT OF A PLASMA BY A MAGNETIC FIELD OF EXTERNAL ORIGIN AND WITH A SHORT RISE TIME*

H. G. Loos
Giannini Plasmadyne Corporation,
Santa Ana, California
(Received March 9, 1959)

Figure 1 shows the basic cylindrical configuration in which a fully ionized plasma is heated and confined by a magnetic field that is suddenly induced by a current in an external conductor. It is assumed that the initial plasma temperature and the rise time of the magnetic field are such that the initial skin depth is small compared with the plasma radius. A good separation between the magnetic field and the confined plasma may be retained in a time interval small compared with the decay time $R^2\mu\sigma$. During such a small time interval the plasma may be manipulated using the "magnetic piston" effect at the plasma boundary. It will be shown that this can be done if the linear ion density $N_i$ is large enough. Furthermore, it appears that heating by translational relaxation with a good separation between field and plasma requires that an additional lower limit condition on $N_i$ is satisfied.

The basic cylindrical configuration of Fig. 1 was proposed by Colgate[1] under the name of "collapse." This concept is incorporated in the Scylla configuration,[2] where magnetic mirrors are placed at the ends of the tube to prevent excessive particle loss. Unaware that this work was going on, we gave the name "punch" to the configuration of Fig. 1 and to related configurations.

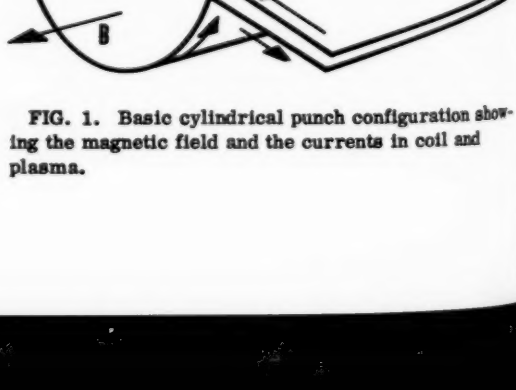


FIG. 1. Basic cylindrical punch configuration showing the magnetic field and the currents in coil and plasma.

Although the basic cylindrical punch configuration does not show any instabilities in the hydrodynamic approximation, but rather an indifferent equilibrium, this feature is lost when magnetic mirrors are placed at the tube ends or when the tube is bent into a toroid. The first configuration is the same as that of Scylla[2] and the exchange instabilities are roughly the same as those in the mirror machine.[3] The second configuration proper does not even have an equilibrium; but there the various ways of establishing a rotational transform, as evolved in the Stellarator program,[4] may perhaps be used to achieve a stable equilibrium. The magnetic field in the punch configuration is radially uniform and hence a large fraction of the energy delivered to the discharge tube appears in the magnetic field, if large compression ratios are used. Strongly nonisentropic heating processes should be used if this inefficiency is to be avoided.

The manipulation of the plasma by using the "magnetic piston" effect at the plasma boundary, as proposed in the punch method, is only possible when plasma and field are well separated. If the index 1 denotes the uniform "final" equilibrium state of the plasma with ion and electron temperatures equal, we have

$$2 n_{i1} k T_1 = B_1^2/2\mu. \tag{1}$$

The number of ions per unit length along the tube is

$$N_i = \pi R_1^2 n_{i1}, \tag{2}$$

and the root mean square of the electron Larmor radius is

$$\tilde{r}_e = m_e \tilde{v}_{e\perp}/eB, \tag{3}$$

where $\tilde{v}_{e\perp}$ is the electron velocity perpendicular to the magnetic field. From (1), (2), and (3) it follows that

$$\alpha \equiv R_1/\tilde{r}_{e1} = (8aN_i)^{\frac{1}{2}}, \tag{4}$$

where $a = e^2/4\pi\epsilon m_e c^2$ is the classical radius of the electron. Neglecting the initial skin depth, as is done throughout this discussion, the thickness of the plasma boundary region in times small compared with the decay time is of the order of $\tilde{r}_{e1} + h_1$, where $h$ is the Debye length. It can be shown that

$$h_1/\tilde{r}_{e1} = \beta_{e\perp 1} + O(\beta_{e\perp 1}^2),$$

where $\beta_{e\perp} = \tilde{v}_{e\perp}/c$. For temperatures of the order of 10 kev the electrons are only slightly relativistic so that the thickness of the plasma boundary region is then of the same order of magnitude as $\tilde{r}_{e1}$. Hence, if the thickness of the plasma boundary region is to be small compared with the plasma radius, at the equilibrium state 1, we must have

$$\alpha = (8aN_i)^{\frac{1}{2}} \gg 1. \tag{5}$$

For nonequilibrium states, condition (5) may not be necessary for good separation of plasma and field; but it seems to be sufficient, possibly with the exception of the case of very rapid expansion with a current sheet velocity very much larger than the mean ion speed. For $\alpha = 20$, we find $N_i = 1.8 \times 10^{16}$/meter.

If collisional relaxation is to be used efficiently for plasma heating, the cycle time must be of the order of the ion-ion collision time $t_{ii}$. Let $m$ relaxation cycles be needed to heat the gas to the required temperature, and let this relaxation heating be done in a small fraction $b$ of the decay time. Then we have, in order of magnitude,

$$m t_{ii} \simeq b t_{\text{decay}} = b\mu R^2 \sigma. \tag{6}$$

Using the expression for $t_{ii}$ in terms of temperature and density, together with an approximate expression for the electric conductivity in terms of temperature, we find from (6)

$$N_i \simeq (5m/b) \times 10^{15} \gg 5m \times 10^{15}, \tag{7}$$

as the condition to be satisfied, in order of magnitude, if collisional relaxation cycles are to be used with good separation between plasma and field. For $b = 10^{-1}$, $m = 10$, (7) requires that $N_i \simeq 5 \times 10^{17}$/meter.

---

*This work was supported by the Air Force Office of Scientific Research.

[1]A. S. Bishop, Project Sherwood - The U. S. Program in Controlled Fusion (Addison-Wesley Press, Cambridge, 1958), pp. 68-70.

[2]Elmore, Little, and Quinn, Phys. Rev. Lett. 1, 32 (1958).

[3]R. F. Post, Proceedings of the Second United Nations International Conference on the Peaceful Uses of Atomic Energy, Geneva, 1958 (United Nations, Geneva, to be published), UN/P-377.

[4]L. Spitzer, Jr., Phys. Fluids 1, 253 (1958).

# POSSIBLE DETERMINATION OF THE HELICITY OF ELEMENTARY EXCITATIONS IN LIQUID He II*

T. D. Lee and F. Mohling†
Department of Physics,
Columbia University,
New York, New York
(Received March 16, 1959)

Recently, at the suggestion of Cohen and Feynman,[1] many groups[2] have directly measured the energy-momentum curve of the excitations in liquid He II by the inelastic scattering of cold neutrons. It is found that associated with a definite momentum transfer $\vec{k}$ of the neutron there is also a definite energy transfer $E(k)$ of a form suggested by Landau.[3] It is customary to call these excitations "phonons" and "rotons." The purpose of this note is to raise the question of the angular momentum of these excitations. In particular, it will be pointed out that the longitudinal component of the angular momentum of an excitation can be experimentally measured by studying the angular distribution of the scattered neutrons.

For definiteness, let us consider the process

$$n(\vec{p}_i) + \text{He(at rest)} \rightarrow n(\vec{p}_f) + \text{He}(\vec{k}), \qquad (1)$$

where $\vec{p}_i$ and $\vec{p}_f$ are, respectively, the incident and final momenta of the neutron. If we denote $\vec{J}$ to be the total angular momentum of liquid He in the final state, then the helicity $H$, defined by

$$H \equiv (\vec{J}\cdot\vec{k})\,k^{-1}, \qquad (2)$$

is a good quantum number.

Physically, if these elementary excitations correspond to longitudinal waves then $H=0$, and if they correspond to transverse waves then the final He state in reaction (1) should be a mixture of states with helicity $\pm|H|$ where $H\neq 0$.

Let $\theta$ be the angle between $\vec{p}_i$ and $\vec{k}$, and $\alpha$ be the angle between $\vec{p}_i$ and $\vec{p}_f$. At the experimental energy range of these cold neutrons the spin states of the neutrons can be regarded (for all practical purposes) as completely unaffected by the collisions. Therefore, conservation of the component of angular momentum along the direction of $\vec{p}_i$ leads to the conclusion that for nonzero helicity the differential cross section for forward scattering must be zero, i.e.,

$$(d\sigma/d\Omega) = 0 \quad \text{at} \quad \theta=0 \quad \text{if} \quad H\neq 0. \qquad (3)$$

Thus a measurement of a nonzero forward scattering cross section would determine unambiguously that these elementary excitations have zero helicity. Furthermore, from a general consideration of rotation invariance it can be shown that if we define $|M|^2$ to be

$$|M|^2 \equiv (p_i/\rho_E)\,(d\sigma/d\Omega), \qquad (4)$$

where $\rho_E$ is the density of final states, then

$$|M|^2 = \sin^{2|H|}\theta \; f(|\vec{p}_i|, |\vec{k}|, \cos\theta), \qquad (5)$$

where $f$ is a polynomial of $\cos\theta$ with a maximum power depending on the number of orbital angular momentum states involved in this collision process.

From (5) we see that in order to determine $H$, it is useful to measure $|M|^2$ for the same $|\vec{k}|$ but at different values of $\theta$ and, in particular, at small $\theta$. Moreover, an important consequence of (5) is that if $|M|^2$ is a function which depends only on the magnitude of $\vec{k}$, then these excitations must have zero helicity. In Fig. 1 we give some rough plots of $(p_i, \theta)$ variations and $(p_i, \alpha)$ variations for fixed $k$ at various typical $k$ values.

We remark that if the interaction between neutron and He atom is represented by a pseudopotential with the correct scattering length $a$, then in the first Born approximation $|M|^2$ is a function of $k$ only. Consequently, only longitudinal waves (i.e., quanta with $H=0$) can be generated. Transverse waves (i.e., quanta with

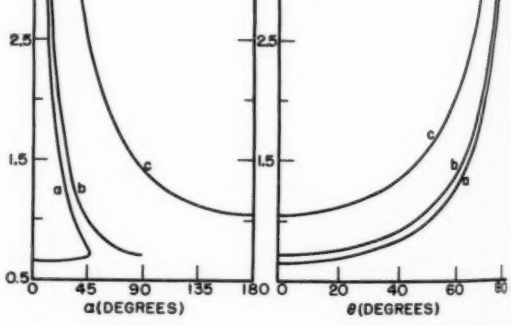


FIG. 1. Rough plots of $(p_i, \alpha)$ variation and $(p_i, \theta)$ variation for fixed momentum transfer $k$, where $\alpha$ is the angle between the incident neutron momentum $\vec{p}_i$ and the final neutron momentum and $\theta$ is the angle between $\vec{p}_i$ and $\vec{k}$. Curves $a$ and $c$ are for $k \cong 0.55$ A$^{-1}$ and 1.90 A$^{-1}$, respectively. Curve $b$ is for $k \cong 0.71$ A$^{-1}$ at which value the corresponding excitation energy equals $\frac{1}{2}k^2$(mass of neutron)$^{-1}$. All plots are based on data taken from Yarnell et al. (reference 2).

$H \neq 0$) can be created through the use of second or higher Born approximations. Because of the extreme smallness of the scattering length as compared to the de Broglie wavelength of the neutron, it is reasonable to expect that the cross section for emitting any transverse wave should be much smaller than the corresponding cross section for a longitudinal wave. Thus, the existing measurements of total cross sections[2,4] already give an indication that these excitations are longitudinal waves. However, because of our limited knowledge concerning the unusual behavior of He II, it is desirable to have a direct experimental determination of the helicity of these excitations as discussed above. If experimentally one finds that both the long-wavelength ($k<1$ A$^{-1}$) excitations and the short-wavelength ones ($k\sim 2$ A$^{-1}$) have zero as their longitudinal angular momentum (helicity) quantum number, then perhaps it would be clarifying to use the same name "phonon" for all of these excitations and regard the variation of $E(k)$ as just a special form of dispersion relation.

The authors wish to thank C. N. Yang, H. Palevsky, and R. Garwin for helpful discussions.

---

*Work supported in part by the U. S. Atomic Energy Commission.

†Boese Postdoctoral Fellow.

[1]M. Cohen and R. P. Feynman, Phys. Rev. 107, 13 (1957).

[2]Palevsky, Otnes, and Larsson, Phys. Rev. 108, 1346 (1957); 112, 11 (1958). Yarnell, Arnold, Bendt, and Kerr, Phys. Rev. Lett. 1, 9 (1958); and Phys. Rev. (to be published). D. G. Henshaw, Phys. Rev. Lett. 1, 127 (1958).

[3]L. Landau, Phys. Rev. 60, 356 (1941). L. Landau, J. Phys. (U.S.S.R.) 5, 71 (1941); 11, 91 (1947).

[4]Sommers, Dash, and Goldstein, Phys. Rev. 97, 855 (1955); see also Cohen and Feynman (reference 1).

---

## FREE INDUCTION DECAYS OF ROTATING SOLIDS*

I. J. Lowe†
Department of Physics,
Washington University, St. Louis, Missouri
(Received February 9, 1959)

Motional narrowing and invariance of the second moment to motional narrowing have been observed for the $F^{19}$ nuclear resonance line shapes in powdered $CaF_2$ and Teflon due to rapid rotation of the sample.[1]

In the usual nuclear resonance experiment one finds that internal motion within the sample is evidenced by a decrease in the sample's observed nuclear resonance line width and its second moment.[2] However, from the Van Vleck[3] expression for the second moment, one expects the second moment to be invariant to internal motion or rotation of the sample since the motional part of the Hamiltonian for the sample commutes with the total spin operator. It can be shown that internal motion increases the fourth moment,[4] which implies that the central portion of the resonance line narrows while the wings increase. The motional modulation of the resonance line produces side bands which add to the wings of the line. The motional contribution of the wings is too weak to be observed because the internal motion has a broad frequency spectrum and thus the side band contribution to the wings is spread over a broad frequency range. However, the nuclear magnetic resonance line shape for a solid sample rotating at a constant angular speed $\omega_s$ should show sharp side bands at frequencies related to $\omega_s$.

Consider a solid containing a single magnetically active nuclear species placed in a uniform magnetic field $H_0\hat{z}$. If the magnetic interaction among the nuclei is purely dipolar, the Hamiltonian[3] describing the solid is (ignoring internal motion and nonsecular terms)

$$\mathcal{H} = \mathcal{H}_0 + \mathcal{H}_1,$$

$$\mathcal{H}_0 = -\gamma\hbar H_0 S_z,$$

$$\mathcal{H}_1 = \tfrac{1}{2}\sum_{j\neq k}(A_{jk}\vec{S}_j\cdot\vec{S}_k + B_{jk}S_{jz}S_{kz}), \qquad (1)$$

$$B_{jk} = -3A_{jk} = -\tfrac{3}{2}(\gamma^2\hbar^2/r_{jk}^3)(3\cos^2\theta_{jk} - 1);$$

$\vec{r}_{jk}$ is the vector connecting the $j$th and $k$th nuclei, $\theta_{jk}$ is the angle $\vec{r}_{jk}$ makes with the $z$ axis, and $\gamma$ is the gyromagnetic ratio of the nuclear species.

If the sample is rotating about an axis oriented at an angle $\theta_H$ with respect to $H_0\hat{z}$, the addition theorem for Legendre polynomials yields

$$(3\cos^2\theta_{jk} - 1) = \tfrac{1}{2}(3\cos^2\theta_H - 1)(3\cos^2\theta_{jk}' - 1) + \tfrac{3}{2}\sin 2\theta_H \sin 2\theta_{jk}' \cos(\phi_{jk}' - \omega_s t) + \tfrac{3}{2}\sin^2\theta_H \sin^2\theta_{jk}' \cos[2(\phi_{jk}' - \omega_s t)], \qquad (2)$$

where $\theta_{jk}'$ is the angle between $\vec{r}_{jk}$ and the axis of rotation. Calculations using the Hamiltonian derived from (1) and (2) are hampered by $\mathcal{H}_1$ not commuting with itself at all times. Using the technique of Lowe and Norberg,[5] the free induction decay and thus the line shape can be calcu-

lated for the case of $A_{jk}=0$ for all $j$ and $k$. The results are that

$$\langle \mu_x(t)\rangle = \frac{\mu_0 \cos\omega_0 t}{N_0} \sum_{j=1}^{N_0} \prod_k{}' \cos\left(\int_0^t B_{jk}(t')dt'/2\hbar\right), \quad (3)$$

the integration in Eq. (3) being trivial. For $\theta_H=0$, $\langle \mu_x(t)\rangle$ is independent of the spinning speed of the sample. The inclusion of $A_{jk}$ in the calculation will not change this result. For $\theta_H=\arccos(1/\sqrt{3})=54.7°$, $\langle \mu_x(t)\rangle$ is a periodic function with a frequency $f_S$. One might facetiously call the extra signals "spinning echoes." The corresponding line shape has side bands at $f_S$ and multiples of $f_S$. The inclusion of $A_{jk}$ in the calculation for $\theta_H=54.7°$ can be shown to make the amplitude of the spinning echoes decay, but it does not wash them out completely. For $\theta_H=90°$, the line shape displays side bands at $2f_S$ and multiples of $2f_S$. Excluding the side band contribution to the line shape, the calculations show the line shape to be narrowed by a factor of two. The inclusion of $A_{jk}$ in the calculation is again expected to change the amplitude of the side bands, but not their position.

Line shape measurements on spinning samples were made by observing the free induction decays of the spinning samples using a standard spin-echo apparatus.[6] The apparatus was operated at 30 Mc/sec, had a crossed coil rf head and a square-law detector and produced rf pulses lasting 4 $\mu$sec that were able to nutate the $F^{19}$ nuclei of the sample by 90°. The applied magnetic field $H_0$ was determined to be homogeneous enough that it did not contribute noticeably to the nuclear magnetic resonance line shape of the solid. The samples were spun at speeds up to 7 kc by using them as rotors of an air-driven turbine. The samples were cylinders 7 mm wide, 7 mm in diameter, and had nylon bearings, and spun on phosphor bronze axles. The spinning frequency was limited only by the strength of the sample. The orientation of the spinning axis could be varied with respect to the applied magnetic field $H_0$. The curves displayed in Figs. 1 and 2 are the free induction decay shapes for spinning and nonspinning samples, and their corresponding Fourier transforms (which are the cw, nuclear magnetic resonance line shapes[5]). It may be noted first that to within the resolution of the drawings (and the original data), the free induction decays have the same initial second derivative. Thus the corresponding cw line shapes have the same second moment, and the

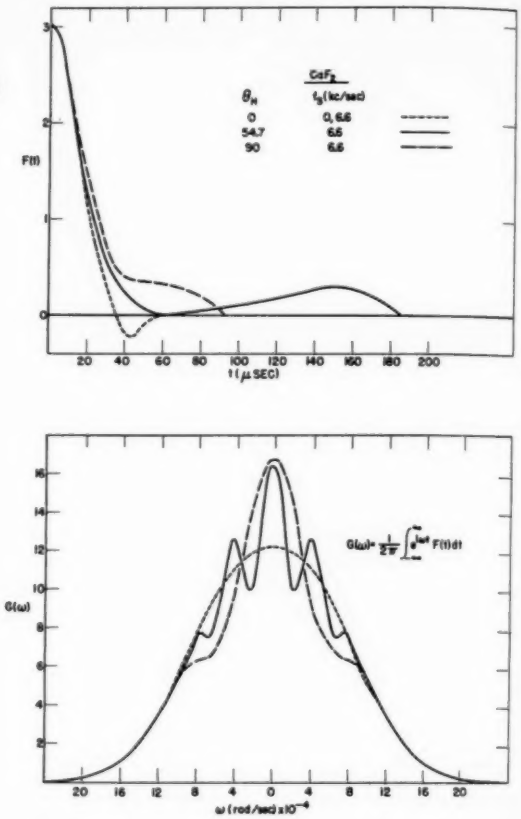


FIG. 1. Free induction decays for spinning and nonspinning samples of powdered $CaF_2$ and their Fourier transforms. The curves are corrected for instrumental nonlinearities.

second moment is invariant to motional narrowing in this case. It is further observed that when $\theta_H=0$, the free induction decay and line shape are the same for the spinning and nonspinning case. When $\theta_H=54.7°$, the free induction decays show a series of peaks or "spinning echoes" at $T_S$, $2T_S$, etc., and the cw line shape's central portion narrows while the intensity in the wings increases at approximately $\omega_S$, $2\omega_S$, etc. For $\theta_H=90°$, the free induction decay is seen to lengthen and the central portion of the cw line shape to narrow correspondingly. One may reasonably interpret the shoulders on the cw line shape to be due to the side band contribution at $2\omega_S$.

With further refinement of this spinning technique and its theory, one might use it to study nondipolar contributions to line shapes in solids.

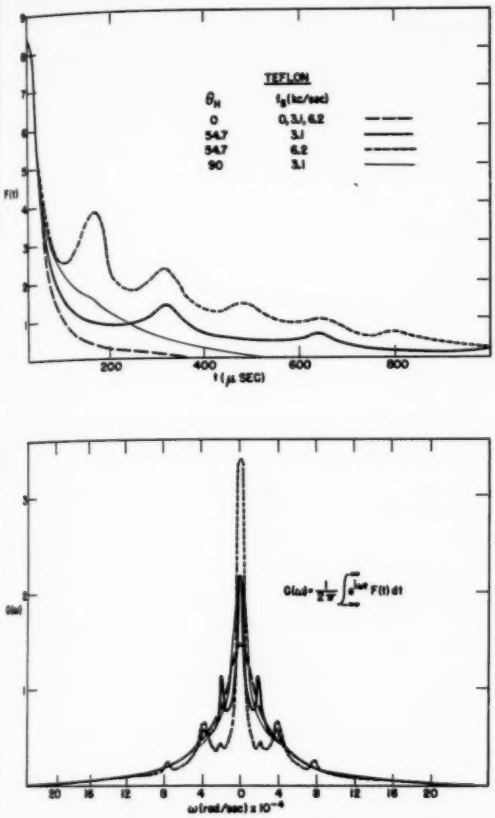





FIG. 2. Free induction decays for spinning and nonspinning samples of Teflon and their Fourier transform. The curves are corrected for instrumental nonlinearities.

I wish to thank Dr. R. E. Norberg for many helpful discussions, Mr. George Theiss for helping to develop the spinning techniques, Mr. Horst Kessemeyer for helping take data, and Mr. William Yen for taking Fourier transforms of free induction decays.

---

*This work was supported in part by the Alfred P. Sloan Foundation and by the Air Force Office of Scientific Research.

†Present address: School of Physics, University of Minnesota, Minneapolis, Minnesota.

[1]Such effects have been independently observed for the $Na^{23}$ nuclear resonance in NaCl by Andrews, Bradbury, and Eades, Arch. sci. Geneva 11, 223 (1958).

[2]H. S. Gutowsky and G. E. Pake, J. Chem. Phys. 18, 162 (1950).

[3]J. H. Van Vleck, Phys. Rev. 74, 1168 (1948).

[4]G. E. Pake, Solid-State Physics, edited by F. Seitz and D. Turnbull (Academic Press, Inc., New York, 1956), Vol. 2.

[5]I. J. Lowe and R. E. Norberg, Phys. Rev. 107, 46 (1957).

[6]E. L. Hahn, Phys. Rev. 80, (1950).

---

## DIFFUSIVE MOTIONS IN LIQUIDS AND NEUTRON SCATTERING

B. N. Brockhouse
Physics Division,
Atomic Energy of Canada Limited,
Chalk River, Ontario, Canada
(Received February 16, 1959)

Measurements of neutron inelastic scattering by a classical liquid provide access to the details of the atomic motions in the liquid, by way of time-dependent correlation functions introduced by Van Hove.[1] The author has discussed some features of these correlation functions in connection with a series of experiments[2] on the isotopic pair—light water which scatters incoherently, and heavy water which scatters coherently. These functions have also been discussed by Vineyard.[3] The partial differential neutron scattering cross sections are Fourier transforms over space and time of the time-dependent correlations,[1] and essentially are functions only of neutron energy transfer and momentum transfer, i.e., of $\omega = \hbar^{-1}(E_0 - E')$ and $\vec{Q} = \vec{k}_0 - \vec{k}'$, where $E_0$, $E'$, $\vec{k}_0$, $\vec{k}'$ are, respectively, the ingoing and outgoing neutron energies and wave vectors. The coherent cross sections are determined by the pair correlation function, which classically is "the probability that, given an atom at position zero at time zero, any atom is at position $\vec{r}$ at time $t$." The incoherent cross sections are determined by the self-correlation function, which classically is "the probability that, given an atom at position zero at time zero, the same atom is at position $\vec{r}$ at time $t$."

The experiments[2] led to the conclusion that the qualitative behavior of the cross sections is largely determined by the asymptotic behavior of the correlation functions at very small times and at large times. Because the correlation functions for any system (solid, liquid, or gas) change very rapidly at small times, the scattering contains an inelastic component which, for a classical system at a given large $Q$, is almost independent of the state of the system, being determined by the temperature and by the mass of the

atoms. At long times, in a nondiffusing solid, the correlation functions become independent of time and hence the scattering contains an elastic component, which is the Fourier transform of the time-independent structure. For coherent scattering this elastic component consists of Bragg peaks whose intensity is modulated by the Debye-Waller form factor of the (Gaussian) "thermal cloud" of an individual atom. For incoherent scattering the intensity of the elastic component is everywhere proportional to the Debye-Waller form factor. In liquid water it was found that a quasi-elastic component of the scattering exists, which for coherent scattering is correlated with the liquid diffraction peak thus showing interference effects,[4] and which for incoherent scattering has intensity proportional to a somewhat non-Gaussian form factor. These facts were interpreted as showing that in a liquid, as in a solid, a "thermal cloud" is quickly set up, the process of setting it up generating the inelastic component of the scattering, but that in a liquid the "thermal cloud" is non-Gaussian. Thereafter the cloud changes only slowly by diffusive processes, the changes in time being reflected in the small energy transfers which actually occur in the quasi-elastic component. The details of these energy transfers, as functions of $Q$, give information on the way diffusion occurs. The measurements could not be reconciled with the simple models of diffusion by large jumps only (activation diffusion), or of diffusion by small motions only (continuous diffusion).

With the resolution available for the earlier experiments, the energy broadening of the quasi-elastic component, from which the above deductions on the nature of the diffusive motions in liquids were made, was just barely detectable in the most interesting region of $Q$. Measurements have now been made at much higher resolution

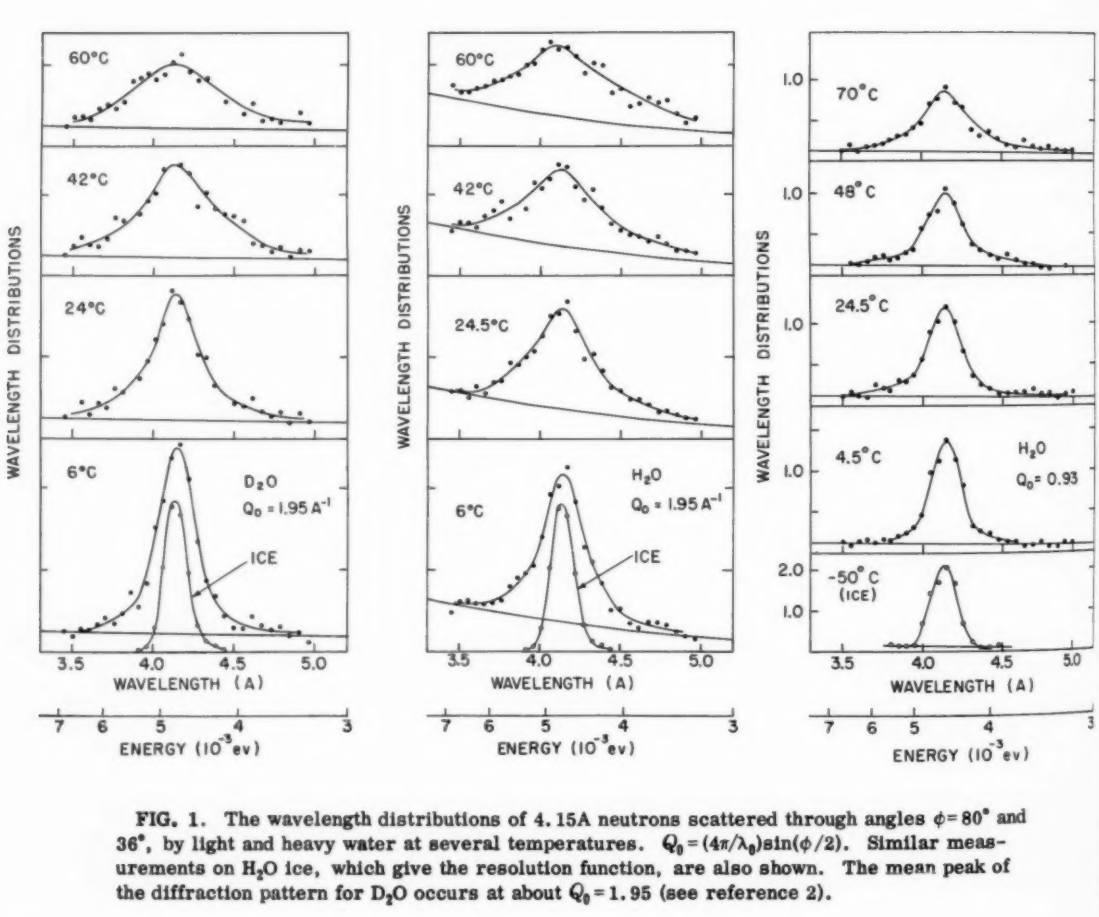


FIG. 1. The wavelength distributions of 4.15A neutrons scattered through angles $\phi = 80°$ and 36°, by light and heavy water at several temperatures. $Q_0 = (4\pi/\lambda_0)\sin(\phi/2)$. Similar measurements on $H_2O$ ice, which give the resolution function, are also shown. The mean peak of the diffraction pattern for $D_2O$ occurs at about $Q_0 = 1.95$ (see reference 2).

with the new rotating crystal spectrometer (at the NRX reactor), briefly described elsewhere.[5] Neutrons of incident wavelength 4.15 A were scattered from fairly thin (~0.3 mean free path) specimens of light and heavy water at angles of 80° and 36°, and the times of flight of scattered neutrons with energies near the initial energy were measured in a 30-channel timesorter. By correcting for counter sensitivity and for frame overlap,[6] the distributions in wavelength shown in Fig. 1 were obtained. The resolution function, obtained from similar measurements on ice, is also shown. The curves represent the quasi-elastic component superposed on the central part of the inelastic component. The inelastic component for $H_2O$ was taken to be the shape of a mass-18 gas distribution, fitted on the wings; for $D_2O$ it was simply drawn in as a straight line. For this region of $Q$ the inelastic component is a very weak function of the temperature.

The shape of the distribution-in-energy of the quasi-elastic component is expected[2] to be approximately that of a Lorentz function $[W^2+(\hbar\omega)^2]^{-1}$, where $W$ is the half-width at half maximum of the distribution. After correction for resolution[7] the spectra of Fig. 1 are consistent within the errors with Lorentz functions. On the approximation of small motions[2] (equivalent to Vineyard's Gaussian approximation[3]), the width $W=Q^2D_S$, where $D_S$ is the coefficient of self diffusion for small motions. In Fig. 2 the measured values of $W/Q^2$ are compared with values of the coefficient of self diffusion of water, as measured using nuclear magnetic resonance by Simpson and Carr,[8] and using tracer methods by Graupner and Winter.[9] Other tracer measurements by Wang, Robinson, and Edelman[10] have given still larger values for $D$. Despite the large errors in the neutron measurements and disagreements in the self-diffusion measurements, it seems clear that the approximation of small motions[2,3] is not adequate and that a variety of diffusive motions must occur.

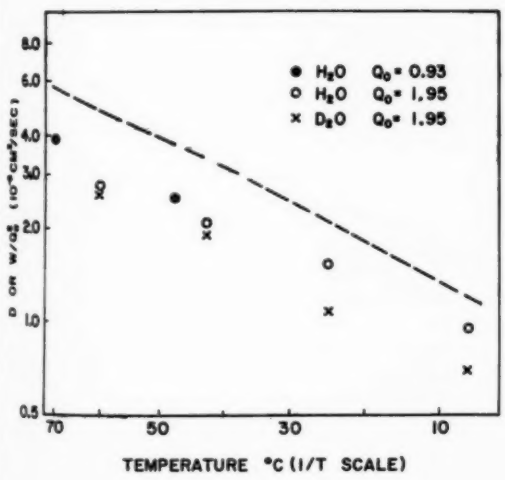


FIG. 2. Values of $W/Q_0^2$(log scale) plotted against the inverse temperature. The dashed line represents the nuclear magnetic resonance measurements of the diffusion coefficient by Simpson and Carr.

---

[1]L. Van Hove, Phys. Rev. 95, 249 (1954); Physica 24, 404 (1958).

[2]B. N. Brockhouse, Suppl. Nuovo cimento 9, 45 (1958); or Acta Cryst. 10, 827 (1957).

[3]G. H. Vineyard, Phys. Rev. 110, 999 (1958).

[4]The inelastic component for $D_2O$ was if anything narrower than that for $H_2O$ at the position of the diffraction maximum of $D_2O$. The energy distributions of $D_2O$ and $H_2O$ were thus markedly different (by as much as 50%) even for quite small energy transfers, which are believed to arise from motion of the molecules as units. On the face of it this fact suggests the failure of Vineyard's convolution approximation for the pair correlation function (reference 3).

[5]B. N. Brockhouse, Bull. Am. Phys. Soc. Ser. II, 3, 233 (1958).

[6]With the flight path of 4.5 meters and the repetition rate of 16 400 bursts/minute, the fastest neutrons inelastically scattered by light water arrived at the detector at the same time as the slower neutrons of the quasi-elastic group from the preceding burst. Approximate corrections were applied using the knowledge gained in the experiments of reference 2. For light water at $Q_0=1.95$ this involved comparatively large corrections between 4.2 and 5 A.

[7]The resolution function is approximately Gaussian. Tables of convolutions of the Lorentz function with a Gaussian resolution function were used to make the resolution corrections [V. L. Sailor, Brookhaven National Laboratory Report BNL-257 (unpublished); and Rose, Miranker, Leak, Rosenthal, and Hendrickson, Westinghouse Electric Corporation Atomic Powers Division Report WAPD-SR-506 (unpublished)].

[8]J. H. Simpson and H. Y. Carr, Phys. Rev. 111, 1201 (1958).

[9]G. Graupner and E. R. S. Winter, J. Chem. Soc. 1145 (1952).

[10]Wang, Robinson, and Edelman, J. Am. Chem. Soc. 75, 466 (1953).

# THEORY OF SOLID $He^3$†

N. Bernardes* and H. Primakoff
Department of Physics,
Washington University, St. Louis, Missouri
(Received March 4, 1959)

We have calculated the properties of solid $He^3$ at pressures $p \approx 30$ atmos and temperatures $T < 1°K$ on the basis of: (A) a gas-phase 12-6 Lennard-Jones potential, modified at small interatomic distances; (B) a Heitler-London type variational wave function, for all the atoms in the solid, constructed from a suitably antisymmetrized product of single-particle orbitals localized on various lattice points; (C) a Dirac vector model to describe the symmetry energy, with an exchange integral deduced from (A) and (B); (D) a spin wave approximation at "low" temperatures, and a Kramers-Opechowski[1] approximation at "high" temperatures, for calculation of the "spin" partition function, and (E) a Debye-phonon model for description of the vibrationally excited states of the solid.

In connection with (A)-(E), we note the following:

(A) The interatomic potential used was

$$V(r_{ij}) = \epsilon [x_{ij}^{-12} - 2x_{ij}^{-6}] \exp(-\lambda x_{ij}^{-10}), \qquad (1)$$

where $r_{ij} = r_0 x_{ij}$ is the distance between atoms $i$ and $j$, $\epsilon = 10.2°K$,[2] $r_0 = 2.88$ A, and $\lambda = 1/15$. The interatomic potential of Eq. (1), in the limit $\lambda \to 0$, is the 12-6 Lennard-Jones potential with constants $\epsilon$ and $r_0$ appropriate to the $He^3$ or $He^4$ gas data. The exponential factor, which modifies the 12-6 potential only at small interatomic distances and consequently does not upset the fit to the gas data, represents, for a suitably chosen $\lambda$, a convenient way of avoiding divergences which arise when a singular potential is used in conjunction with variational wave functions lacking the proper atom-atom correlation at these small distances. The choice $\lambda = 1/15$ was found to give the best description of available data for (1) the cohesive energy and lattice constant of solid $He^4$ at pressures $\approx 30$ atmos and (2) the root mean square deviation ($d_{\text{rms}}$) of a $He^4$ atom from its lattice site at these pressures.

(B) We used single-particle localized orbitals of the form

$$C \exp[-\tfrac{1}{2}\alpha^2(\vec{r}_i - \vec{R}_n)^2], \qquad (2)$$

where $C$ is a normalization constant, $\vec{R}_n$ gives the position of a lattice point, and $\alpha$ is a variational parameter proportional to $(d_{\text{rms}})^{-1}$.

From (A)-(E) we may write the energy of solid $He^3$ as

$$E(R,\alpha,H) = E_0(R,\alpha) - \tfrac{1}{2}J(R,\alpha)\sum_{n=1}^{N}\sum_{m}(1+\vec{\sigma}_n\cdot\vec{\sigma}_m)$$

$$-\mu H\sum_{n=1}^{N}\sigma_n^{(z)} + E_{\text{phonons}}, \qquad (3)$$

where the second term is the symmetry energy, $J(R,\alpha)$ is the exchange integral, the $\vec{\sigma}$'s are spin operators, $R$ is the distance between nearest neighbor lattice points, the sum over $m$ for a given $n$ runs over the nearest neighbors of $n$, $\mu$ is the magnetic moment of a $He^3$ nucleus, and $H$ is an external magnetic field. Equation (3) expresses the symmetry energy by means of the Dirac vector model; the validity of this vector model is only approximate in the present case since we use nonorthogonal orbitals. The spin-spin magnetic interaction energy ($\sim N\mu^2/R^3$) is negligible compared to the symmetry energy and is not included in Eq. (3).

In our variational procedure we first find the optimum value of $\alpha$ which minimizes the right-hand side of Eq. (3) for states with $E_{\text{phonons}} = 0$. In this minimization we also neglect the symmetry energy since it represents only a small part of the total cohesive energy (the Curie temperature of solid $He^3$ is $\approx 0.1°K$,[3] while the cohesive energy per atom is $\approx 1$–$2°K$). Furthermore, in evaluating $E_0(R,\alpha)$ numerically we assume an fcc lattice and sum over the first 42 neighbors. Following this procedure, we obtain the results (1)-(7):

(1) For an empirical nearest neighbor distance $R_0 = 3.8$ A, appropriate to solid $He^3$ at $p \approx 30$ atmos, the optimum value of $\alpha$ is found to be $\alpha_0 = 2.6/r_0$; this yields $d_{\text{rms}} = 0.36R_0$, slightly larger than the corresponding (experimentally known) value for solid $He^4$.

(2) The cohesive energy per $He^3$ atom is found to be $\cong 2.5°K$, which may be somewhat too large.

(3) The exchange integral (whose dominant contribution comes from the kinetic energy operator) is found to be $J(R_0,\alpha_0) \equiv J_0 \cong -\epsilon/200 = -0.05°K$, so that the ground state of solid $He^3$ at $p \approx 30$ atmos corresponds to an antiferromagnetic configuration.

The spin entropy of the solid was calculated, as a function of $T$ and $H$, (a) in the limit of "high" temperatures ($T > 6|J_0|$) using an approximation developed by Kramers and Opechowski,[1] and (b) in the limit of "low" temperatures ($T < 6|J_0|$)

using a spin wave approximation based on a two-sublattice model[4] of antiferromagnetism (not exactly valid for a close-packed lattice). From this calculated expression for the "high"-temperature spin entropy, we can express the magnetic susceptibility of solid $He^3$, $\chi$, as a power series in $J_0/T$ which can be approximated by a Curie-Weiss law:

$$\chi = N\mu^2/(T+T_C), \tag{4}$$

where $T_C = 6|J_0| = 0.3°K$. Empirically,[3] $\chi$ indeed appears to be given by an expression of the form of Eq. (4), but with $T_C$ closer to 0.1°K than to 0.3°K. Our estimate of $T_C$ agrees with the result of Primakoff[5] but disagrees with the estimate $T_C \approx 10^{-7}$°K suggested by Pomeranchuk[6] in a treatment where the symmetry energy is assumed negligible compared to the spin-spin magnetic interaction energy.

From our theoretical values for the total entropy of the solid, $S = S_{spin} + S_{phonon}$, we further calculate that:

(4) $C_V \equiv T(\partial S/\partial T)_V$ exhibits an anomaly at $T \approx 0.2°K$;

(5a) $(\partial S/\partial p)_T > 0$ for $T < 0.5°K$,

and

(5b) $(\partial S/\partial p)_T < 0$ for $T > 0.5°K$,

so that $(\partial V/\partial T)_p$ of solid $He^3$ at $p \approx 30$ atmos should become negative below 0.5°K.

From (5a) it follows that

(6) below 0.5°K it should be possible to cool solid $He^3$ by an adiabatic compression.

(7) Finally, we construct the "low"-temperature part of the melting curve, by means of the Clapeyron equation

$$dp/dT = (S_{liq} - S_{sol})/(V_{liq} - V_{sol})$$

and with use of (a) one experimental point: $p = 30$ atmos, $T = 0.05°K$,[7] (b) our theoretical values (suitably interpolated) for the entropy of the solid, (c) the experimental values of $S_{liq}$, obtained from specific heat measurements,[8] and (d) a temperature-independent $V_{liq} - V_{sol} = 1.0$ cm³/mole.[9]

The resulting melting curve is presented in Fig. 1 (together with typical experimental points obtained by the blocked capillary method[7]) for three different values of the exchange integral $J_0$ and $T_{Debye} = 20°K$. The results contained in Fig. 1 indicate that the melting curve should have a minimum near 0.4°K with a difference $[p(0.1°K) - p(0.4°K)]$ sufficiently large ($\cong 4$ atmos) for experimental observation. The failure to detect this minimum up to now may therefore be ascribed to the suggested inadequacy[10] of the blocked capillary method.

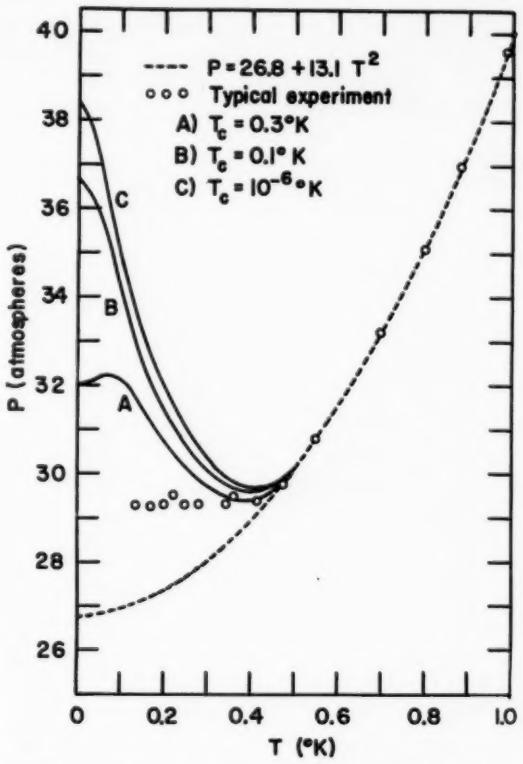


FIG. 1. Melting curve of $He^3$: solid lines $A$, $B$, and $C$ calculated as described in the text; the circles correspond to experimental points.[7]

---

†This research was supported by the U. S. Air Force through the Air Force Office of Scientific Research of the Air Research and Development Command.

*Now at Department of Physics, Iowa State College, Ames, Iowa.

[1]W. Opechowski, Physica 4, 181 (1937).

[2]We choose our units so that the Boltzmann constant is a pure number equal to unity; hence energy will be expressed in degrees Kelvin.

[3]W. M. Fairbank and G. K. Walters, Suppl. Nuovo cimento 9, 297 (1958).

[4]J. Van Kranendonk and J. H. Van Vleck, Revs. Modern Phys. 30, 1 (1958).

[5]H. Primakoff, Bull. Am. Phys. Soc. Ser. II, 2, 63 (1957).

[6]I. Pomeranchuk, J. Exptl. Theoret. Phys. U.S.S.R.

20, 1919 (1950).
[7]Weinstock, Abraham, and Osborne, Phys. Rev. 85, 158 (1952).
[8]Brewer, Sreedhar, Kramers, and Daunt, Phys. Rev. 110, 282 (1958).
[9]R. L. Mills and E. R. Grilly, Symposium on Liquid and Solid He³, Ohio State University, 1957 (unpublished).
[10]See K. Mendelssohn, in Handbuch der Physik, edited by S. Flügge (Springer-Verlag, Berlin, 1956), Vol. 15, pp. 399-400.

## CYCLOTRON RESONANCE EFFECTS IN ZINC

J. K. Galt, F. R. Merritt, W. A. Yager, and H. W. Dail, Jr.
Bell Telephone Laboratories, Murray Hill, New Jersey
(Received March 12, 1959)

We have observed cyclotron resonance effects in single-crystal samples of zinc at about 1.3°K and at both 24 000 Mc/sec and 72 000 Mc/sec. We have done the experiment both with the magnetic field along a twofold and along a sixfold axis.

The experiments were done by using the same technique used previously in experiments on bismuth[1,2] and graphite.[3] The crystallographically oriented plane surface of a disk sample was made to form part of the wall of a microwave cavity in an area where circularly polarized radiation was incident upon it. In the experiments on zinc, the sensitivity of the experiment was increased by making the sample form a larger part of the cavity end-wall than in the earlier work. As a result, the two circular polarizations in the radiation incident on the sample have a ratio as low as 7.5 in some cases, but this does not seem to have led to vital difficulties.

Single-crystal boules of zinc were grown in a stream of hydrogen at atmospheric pressure by pulling a seed from a melt formed from New Jersey Zinc Company's "super-purity" zinc. Disks with at least one plane, carefully oriented surface were cut from these, some with the plane surface normal to a twofold axis, ⟨10·0⟩, so that a sixfold axis was in the surface, and some with the plane surface normal to a sixfold axis in which case twofold axes were in the plane. The data in the figures are from two samples, both cut from a crystal in which the dc resistance ratio $R(300°K)/R(4.2°K)$ was about 9000.

For each sample type, experiments were done both with the field in the plane of the sample and normal to it. When the field was in the plane of the sample, the behavior observed was like that predicted by Azbel' and Kaner[4] and observed by others in tin, lead and copper.[5] Data taken under these conditions at 24 000 Mc/sec showed the appropriate frequency dependence and generally confirmed those taken at 72 000 Mc/sec but were not as good, and only the latter are presented.

Figure 1 shows data taken with the field in the sample plane and along a sixfold axis. The data

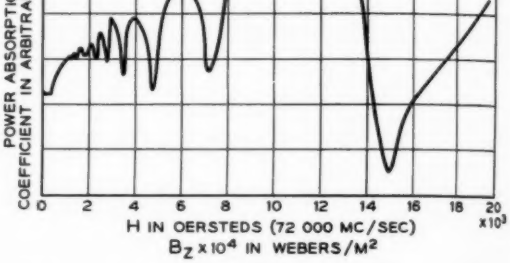


FIG. 1. Cyclotron resonance data at 72 000 Mc/sec and 1.3°K for zinc with magnetic field in sample plane and along a sixfold axis.

below one kilogauss do not constitute a well-resolved signal, but they do indicate the presence of a carrier of cyclotron mass less than $0.015m_0$. This part of the data agrees qualitatively with de Haas-van Alphen data,[6] which give a cyclotron mass of $0.005m_0$ for carrier motions about this axis. The high-field region in Fig. 1 shows a well-resolved signal of the type predicted by Azbel' and Kaner which is from another carrier. These data fit reasonably well the behavior of $R(H)/R(0)$ derived from the formula given by Azbel' and Kaner[4] for $Z(H)/Z(0)$ using a mass of $0.55m_0 \pm 5\%$, an $\omega\tau$ of about 20, and a phase of $e^{-i\pi/3}$ in $Z(0)$. This signal also has the characteristic predicted by Azbel' and Kaner that it disappears unless the field is within about one degree of the sample surface. The fit to the theory is not perfect, but the misfit probably arises primarily from imperfect tracking of the cavity and signal oscillator frequencies, so that the signal partly reflects the surface reactance as well as the surface resistance.

Figure 2 shows data taken with the field in the sample plane and along a twofold axis. Here we

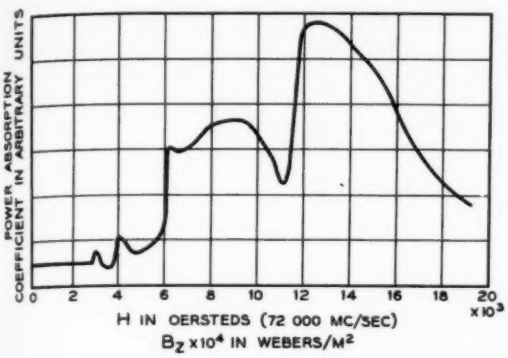
POWER ABSORPTION COEFFICIENT IN ARBITRARY UNITS
0 2 4 6 8 10 12 14 16 18 20
x10³
H IN OERSTEDS (72 000 MC/SEC)
Bz x10⁴ IN WEBERS/M²

FIG. 2. Cyclotron resonance data at 72 000 Mc/sec and 1.3°K for zinc with magnetic field in sample plane and along a twofold axis.

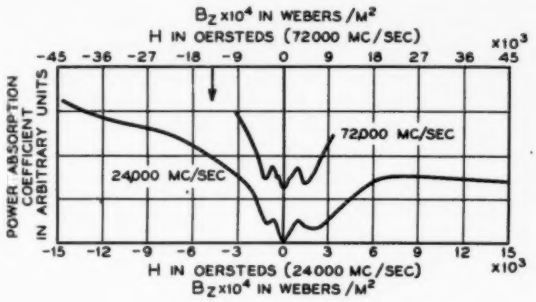
Bz x10⁴ IN WEBERS/M²
H IN OERSTEDS (72000 MC/SEC)
-45 -36 -27 -18 -9 0 9 18 27 36 45
x10³
POWER ABSORPTION COEFFICIENT IN ARBITRARY UNITS
72000 MC/SEC
24000 MC/SEC
-15 -12 -9 -6 -3 0 3 6 9 12 15
x10³
H IN OERSTEDS (24000 MC/SEC)
Bz x10⁴ IN WEBERS/M²

FIG. 3. Cyclotron resonance observations at 72 000 Mc/sec and 24 000 Mc/sec at 1.3°K on zinc with magnetic field normal to sample plane and along a sixfold axis. Field scales are adjusted so that cyclotron fields for both curves are on the same vertical line. The cyclotron field deduced from the data in Fig. 1 is shown by an arrow. Electrons resonate on the negative-field side of the figure, holes on the positive-field side.

were unable to detect a signal from the very-low-mass carrier apparent from the de Haas-van Alphen data,[6] but a signal is observed in the higher field region. The signal here fits fairly well the behavior of $R(H)/R(0)$ derived from the formula given by Azbel' and Kaner for $Z(H)/Z(0)$ using a mass of $0.43m_0 \pm 10\%$, an $\omega\tau$ of about 10, and a phase of $e^{i\pi/3}$ in $Z(0)$; it will be noted that the phase in $Z(0)$ is different for this curve than for that in Fig. 1. Here again as in Fig. 1, and presumably for the same reasons, the fit to the theoretical curve is not perfect, and in particular the curve has an extra bump in the field range between 7 and 11 kilogauss. The signal in Fig. 2 did not change drastically until the field was rotated more than 5 degrees out of the plane of the sample.

Figure 3 shows data taken at both experimental frequencies with the magnetic field normal to the sample plane and along a sixfold axis. Caution must be used in interpreting these data because they are observed under anomalous skin effect conditions and no theory of the shape of the curve is now available, but they are important because they are a basis for distinguishing effects due to holes from those due to electrons. Furthermore, they do correspond broadly to what might be expected from the data in Fig. 1, which is taken with the magnetic field along the same crystal direction, i.e., low-field structure from a very-low-mass carrier and broad variations at higher fields from the higher-mass carrier. There are indications from the differences in behavior for magnetic fields of the two signs that the carrier with mass $0.55m_0$ (as determined from the data in Fig. 1) is an electron.

Figure 4 shows data taken at both experimental frequencies with the magnetic field normal to the sample plane and along a twofold axis. Here again, anomalous skin effect conditions prevail, but two comments may be made. First, the unresolved structure at low fields indicates the presence of a very-low-mass carrier, presumably the one observed in de Haas-van Alphen experiments.[6] Second, on the negative field side the curve indicates that as the field increases the surface impedance is almost independent of

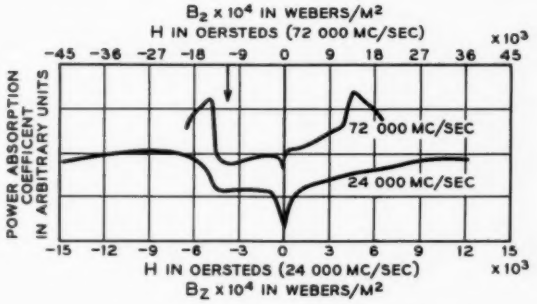
Bz x10⁴ IN WEBERS/M²
H IN OERSTEDS (72 000 MC/SEC)
-45 -36 -27 -18 -9 0 9 18 27 36 45
x10³
POWER ABSORPTION COEFFICIENT IN ARBITRARY UNITS
72 000 MC/SEC
24 000 MC/SEC
-15 -12 -9 -6 -3 0 3 6 9 12 15
x10³
H IN OERSTEDS (24 000 MC/SEC)
Bz x10⁴ IN WEBERS/M²

FIG. 4. Cyclotron resonance observations at 72 000 Mc/sec and 24 000 Mc/sec at 1.3°K on zinc with magnetic field normal to sample surface and along a twofold axis. Field scales are adjusted so that cyclotron fields for both curves are on the same vertical line. The cyclotron field deduced from the data in Fig. 2 is shown by an arrow. Electrons resonate on the negative-field side of the figure, holes on the positive-field side.

field until after the resonance of the high-mass carrier shown by the data in Fig. 2 is passed. It seems likely that this lack of change is a result of anomalous skin effect conditions, and that the sharp rise observed at a field just above the resonance represents at least partial emergence from the anomalous skin effect region.[7] This occurs for the sign of field corresponding to electron resonance, and indicates that the carrier of mass $0.43m_0$ observed in Fig. 2 is an electron.

We wish to thank B. B. Cetlin for help in sample preparation, W. H. Richards for growing zinc crystals, and D. F. Gibbons for a residual resistance measurement.

---

[1]Galt, Yager, Merritt, Cetlin, and Dail, Phys. Rev. 100, 748 (1955).

[2]Galt, Yager, Merritt, Cetlin, and Brailsford, Phys. Rev. (to be published).

[3]Galt, Yager, and Dail, Phys. Rev. 103, 1586 (1956).

[4]M. Ia. Azbel' and E. A. Kaner, Zhur. Eksptl. i Teoret. Fiz. 30, 811 (1956) [translation: Soviet Phys. JETP 3, 772 (1956)]; J. Phys. Chem. Solids 6, 113 (1958).

[5]E. Fawcett, Phys. Rev. 103, 1582 (1956); Kip, Langenburg, Rosenblum, and Wagoner, Phys. Rev. 108, 494 (1957); P. A. Bezuglyi and A. A. Galkin, Zhur. Eksptl. i Teoret. Fiz. 33, 1076 (1957) [translation: Soviet Phys. JETP 6, 831 (1958)].

[6]D. Shoenberg, Proc. Roy. Soc. (London) A170, 341 (1939).

[7]M. Ia. Azbel' and M. I. Kaganov, Doklady Akad. Nauk S.S.S.R. 95, 41 (1954).

---

## DIRECT OBSERVATION OF ANTIPARALLEL DOMAINS DURING POLARIZATION REVERSAL IN SINGLE-CRYSTAL BARIUM TITANATE

Robert C. Miller and Albert Savage
Bell Telephone Laboratories,
Murray Hill, New Jersey
(Received March 13, 1959)

This communication describes a new and better method than others previously reported for the continuous, direct observation of the antiparallel ferroelectric domain structure in $BaTiO_3$ during polarization reversal. This method has been applied to both liquid- and metal-electroded crystals and some of the more interesting results concerning domain growth and domain-wall motion in metal-electroded crystals are given.

The study of the domain dynamics of polarization reversal in $c$-domain $BaTiO_3$ crystal plates has been rather severely hampered due to the difficulty experienced in trying to observe directly the antiparallel domains in question.[1] Under conditions where the applied electric field is either parallel or antiparallel to the spontaneous polarization in $BaTiO_3$, it has generally been considered that domains of opposite polarization cannot be discerned by direct optical observation. Several investigators[2-4] have observed directly the antiparallel domain configuration during polarization reversal; however, in each case it was necessary to subject the $BaTiO_3$ samples to a "perturbing" electric field applied in a direction normal to the spontaneous polarization. This field rotates the optic axes of the antiparallel domains by small amounts, in opposite directions, so that with the appropriate experimental arrangement, one can discern the antiparallel domain structure. Some of the experimental results of these investigations seem to be in conflict with other work in which the perturbing electric field was omitted. However, it is difficult to interpret some of the results obtained by direct observation, as mentioned above, in terms of polarization reversal in the usual sense where the only applied field is one parallel to the ferroelectric axis.

Two other methods which have frequently been employed to observe a stationary antiparallel domain pattern in $BaTiO_3$ are the acid etch technique[5] and the electrostatically charged powder technique.[6] Unfortunately, although very valuable, these latter two techniques are not suitable for a continuous direct observation of the antiparallel domain configuration during polarization reversal. The ideal method for the study of domain dynamics is, of course, one in which the field is applied parallel to the ferroelectric axis and the domain configuration observed continuously through transparent, or semitransparent, electrodes. The authors have found that this is indeed possible.

In the course of experiments on the electric field dependence of 180° domain-wall velocity in $BaTiO_3$, it was noted that occasionally one could differentiate antiparallel domains without recourse to any of the aforementioned techniques. That is, portions of the antiparallel domain configuration of liquid-electroded samples[7] which were partially reversed with fields of the order of a thousand volts per centimeter and then washed in water to remove the electrolyte, were sometimes visible when the sample was mounted

between crossed polaroids and viewed with white light. The reversed domains generally appeared somewhat darker in shade than the surrounding regions.

This most interesting result led to attempts to observe the $c$-domain structure during polarization reversal by looking along the ferroelectric axis through transparent aqueous lithium chloride electrodes,[7] again with crossed polaroids. It was found that the antiparallel domain configuration could be discerned in this manner. Furthermore, one could also observe the antiparallel domain structure of semitransparent metal-electroded $BaTiO_3$ crystals. A photomicrograph of a portion of the antiparallel domain configuration observed directly during polarization reversal with a metal-electroded crystal is shown in Fig. 1. The metal electrodes consisted of 200A films of gold evaporated on to opposite sides of the crystal plate. Motion pictures of the domain pattern as viewed during polarization reversal have also been made. The visual characteristics of the antiparallel domains are somewhat variable and depend on the lighting conditions. However, it has been possible to discern the antiparallel domain structure of every sample which has been investigated to date. The origin of the effects which enables one to observe the $c$-domain structure in the samples viewed in the manner described above is not understood.

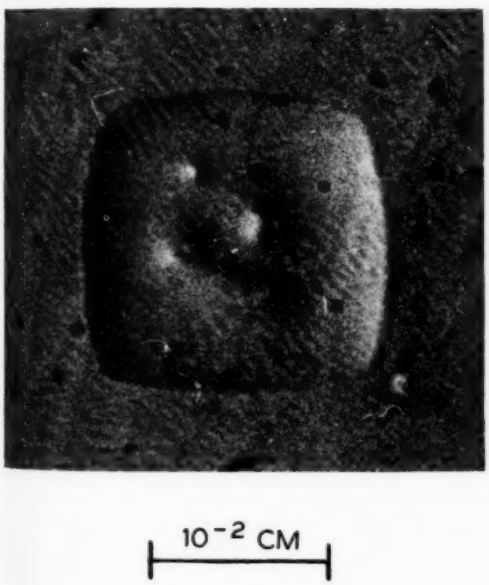


FIG. 1. Photomicrograph showing a portion of the antiparallel domain configuration of a partially reversed $BaTiO_3$ crystal as observed directly through semitransparent gold electrodes. The single reversed domain shown in the figure is approximately square with the sides at about 45° to the crystalline $a$ axes. The sample was placed between crossed polaroids and viewed with white light.

Some of the most interesting results obtained using this new technique are those concerned with the domain dynamics of polarization reversal of metal-electroded crystals. "Extensive" sidewise 180° domain-wall motion has been found to occur when the spontaneous polarization of liquid-electroded $BaTiO_3$ crystals is reversed with applied fields of several hundred volts per centimeter.[7] The quantitative aspects of this wall motion have also been given.[8] The authors call sidewise domain wall motion "extensive" if the domain walls in question move sidewise through distances which are a significant fraction of the diameter ($\approx 1$ mm) of the electroded area. In the case of metal-electroded crystals, the published data on sidewise domain-wall motion are somewhat conflicting. However, there is good evidence that some sidewise 180° domain-wall motion occurs in metal-electroded crystals during polarization reversal with fields of several thousand volts per centimeter[3,9] and also with fields of several hundred volts per centimeter.[7,10] Direct observations in the present research indicate that many of the salient features of sidewise wall motion and polarization reversal are the same for metal- and liquid-electroded crystals.[7,8] In particular, with applied fields of hundreds of volts per centimeter, extensive sidewise wall motion does indeed occur in metal-electroded crystals; and in some cases, the entire electroded area (2.5 mm in diam) can be reversed with a single growing domain, expanding through sidewise 180° domain-wall motion. As in the case of liquid-electroded crystals, the reversed growing domains generally tend to be approximately square in shape, as shown in Fig. 1, with the sides at about 45° to the crystalline $a$ axes. Measurements of the rate of growth of a single reversed domain as a function of the applied field $E$ indicate that the sidewise wall velocity is given by $v\exp[-(\text{const}/E)]$. The same field dependence has been found with liquid-electroded crystals[8]; however, it appears that the sidewise wall velocity measured with metal-electroded crystals is something like several orders of magnitude less than that found for the same field with liquid-electroded crystals.

Since one can now observe directly the anti-

parallel domain structure during polarization reversal under the conditions given above, there are many important experiments which are possible and which will undoubtedly lead to a better understanding of ferroelectric $BaTiO_3$. Among those which the authors are currently investigating are the following: the phenomena which give rise the visibility of the antiparallel domains, the quantitative aspects of sidewise wall motion in metal-electroded crystals, the nucleation sites for reversed domains, the origin and characteristics of ferroelectric Barkhausen pulses, and the effects of various electrodes and impurity dopings on the characteristics of polarization reversal.

---

[1]For a general discussion of the published work on this subject, the reader is referred to W. Känzig, in Solid State Physics, edited by F. Seitz and D. Turnbull (Academic Press, Inc., New York, 1957), Vol. 4.

[2]W. J. Merz, Phys. Rev. 88, 421 (1952). W. J. Merz, Phys. Rev. 95, 690 (1954).

[3]E. A. Little, Phys. Rev. 98, 978 (1955).

[4]D. Meyerhofer, Phys. Rev. 112, 413 (1958).

[5]J. A. Hooton and W. J. Merz, Phys. Rev. 98, 409 (1955).

[6]G. L. Pearson and W. L. Feldmann, J. Phys. Chem. Solids 9, 28 (1959).

[7]R. C. Miller, Phys. Rev. 111, 736 (1958).

[8]R. C. Miller and A. Savage, Phys. Rev. 112, 755 (1958).

[9]S. Triebwasser and E. F. Hahn, Bull. Am. Phys. Soc. Ser. II, 4, 184 (1959).

[10]R. C. Miller and A. Savage (unpublished).

---

## SUPERCONDUCTIVITY OF $\beta$ MERCURY*

J. E. Schirber and C. A. Swenson
Institute for Atomic Research
and Department of Physics,
Iowa State College, Ames, Iowa
(Received March 12, 1959)

Solid mercury ordinarily crystallizes in a rhombohedral structure which is stable to absolute zero under normal pressures. Recent experiments have shown, however, that a new type of solid mercury can be produced which is actually the more stable form at temperatures below 79°K.[1] The first indications that this new modification existed were found in the course of a series of experiments in which the effect of pressure on the superconducting transition temperature of normal ($\alpha$) mercury was studied.[2] The results of these experiments implied (although not conclusively) that the new ($\beta$) phase was also superconducting. The theory of superconductivity, as given by Bardeen, Cooper, and Schrieffer,[3] is relatively insensitive to the band structure, and, hence, for a given element, the superconducting transition temperature in zero field should be dependent to a first approximation only on the density.[4] Lanthanum, which is far from an ideal superconductor,[5] represents what has been the only known example of an element that exists in two superconducting crystallographic modifications. The two forms of mercury seemed to offer a more ideal opportunity for checking the dependence of the superconducting transition temperature on crystal structure, and in order to investigate this point we have recently investigated the initial part of the critical field curve for $\beta$ mercury. The zero-field transition temperature which was found for $\beta$ mercury can be explained quantitatively in terms of the known difference in molar volume[1] (about 1.5%) between the two forms of solid mercury, and the pressure-effect data for $\alpha$ mercury.[2]

Although $\beta$ mercury is stable at zero pressure below 79°K, and metastable for temperatures below 90°K, it can be formed only at relatively high pressures (4000 atmos). Above 90°K the low-temperature $\beta$ phase anneals rapidly into the $\alpha$ phase in an irreversible manner, so care must be taken in handling samples once they have been obtained. In our case, a fine wire of the $\beta$ phase, 0.4-mm diam, was formed by extruding solid mercury under liquid nitrogen from a 0.250-in. diam cylinder through a 0.016-in. diam hold. A pressure of 8000 atmos was necessary to initiate extrusion, so $\beta$ mercury was formed in the cylinder before the extrusion began. The extrusion rate was kept small (about one inch of wire per hour) in order to prevent local heating and annealing. A convenient, though destructive, test for the existence of the $\beta$ phase was made by measuring the resistance of a piece of wire in liquid nitrogen before and after heating in air to 100°K. The existence of the $\beta$ phase was indicated by an irreversible resistance increase of a factor of two due to the $\beta \rightarrow \alpha$ transition.

The critical field curve to 200 gauss was determined by placing the wire in the center of a small solenoid which was later placed in a liquid helium Dewar, all manipulations taking place under liquid nitrogen. The transitions were observed by using an ac mutual inductance method at 33 cps, with a measuring field of 0.02 gauss rms superimposed on the dc field. The results of three runs on both $\alpha$ and $\beta$ mercury are given

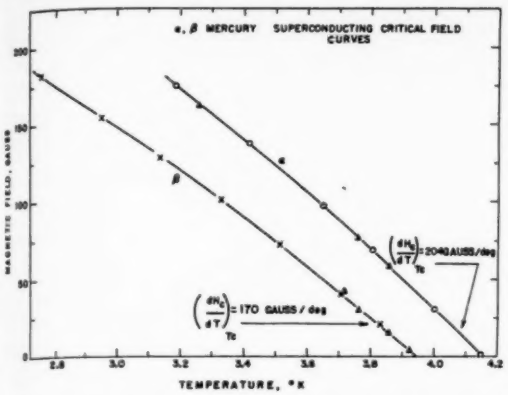
α, β MERCURY SUPERCONDUCTING CRITICAL FIELD CURVES
MAGNETIC FIELD, GAUSS
TEMPERATURE, °K
(dHc/dT)Tc = 204 GAUSS/deg
(dHc/dT)Tc = 170 GAUSS/deg

FIG. 1. The critical-field curves for the $\alpha$ and $\beta$ forms of mercury.

in Fig. 1. In the first run, the sample (0.4-mm diam) was inadvertently allowed to warm above 90°K, and only the $\alpha$ transitions were noted. An identical piece of wire was used in the second run, and only the $\beta$ transitions were found. Finally, a third run was made with a slightly larger wire (about 0.55-mm diam) which, for some unexplained reason, seemed to contain a mixture of both phases, and two sets of transitions were found, neither being of the same quality as in the first two runs. The consistency within a given run was about $\pm 0.1$ gauss, with an agreement between different runs of about one gauss. The wire used in the first two runs may have been fairly strain-free, since it had been kept under liquid nitrogen for two weeks before the runs were made. The second lot of wire was run almost immediately after extrusion, and may have been quite strained, since changes in hardness of the wire with time have been observed in the course of this work. Thus, we tend to rely on the first two runs as being the more dependable, and on the third run as furnishing a qualitative confirmation of the first two.

The changes in both the zero-field transition temperature (from 4.1536°K for $\alpha$ mercury to 3.94°K for $\beta$ mercury) and the shape of the critical-field curve are quite marked. Our data for $\alpha$ mercury agree with Maxwell and Lutes[6] in that, within our accuracy and the limited range of our magnetic fields, the critical-field curve is strictly parabolic, with an $H_0$ of 426 gauss, compared with their 410 gauss. The critical-field curve for $\beta$ mercury appears to deviate appreciably from parabolic shape in the same sense as tin and indium, although no attempt was made to fit the data to an analytic curve to determine a value for $H_0$. The measured initial slopes of the critical-field curves are -204 gauss/deg for $\alpha$ mercury and -170 gauss/deg for $\beta$ mercury.

The change in the zero-field transition temperature (-0.21°) can be explained almost completely by the change in volume due to the crystallographic transformation. The pressure-effect experiments[2] give $(dT_c/dV) = 0.91$ deg/(cm$^3$/mole), and the compression measurements give $\Delta V = V_\alpha - V_\beta = 0.206$ cm$^3$/mole at 4°K.[1] Thus, on the basis of these data, a change in $T_c$ of -0.19° would be predicted, well within the experimental uncertainties. On the basis of this same assumption, the observed difference in the slopes of the critical-field curves can be explained only if $(\partial H_c/\partial V)_T$ were to increase with decreasing temperature. This does not correspond with what is known of any other superconductor,[7] and we hope to investigate this point at a later date.

An x-ray powder camera for use at either liquid nitrogen or liquid helium temperatures was constructed in order to determine the structure of $\beta$ mercury. The results of this work are only tentative, but the pictures which have been obtained show conclusively that the structure of $\beta$ mercury is quite different from that of $\alpha$ mercury. The powder diffraction patterns from $\beta$ mercury can be explained by a body-centered tetragonal structure, although a definite statement cannot be made until further data are obtained.

The authors are indebted to Dr. M. Atoji for his collaboration in the design of the x-ray cryostat, and for his determination of the structure from the pictures which were taken. More complete accounts of the x-ray and superconductivity experiments will be published as separate papers at a later date.

*Contribution No. 728. Work was performed in the Ames Laboratory of the U. S. Atomic Energy Commission.

[1]C. A. Swenson, Phys. Rev. 111, 82 (1958).

[2]L. D. Jennings and C. A. Swenson, Phys. Rev. 112, 31 (1958).

[3]Bardeen, Cooper, and Schrieffer, Phys. Rev. 108, 1175 (1957).

[4]For a discussion of the effects of crystal structure, see D. Pines, Phys. Rev. 109, 280 (1958).

[5]Anderson, Legvold, and Spedding, Phys. Rev. 109, 243 (1958).

[6]E. Maxwell and O. S. Lutes, Phys. Rev. 95, 333 (1954).

[7]J. L. Olsen and H. Rohrer, Helv. Phys. Acta 30, 49 (1957).

# ATTENUATION OF HYPERSONIC WAVES IN QUARTZ

H. E. Bömmel and K. Dransfeld
Bell Telephone Laboratories,
Murray Hill, New Jersey
(Received February 13, 1959)

We have measured the acoustic absorption in crystalline quartz at frequencies between 1000 Mc/sec and 4000 Mc/sec from room temperature to 4.2°K. Figure 1 shows the experimental arrangement. A cylindrical quartz rod, 25 mm long and 3 mm in diameter, with both end faces polished optically flat and parallel, extended between two cavities of the same frequency. Sound waves were generated by surface excitation, as described previously,[1] in the electric field of one cavity and similarly detected in the other.

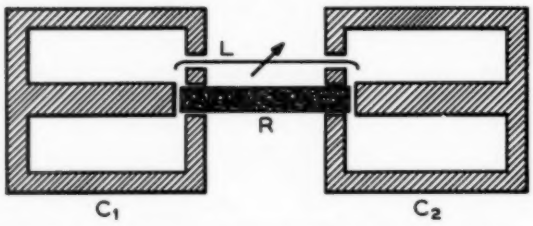


FIG. 1. Schematic diagram of the two cavities coupled acoustically by the quartz rod $R$ and a variable electric coupling $L$.

The transmitter cavity $C_1$ was coupled to a pulsed rf-power source, and the receiver cavity $C_2$ to a sensitive receiver and oscilloscope. A variable electric coupling between the two cavities provided a means to compare the acoustically transmitted pulse with a calibrated electric leakage signal. This made it possible to measure relative changes of the acoustic attenuation, since changes in the quality factor of the cavities with temperature affected both signals in the same way. Changes in the electrical coupling due to thermal expansion were negligible below 70°K and were corrected for at higher temperatures.

Three different crystal orientations were used. For longitudinal waves, the rod axis was parallel to the $x$ axis. For transverse waves, two rotated $y$-cuts were used: an $AC$-cut and a $BC$-cut, with the rod axis making an angle of -59° and +31°, respectively, with the $z$ axis. In these two orientations transverse waves travel parallel to the rod axis and have no cross-coupling to other modes.

Some of the results for longitudinal and transverse waves are shown in Figs. 2 and 3, where

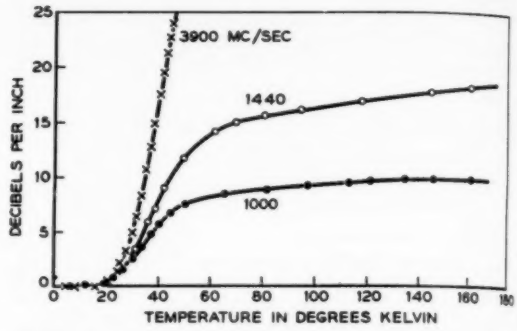


FIG. 2. Temperature-dependent part of attenuation of longitudinal waves vs temperature at different frequencies.

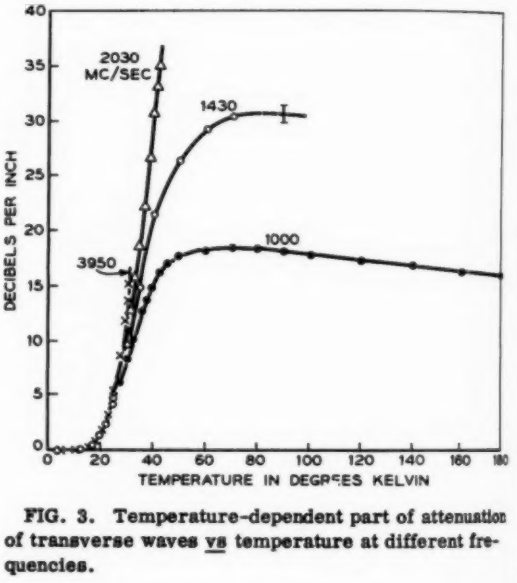


FIG. 3. Temperature-dependent part of attenuation of transverse waves vs temperature at different frequencies.

the temperature-dependent part of the absorption is plotted versus the temperature. The attenuation changes relatively little between room temperature and 60°K, but drops fast between 60°K and 20°K. It was only below 20°K that a large number of echoes could be observed, as shown in Fig. 4, thus making it possible to determine the absolute value of the absorption. The residual temperature-independent attenuation below 15°K was always only a small fraction between 1% and 10% of the room-temperature value and is not shown in Figs. 2 and 3. Therefore, below 20°K there should be no difficulty in extending such measurements to appreciably higher frequencies. None of the relaxation peaks observed in earlier work[2] at lower frequencies could be

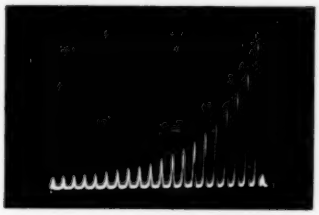

FIG. 4. Multiple reflections of longitudinal waves at 1000 Mc/sec and 15°K.

seen at 1000 Mc/sec and above. The uncertainty of the absolute values of each curve in Figs. 2 and 3 is estimated to be about 10%. The relative values are considerably more accurate, the main source of error being the calibration of the leakage signal. The frequency dependence of the attenuation is different at high and at low temperatures. Below about 25°K there is practically no variation with frequency, while above 60°K the frequency dependence appears to be between linear and quadratic. Further experiments over a wider frequency range will clarify this point.

At present we have no satisfactory explanation for our observation. It appears to be more difficult to account for the magnitude of the absorption than for its temperature dependence. It is interesting to note, in this connection, that the attenuation drops to half of its high-temperature value where the mean free path of the thermal phonons is of the same order as the acoustic wavelength, particularly in the case of transverse waves; thus this appears to be an example of interaction between sound waves and the thermal phonons. The small variation of the attenuation above this temperature may be related to the fact that here the product of the total phonon energy[3] $E$ and the phonon mean free path $l$ is nearly constant. A naive assumption of a "phonon-viscosity,"

$$\eta = E \times l/3\bar{c}, \quad (\bar{c} = \text{average sound velocity})$$

would therefore qualitatively explain the temperature dependence, but it would account for only about 15% of the observed absorption of transverse waves above 60°K. In the case of longitudinal waves our data would, in addition, require the assumption of a considerable compressional viscosity.

Absorption due to heat conduction, as calculated for example by Lücke[4] and others, is one order of magnitude smaller than observed and would not account for the absorption of transverse waves.

Akhieser[5] and Pomeranchuk[6] treated the interaction between sound waves and thermal phonons in ideal crystals. Unfortunately Akhieser only considers temperatures much higher and much lower than the Debye temperature, so that a comparison with our results is not yet possible. Pomeranchuk's results do not agree with our observed temperature dependence.

Eshelby,[7] Leibfried,[8] and Nabarro[9] estimated the sound absorption arising from the fact that the motion of dislocations is damped by interaction with thermal phonons. But the observed temperature dependence and the strong longitudinal absorption are difficult to understand on the basis of their models.

We should like to acknowledge gratefully very interesting discussions with C. Herring, H. J. McSkimin, and W. P. Mason of these Laboratories. We also wish to thank A. DiGiovanni for his very valuable assistance with the experiments.

[1]H. Bömmel and K. Dransfeld, Phys. Rev. Lett. 1, 234 (1958).

[2]Bömmel, Mason, and Warner, Phys. Rev. 102, 64 (1956).

[3]We are indebted to Dr. E. F. Westrum of the University of Michigan, Ann Arbor, for permission to use his data on the specific heat of crystalline quartz prior to publication.

[4]K. Lücke, J. Appl. Phys. 27, 1433 (1956).

[5]A. Akhieser, J. Phys. U.S.S.R. 1, 277 (1939).

[6]I. J. Pomeranchuk, J. Phys. U.S.S.R. 4, 529 (1941).

[7]J. D. Eshelby, Proc. Roy. Soc. (London) A197, 396 (1949).

[8]G. Leibfried, Z. Physik 127, 344 (1950).

[9]F. R. N. Nabarro, Proc. Roy. Soc. (London) A209, 278 (1951).

## RESONANCE PHENOMENA IN LARGE-ANGLE HELIUM ION–HELIUM ATOM COLLISIONS*

F. P. Ziemba and E. Everhart
Physics Department,
University of Connecticut,
Storrs, Connecticut
(Received February 16, 1959)

When $He^+$ ions are scattered from He atoms at kev energies, a small fraction of these collisions result in large-angle scattering of the incident particle. Scattered particles from this collision (and other combinations as well) have been analyzed to determine their charge state in two previous papers,[1,2] the data being taken at 25, 50, and 100 kev incident energies. Two interesting facts appear from the $He^+$ on He data of these

papers. Firstly, there is hardly any variation to the charge-state fractions of the scattered helium particle as the angle of scattering varies from 1° to 20°. Secondly, the fraction of neutral helium is unexpectedly higher at 50 kev than at 25 or 100 kev, indicating that this quantity must reach a maximum within this region.

A detailed investigation of this second anomaly has uncovered several resonance peaks as shown in Fig. 1. The curve $P_0$ is the fraction of the particles scattered at 5° which are neutral. There are maxima in $P_0$ at 2.7, 4.0, 5.8, 9.6, 17.5, and 43 kev, and indications of a maximum at about 250 kev. Although the data are plotted for 5° scattering, the curve for 10° scattering is coincident at energies in excess of 15 kev. At lower energies, where the analysis is to some extent a function of the scattering angle, the peaks would be shifted if the 10° data were plotted. The curve for $P_2$, the fraction scattered as $He^{++}$, is plotted also. This curve shows peaks at 80, 26, and 13.5 kev and is zero at lower energies. Peaks for $P_2$ occur where $P_0$ is a minimum. The values for $P_1$, the fraction scattered as $He^{+}$, are not shown but are readily found since $P_0$, $P_1$, and $P_2$ must add to unity.

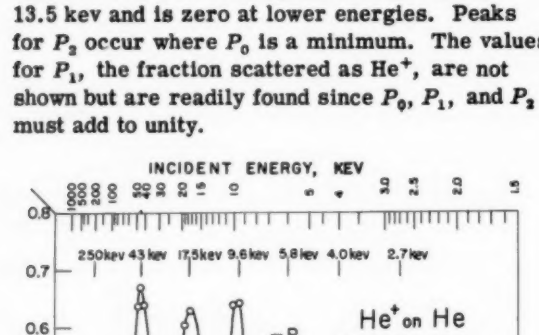
INCIDENT ENERGY, KEV
250kev 43 kev 17.5kev 9.6kev 5.8kev 4.0kev 2.7kev
He+ on He
5° scattering
P0
80kev 26kev 13.5kev 7.2kev 4.8kev 3.3kev 2.2kev
P2
FRACTIONS P0 AND P2
COLLISION TIME, UNITS OF (KEV)-½
0 0.1 0.2 0.3 0.4 0.5 0.6 0.7 0.8

FIG. 1. The particles scattered at 5° from a $He^{+}$ on He collision are analyzed to determine the fractions $P_0$ and $P_2$ which are neutral and doubly ionized, respectively. These fractions are plotted as a function of collision time on the lower axis and incident energy in kev on the upper axis. Several resonance peaks are shown.

The data are plotted on a scale spaced in proportion to the collision time, which varies as the inverse square root of the energy. It is immediately evident that the high-energy peaks are evenly spaced on this scale and there is a strong indication that the peak at about 250 kev is the first one in the series. The low-energy peaks are spaced progressively further apart.

A qualitative explanation of these phenomena may be the following: At 250 kev the collision time is so short that an electron from the neutral target atom has just time to jump to the ion and neutralize it. At 80 kev the electron has time to jump to the ion and back to its original atom. At 43 kev the electron has time to jump on and off and on again, and so on. The formation of the $He^{++}$ is a nonresonant competing process at high energies upon which effects of the resonant capture process are superimposed.

It is most interesting that Firsov[3] and Massey, Bates, and Stewart[4] have predicted that the differential cross section for elastic scattering with charge exchange of an ion in its own gas should vary as $\sin^2[kE^{-\frac{1}{2}}]$, where $E$ is the energy and $k$ is a constant. Our data clearly show this sort of energy dependence. However, their theories were expected to be valid at low energies, of the order of a few kev or less.

Our data were taken with essentially the same apparatus as in our previous work[1,2] except that the detector is now a secondary electron multiplier which counts the scattered particles individually. We have not yet developed a method of calibrating and comparing the counting efficiencies for neutrals and singly-ionized atoms below 25 kev. The heights of the peaks and depths of the valleys may need later adjustment when this calibration is made. The gradual falling off of peak heights of $P_0$ at low energies might simply reflect a decreased efficiency in the counting of neutrals. The energies at which the peaks and valleys occur should not depend on this calibration.

We would express our thanks to Dr. Arnold Russek for valuable discussions of this phenomenon and to Mr. Grant Lockwood for his help in obtaining the data.

---

*Sponsored by the Office of Ordnance Research, U. S. Army.

[1]Fuls, Jones, Ziemba, and Everhart, Phys. Rev. 107, 704 (1957).

[2]Jones, Ziemba, Moses, and Everhart, Phys. Rev. 113, 182 (1959).

[3]O. B. Firsov, J. Exptl. Theoret. Phys. (U.S.S.R.)

21, 1001 (1951).
[4]Bates, Massey, and Stewart, Proc. Roy. Soc. (London) A216, 437 (1953).

## ROTARY SPIN ECHOES

I. Solomon
Centre d'Etudes Nucléaires de Saclay,
BP2 à Gif-sur-Yvette
(Seine et Oise), France
(Received March 9, 1959)

Torrey[1] has observed the free precession of nuclear spins around an rf field $H_1$, fixed in a frame rotating at the Larmor frequency $\omega_0=\gamma H_0$ around a large dc magnetic field $H_0$. He showed that, for an $H_1$ much larger than the inhomogeneity of $H_0$, the latter has a negligible effect on the decay of the spin magnetization which is mainly due to the inhomogeneity of $H_1$. We report here on a method of overcoming the inhomogeneity of $H_1$ by the production of echoes in the rotating frame ("rotary echoes") which are very similar to the usual spin echoes.[2] The rotary echoes, however, have some additional specific features that make them particularly suitable for the measurement of long relaxation times.

Consider the rotating frame with the $z$-axis along $H_0$ and the $x$-axis along the rf field $H_1$. If at the time $t=0$ we suppose that the spin magnetization $M$ is along the $z$-axis, $M$ will precess in the $yz$ plane and, at $t=\tau$, the angle of precession is $\phi=\gamma H_1\tau$. In practice $H_1$ is inhomogeneous, with a half-width $\Delta H_1$, and will vary within the sample. Therefore, the total magnetization, sum of magnetization vectors at different points of the sample, will fan out in the $yz$ plane in a time of the order of $1/\gamma\Delta H_1$.

At $t=\tau$, we perform a 180° phase shift on the rf field so that $H_1$ is suddenly reversed in the rotating frame. From then on, the magnetization vector, at each point, will precess at the same rate as before, but in the opposite direction. Therefore, at time $t=2\tau$, the angle of precession will cancel out and all the magnetization vectors will be in phase again on the $z$-axis producing an "echo," as shown in Fig. 1.

In that way, we overcome the effect of the inhomogeneity of $H_1$ and we measure only the effect of spin relaxation. For example, in a liquid where the Bloch equations[3] are valid, the envelope of the echoes, when $\tau$ is varied, is an exponential curve with a time constant $T$ given by[1]

$$-\frac{1}{T}=\tfrac{1}{2}\left(\frac{1}{T_1}+\frac{1}{T_2}\right),$$

where $T_1$ and $T_2$ are the longitudinal and transverse relaxation times, respectively. The main limitation of the rotary echo method is due to self-diffusion in the liquid just as in the standard spin-echo experiment. Its effect can be greatly reduced, as in the Carr-Purcell[4] method, by reversing $H_1$ (which corresponds to a 180° pulse in a spin-echo experiment) not only at $t=\tau$ but also at $t=3\tau$, $t=5\tau,\ldots$, $t=(2n+1)\tau$; the echoes then occurring at $t=2\tau$, $t=4\tau,\ldots$, $t=2(n+1)\tau$.

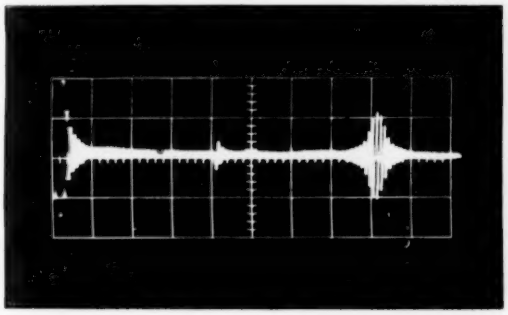

FIG. 1. A "rotary echo" in doped water. The total trace is 100 msec long.

The main difficulty in applying the spin-echo method in the measurement of long relaxation times is that (a) in order to overcome diffusion a large number of 180° pulses must be applied, and (b) the errors on the 180° pulses being cumulative, a large number of pulses give poor reproductibility. A remarkable feature of the "rotary echoes" is that the errors on the reversals of $H_1$ are not cumulative. This can be seen by a detailed analysis in the rotating frame in a manner analogous to that described by Meiboom and Gill[5] for their modified Carr-Purcell method. The result is the possibility of obtaining a large number of echoes (1000 are shown in Fig. 2) with good stability, while it was practically impossible to obtain in the same magnet more than 30 echoes of the Carr-Purcell type. Figure 2 shows a measurement of relaxation time in oxygen-free benzene which yields the value $T_2=19.6\pm1.5$ sec.

We use a crossed coil spectrometer. The transmitting coil is fed by a gated oscillator giving an rf field $H_1$ up to 1.5 gauss (rotating component). As in Torrey's experiment,[1] we

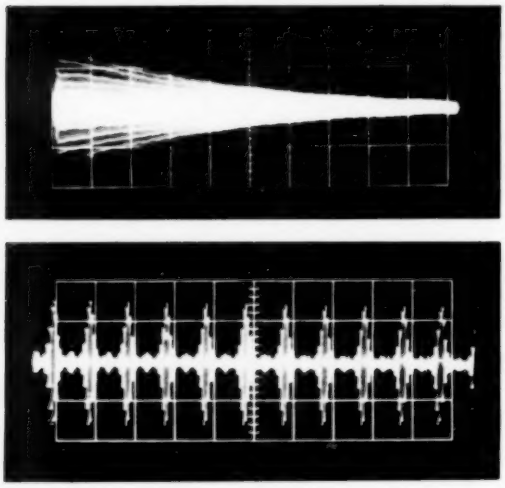

FIG. 2. Rotary echoes of the Carr-Purcell type in oxygen-free benzene. Upper photograph: the whole pattern. The pulse rate is 50 per second, and the total trace is 40 sec long. The rotary echoes are too close to be resolved on the photograph. Lower photograph: part of the same pattern enlarged 100 times to show the detail of the echoes.

turn on the oscillator at $t=0$, and the magnetization $M$ precesses around $H_1$ in the $yz$ plane. The receiving coil is tuned in the absorption mode, so that the audio signal observed after detection is directly proportional to $My$. Since the magnetization $M$ precesses around the $x$-axis at the frequency $\gamma H_1$, the frequency of the audio signal on the cathode ray oscilloscope gives the magnitude of $H_1$, while its decay gives the inhomogeneity of $H_1$. The reversal of $H_1$ at $t=\tau$ is obtained by the application on the grid of the oscillator of a strong pulse of variable length (1 to 20 microseconds). The frequency is then slightly changed for a short time and a phase shift occurs. This shift can be set to be 180°, either by direct observation of the rf voltage on a fast cathode ray oscilloscope, or by tuning the pulse length for maximum echo amplitude.

[1]H. C. Torrey, Phys. Rev. 76, 1059 (1949).
[2]E. L. Hahn, Phys. Rev. 80, 580 (1950).
[3]F. Bloch, Phys. Rev. 70, 460 (1946).
[4]H. Y. Carr and E. M. Purcell, Phys. Rev. 94, 630 (1954).
[5]S. Meiboom and D. Gill, Rev. Sci. Instr. 29, 688 (1958).

## PROPOSAL FOR A "STAIRCASE" MASER*

A. E. Siegman and R. J. Morris
Stanford Electronics Laboratories,
Stanford University,
Stanford, California
(Received February 27, 1959)

Inversion by adiabatic fast passage of a single electron spin resonance transition in a multilevel system with unequal level spacings has recently been demonstrated.[1,2] Using this phenomenon, it appears feasible to construct a "staircase" maser which will radiate at approximately twice the pump frequency. Consider the three-level system of Fig. 1. If the 1—2 transition is

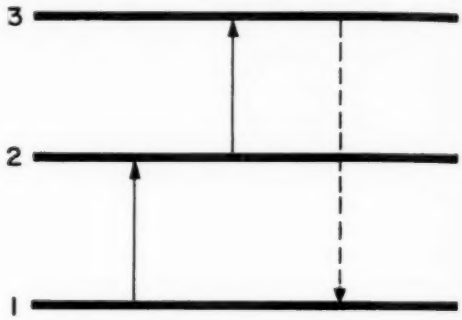


FIG. 1. In the staircase maser scheme, the 1⟷2 and 2⟷3 transitions are successively inverted by fast passage, followed by double-frequency amplification on the 1⟷3 transition.

inverted by fast passage, followed in a time less than the spin-lattice relaxation time by inversion of the 2—3 transition, a population inversion between levels 3 and 1 will result, permitting amplification on the 1—3 transition at roughly double the pump frequency. Operating points can be found in common maser materials at which the two successive inversions can be performed by the same pump oscillator in a single sweep of the dc magnetic field. Extension of the method to more than two steps up a staircase is conceivable. Cross relaxation between the two nearly equal pump transitions may be the major difficulty in implementing this scheme.[3]

*This work was supported by the U. S. Air Force.
[1]Wagner, Castle, and Chester, Bull. Am. Phys. Soc. Ser. II, 4, 21 (1959).
[2]W. W. Anderson, Electrical Engineering Depart-

ment, Stanford University, California (private communication).

[3]Bloembergen, Shapiro, Pershan, and Artman, Technical Report No. 285, Cruft Laboratory, Harvard University, Cambridge, Massachusetts, October 15, 1958 (unpublished).

## OBSERVATION OF CHARGED-PARTICLE REACTION PRODUCTS

J. M. McKenzie and D. A. Bromley
Atomic Energy of Canada Limited,
Chalk River, Ontario, Canada
(Received January 29, 1959)

Nuclear reactions of the type $(X, \alpha\gamma)$ have received, as yet, little detailed experimental study despite their particular interest in terms of the reaction mechanisms involved. This neglect has resulted largely from the inherent difficulties in resolving the product alpha particles from backgrounds of neutrons, gamma rays, and longer range charged particles. Detectors such as gridded ionization chambers, which provide adequate energy resolution, have pulse rise-time characteristics insufficiently short to permit millimicrosecond particle-gamma and particle-particle coincidence studies.

The use of Au-Ge junctions for the detection of alpha particles[1] and fission fragments[2] has been reported. It is the purpose of this Letter to summarize the results of a number of new measurements on the physical characteristics of the junctions. These measurements serve to demonstrate the great potential usefulness of junction detectors in heavy-particle nuclear spectroscopy.

The measurements have been carried out on junctions made according to the technique developed by Pantchechnikoff.[3] By comparison of the voltage pulses produced by $Pu^{240}$ alpha particles absorbed in the junction with those from a calibrated signal generator injected through a known small capacitor, a value of $2.84 \pm 0.12$ ev per electron hole pair was found for germanium. This is in accord with the previously reported value[4] $2.94 \pm 0.15$ ev. By measuring the junction capacitance a junction thickness is obtained; this thickness varies with method and conditions of manufacture, and increases with applied voltage.

For protons, $He^3$ ions, and $He^4$ ions (from a Van de Graaff generator) the output pulse is proportional to the incident energy provided that the particle range is less than the junction thickness. Figure 1(a) shows results obtained with a liquid nitrogen cooled $2 \times 2$ mm junction of thickness appropriate to the energies available. The proton curve shows clearly a loss of pulse height for longer range particles.

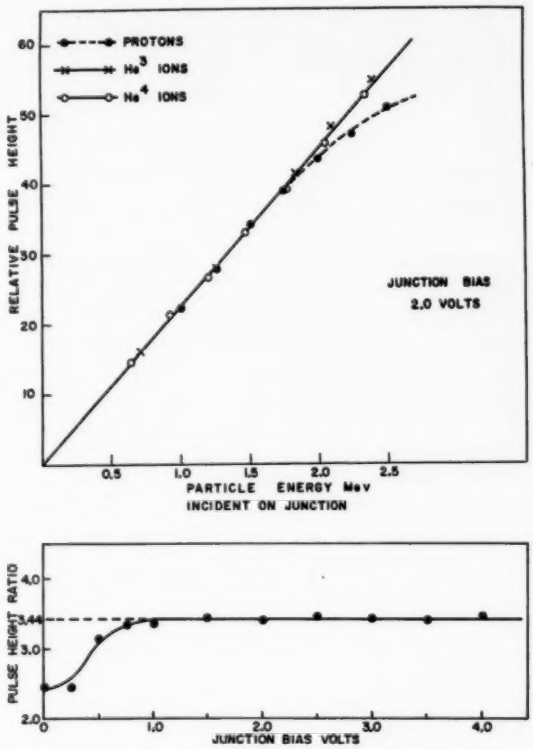


FIG. 1. (a) The junction response to protons, $He^3$ ions, and $He^4$ ions as a function of the energy of the incident particle. At the higher energies the proton range exceeds the effective junction thickness. (b) Pulse-height ratio, for 5.16-Mev alpha particles and 1.5-Mev protons, as a function of junction bias voltage. The energy ratio is 3.44.

The curve Fig. 1(b) is the pulse-height ratio (of 5.16-Mev alpha particles to 1.5-Mev protons) as a function of junction bias. As these particles have a range less than the junction thickness, the curve shows that the response is independent of particle specific ionization (i.e., pulse-height ratio is equal to the energy ratio) provided the junction bias is sufficient to prevent recombination. The decrease in the pulse-height ratio at low applied voltage is consistent with the greater electron-hole recombination in the denser alpha-

particle ionization column.

At a given energy input the output pulse is independent of the junction temperature if, as the temperature is increased, the applied voltage is maintained constant, by increasing the quiescent series current, to avoid changing the junction capacitance. The noise, however, becomes serious at higher temperatures.

For a 2×2 mm junction at liquid nitrogen temperature Fig. 2 shows a charged particle spectrum, at 90° to the incident beam, from the reactions induced by 2.0-Mev $He^3$ ions on isotopically pure $Li^7$. This reaction was selected because it provided proton, deuteron, and alpha groups with energies ranging up to 11.3 Mev, 10.4 Mev, and 8.6 Mev, respectively, together with proton and effective deuteron continua extending downward in energy from ~8.4 Mev and ~7.5 Mev. A 2.73-mg/cm² Al foil was placed between the target and detector to absorb the elastically scattered $He^3$ ions. As expected the detector behaves as a thin ionization chamber; the groups labelled *A*, *B*, and *C* correspond to alpha particles which are stopped in the junction.

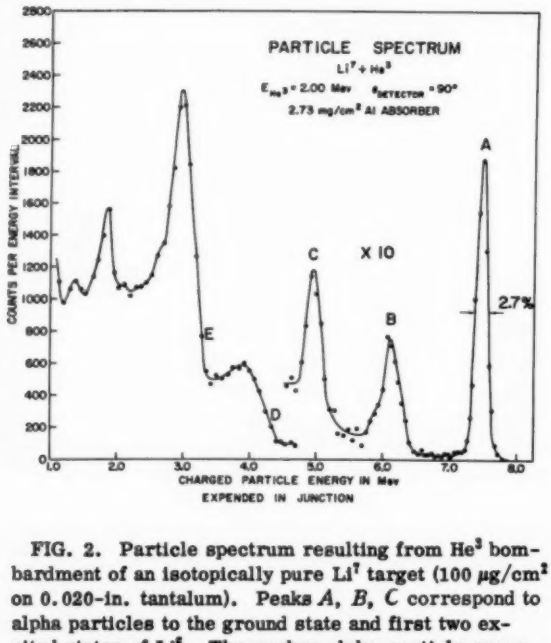


FIG. 2. Particle spectrum resulting from $He^3$ bombardment of an isotopically pure $Li^7$ target (100 μg/cm² on 0.020-in. tantalum). Peaks *A*, *B*, *C* correspond to alpha particles to the ground state and first two excited states of $Li^6$. The weaker alpha-particle group corresponding to the low-energy shoulder on peak *B* results from the prolific $F^{19}(p,\alpha)O^{16}$ reaction with the $HHH^+$ beam contaminant on the $F^{19}$ target contamination. As discussed in detail in the text, the pulse-height steps at *D* and *E* correspond to deuterons and protons, respectively.

The steps at *D* and *E* correspond respectively to the maximum pulse heights obtainable from continua of incident deuterons and protons. This follows from the observations that with increasing absorber interposed between the target and detector, the steps individually remain fixed in pulse height, but decrease in intensity, until the absorber thickness is sufficient to reduce the particle energies below those corresponding to a range equal to the junction thickness. Beyond this point the pulse height decreases. The steps for this junction correspond to proton energies of 3.3 ± 0.1 Mev and deuteron energies of 4.4 ± 0.1 Mev giving an effective junction thickness of $(6 \pm 0.3) \times 10^{-3}$ cm in fair agreement with that obtained with the capacitance measurement. The indicated energy resolution for the highest energy alpha group is 2.7%. Using a $Pu^{240}$ source, energy resolutions of 2% have been obtained. For these particles the energy resolution is not determined by the signal to noise ratio.

Simultaneous examination of natural alpha particles and elastically scattered proton beams has demonstrated that, for counting rates up to $5 \times 10^4$ counts/sec, the gain shift with counting rate is less than ½%. By using a delay cable to reflect the leading edge the pulse rise time was found to be less than $3 \times 10^{-9}$ sec. An approximate calculation, assuming a junction thickness of $6 \times 10^{-3}$ cm and the published hole mobilities[5] in Ge at liquid nitrogen temperature, suggests a pulse rise time of $5 \times 10^{-10}$ sec.

Although the measurements reported herein have been carried out with 2×2 mm junctions, a 10×10 mm unit has been tested but had decreased resolution due to increased noise. Further work is directed toward the problems of producing junctions of controlled thickness and to the examination of the characteristics of both Ge and Si crystals[6,7] with other junction components.

Among the advantages which these detectors have for nuclear charged particle spectroscopy are the following: (a) fast pulse rise for coincidence applications; (b) the minimizing of vacuum problems both because of the low voltages involved and the elimination of the windows required in gas counters; (c) small geometric size for minimal scattering of associated radiation; (d) convenience in assembly of complex detection systems, for example, in the focal plane of high-resolution magnetic spectrographs; (e) stability both in time and under high counting rates; (f) insensitivity to both gamma radiation and neutrons; however, the addition of a $B^{10}$ foil over

the junction has permitted the detection of neutrons by the $B^{10}(n,\alpha)Li^7$ reaction.

We are indebted to Mr. R. J. Toone for his assistance in the measurements reported.

[1]J. Mayer and B. Gossick, Rev. Sci. Instr. 27, 407 (1956).

[2]Dabbs, Walter, and Roberts, Oak Ridge National Laboratory Report ORNL-2501, 1958 (unpublished), p. 73.

[3]J. I. Pantchechnikoff, Rev. Sci. Instr. 23, 135 (1952).

[4]K. G. McKay and K. B. McAfee, Phys. Rev. 91, 1079 (1953).

[5]E. M. Conwell, Proc. I.R.E. 46, 1281 (1958).

[6]A. V. Airapetiants and S. M. Ryvkin, Zhur. tekh. Fiz. 27, 95 (1957) [translation: Soviet Phys. Tech. Phys. 2, 79 (1957)].

[7]R. V. Babcock et al., Westinghouse Electric Corporation, Scientific Paper No. 5806-6600-13, 1958 (unpublished).

## NUCLEAR MAGNETIC MOMENT AND SPIN OF EUROPIUM-152$m$*

V. W. Cohen and J. Schwartz
Brookhaven National Laboratory,
Upton, New York

and

R. Novick
Department of Physics,
University of Illinois,
Urbana, Illinois†

(Received March 13, 1959)

Goldhaber, Grodzins, and Sunyar[1] have made a determination of the helicity of the neutrino by studying the decay of the 9.3-hour isomeric state of $Eu^{152}$. Their conclusions rest, in part, upon a knowledge of the spin and parity of this state. At the time their experiment was performed, the possible assignments for this state were considered to be $0^-$, $1^-$, and $1^+$. Higher spin values were ruled out by the fact that the partial lifetime for the decay of the isomeric state to the spin 3 ground state of $Eu^{152}$ was found to be greater than 5000 hours. From a study of the $\beta$-$\gamma$ correlation in the decay of $Eu^{152m}$ to $Gd^{152}$, Grodzins and Sunyar[2] have been able to rule out definitely the $1^+$ assignment.

We have performed an atomic beam flop-in experiment with radioactive detection on $Eu^{152m}$ in order to distinguish between the 0 and 1 assignments. A $Eu^{152m}$ beam was formed by evaporating neutron-irradiated Eu metal from a tantalum oven at about 650°C. Detection was effected with sulfur-coated metal buttons. A $Eu^{152m}$ resonance obtained at a field value of 1.4 gauss is shown in Fig. 1. Resonance curves have also been obtained at 0.8 and 1.0 gauss. The resonance frequency has been found to vary linearly with the field and to correspond to a Landé $g$ factor of nearly 2.0. Woodgate[3] has found that $g_J = 1.994$ for europium. These observations show either that the spin of $Eu^{152m}$ is zero or that if the spin were different from zero, the hfs splitting of the atomic ground state must be very small compared with 4 Mc/sec. If the spin were 1 or 2 and if the splitting were large, the apparatus would detect the transition $\Delta F = 0$, $m_F(-F \leftrightarrow -F+1)$ and a resonance would have occurred at the points marked 1 or 2 in Fig. 1. If the spin were different from zero and

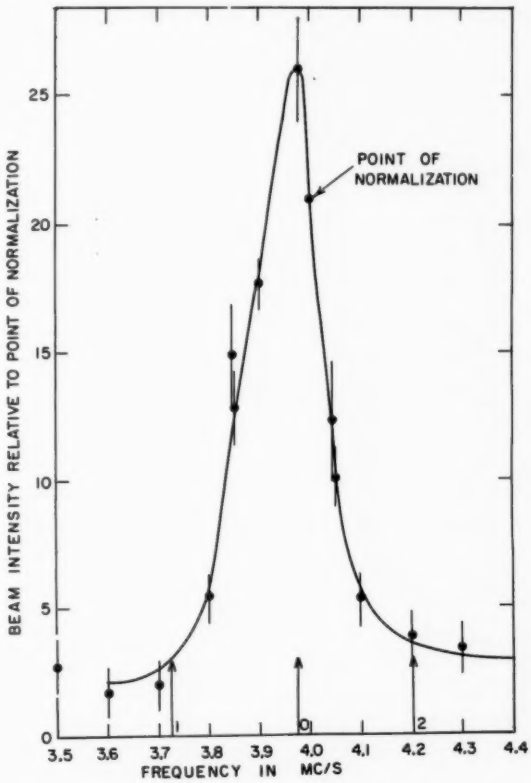


FIG. 1. Resonance curve obtained for $Eu^{152m}$ at a field of 1.4 gauss. A counter background of about 9 cpm has been subtracted from all of the observations and the data have been corrected for decay. The beam intensity showed a steady decrease with time. Every fifth observation was taken at 4.0 Mc/sec and this information was used to normalize the points on the remainder of the curve.

if the hfs splitting were comparable to 4 Mc/sec (intermediate field case), the resonance frequency might accidentally occur at the spin-zero value at one field but it would not vary linearly with the field. If the spin were 1 and if the hfs splitting were very small (Back-Goudsmit region), the apparatus would indicate the transition $m_j(+1/2 \rightarrow -1/2)$, $\Delta m_i = 0$, and we would observe three resonances centered about the spin-zero frequency with a spacing equal to the hfs interaction energy $a$ of the $Eu^{152m}$ atom.[4] If there were such a multiplicity of lines unresolved by our apparatus, we could obtain an upper limit for $a$ by a consideration of the line width. Aside from possible unresolved hyperfine structure, the line width is determined by the inhomogeneities in the transition magnetic field and time spent in the oscillating field. The latter effect is calculated to be roughly 30 kc/sec for Eu and 50 kc/sec for a potassium beam used in calibrating the magnetic field. The effect of field inhomogeneities is expected to be four times greater for Eu than for K since the $g$ factors are in the ratio of four to one. A study was made of the shape of the K resonance and it was found that the width of this resonance could be varied over a range of 60 to 120 kc/sec by changes in the magnetic history of the transition magnet. This shows that, at least in the case of K, the line shape is determined by field inhomogeneities. Before the data shown in Fig. 1 were obtained, the transition magnet was carefully manipulated to obtain the narrowest possible $K^{39}$ resonance (60 kc/sec). If this 60-kc/sec width were due entirely to field inhomogeneity, then we would expect a 240-kc/sec width for the $Eu^{152m}$ resonance. In fact, the 60-kc/sec width for K results from a combination of natural broadening and inhomogeneity broadening. Lacking detailed knowledge of the distribution of both the steady and oscillating magnetic fields in the transition region, we cannot make an exact estimate of the width to be expected for the $Eu^{152m}$ resonance. The observed 170-kc/sec width is less than the extreme value estimated above and is entirely consistent with the assumption that there is no unresolved hyperfine structure. We can obtain an absolute upper bound on $a$ by assuming that the observed 170-kc/sec width results entirely from the blending of three lines, each of which has a width of 30 kc/sec (the natural width for Eu in our apparatus). In this way we find that $a \leq 60$ kc/sec. By comparing this limit of $a$ with the value, $a = -20.0$ Mc/sec, obtained by Woodgate[3] for $Eu^{151}$, for which $I = 5/2$ and $\mu = 3.4$ nm,[4] we can evaluate $\mu(Eu^{152m}) \leq 4.0 \times 10^{-3}$ nm. It should be emphasized that this is an absolute upper bound and that there is nothing in our data that requires us to assume that the value is different from zero.

The nuclear moments of deformed odd-odd nuclei have recently been discussed by Gallagher and Moszkowski[5] and by Hooke[6] in the context of the Nilsson model.[7] In Table I we list the moments predicted for a possible $1^-$ state of $Eu^{152m}$ on the basis of this model, for several different proton and neutron assignments and for three different values of the nuclear deformation parameter ($\delta$). The range of deformation considered lies between the values appropriate to $Eu^{151}$ and $Eu^{153}$. A comparison of these values with our limit shows that, if the Nilsson model

Table I. Nuclear magnetic moments predicted for a possible $1^-$ state of $Eu^{152m}$ on the basis of the Nilsson model for several proton and neutron assignments and for three values of the nuclear deformation parameter ($\delta$). The assignments are listed in order of decreasing likelihood for each value of $\delta$.

| $\delta = +0.15$ | | $\delta = +0.20$ | | $\delta = +0.25$ | |
|---|---|---|---|---|---|
| Assignment | $\mu$ (nm) | Assignment | $\mu$ (nm) | Assignment | $\mu$ (nm) |
| *e* | +1.5 | *e* | +1.4 | *a* | +2.6 |
| *c* | +1.0 | *h* | +0.6 | *c* | +1.2 |
| *b* | -1.1 | *a* | +2.5 | *h* | +0.4 |
| *f* | -0.5 | *c* | +1.1 | *g* | +2.1 |
| *d* | -1.5 | *g* | +1.9 | *b* | -0.9 |
| *a* | +2.4 | *b* | -1.0 | | |

| Assignment | Proton state[a] | Neutron state[a] |
|---|---|---|
| *a* | 5/2-(532+) | 3/2+(651+) |
| *b* | 3/2+(411+) | 5/2-(523-) |
| *c* | 5/2+(413-) | 3/2-(521+) |
| *d* | 3/2-(541+) | 5/2+(642+) |
| *e* | 3/2-(541+) | 1/2+(660+) |
| *f* | 1/2-(550+) | 3/2+(651+) |
| *g* | 3/2+(411+) | 1/2-(530+) |
| *h* | 5/2+(413-) | 3/2-(532-) |

[a]The nucleon states are characterized by $\Omega$ (the component of angular momentum along the nuclear axis), parity, and the asymptotic quantum numbers ($N$, $n_z$, $\Lambda$, $\Sigma$).

is valid, our result provides strong support for the supposition that the spin of $Eu^{152m}$ is zero. The possibility that the spin is different from zero and that states exhibiting positive and negative moments are mixed so that the moment accidentally vanishes can, of course, never be completely ruled out.[8] In this connection it is important to note that the simple Nilsson model without mixing correctly predicts the spin, parity, and moments of the ground states of $Eu^{151}$, $Eu^{152}$, and $Eu^{153}$, and furthermore that a $0^-$ isomeric state of $Eu^{152}$ can be formed with plausible proton and neutron assignments. Lastly, it is noteworthy that there is only one measured moment smaller than our limit, namely $Tl^{198}$, for which $\mu < 0.002$ nm.[9]

The authors would like to acknowledge their appreciation to Dr. M. Goldhaber for many helpful discussions, and to A. W. Kane and J. Ciperano for their painstaking technical assistance throughout the course of this work. One of the authors (RN) would like to acknowledge the hospitality extended to him while he was a guest of the Brookhaven National Laboratory. He would also like to thank Dr. J. D. Jackson and Dr. H. Lipkin for many helpful discussions of the Nilsson model. Finally, we would also like to thank R. L. Cohen for his very enthusiastic assistance in the early stages of this experiment.

*Work performed at the Brookhaven National Laboratory under the auspices of the U. S. Atomic Energy Commission.

†One of the authors (RN) participated in this experiment as a guest of the Brookhaven National Laboratory.

[1]Goldhaber, Grodzins, and Sunyar, Phys. Rev. 109, 1015 (1958).

[2]L. Grodzins and A. W. Sunyar, following Letter [Phys. Rev. Lett. 2, 307 (1959)].

[3]G. K. Woodgate (private communication in advance of publication).

[4]T. Schmidt, Z. Physik 108, 408 (1938).

[5]C. J. Gallagher, Jr., and S. A. Moszkowski, Phys. Rev. 111, 1282 (1958).

[6]W. M. Hooke, Bull. Am. Phys. Soc. Ser. II, 3, 186 (1958).

[7]B. R. Mottelson and S. G. Nilsson, Kgl. Danske Videnskab. Selskab, Mat.-fys. Medd. (to be published), and Phys. Rev. 99, 1615 (1955).

[8]Such mixing may account for the fact that the observed moment in $Au^{192}$ is 0.008 nm whereas the value predicted from the Nilsson model is about 0.5 nm.

[9]Lindgren, Johansson, and Axensten, Phys. Rev. Lett. 1, 473 (1958).

## EVIDENCE CONCERNING THE SPIN AND PARITY OF $Eu^{152m}$†

L. Grodzins* and A. W. Sunyar
Brookhaven National Laboratory,
Upton, New York
(Received March 13, 1959)

The importance of measuring the spin and parity of $Eu^{152m}$ has greatly increased with the recent experiment by Goldhaber et al.,[1] which measured the helicity of the neutrinos emitted by this isotope when decaying by $K$-capture to a $1^-$ level in $Sm^{152}$. Arguments were presented in that paper for assuming the spin-parity to be $0^-$, in which case the neutrino has negative helicity. The conclusion is the same, though the argument becomes more complicated, if the spin-parity is $1^-$; no conclusion can be drawn from the data if the spin-parity has the unlikely value $1^+$. Because of the importance of the neutrino helicity experiment (which has been confirmed by various nuclear recoil experiments[2]) an effort has been made to find more convincing evidence for the parity and, if possible, the spin of $Eu^{152m}$ than the circumstancial evidence presented by Goldhaber et al.[1]

Various groups have pursued four distinct lines of research. (1) A more intensive search was made for the isomeric transition to the $3^-$, 13-year $Eu^{152}$ ground state[3] (see Fig. 1 for pertinent

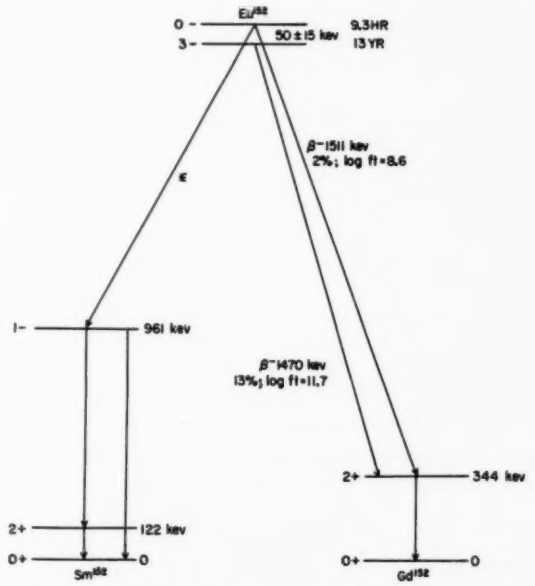


FIG. 1. Partial decay scheme for $Eu^{152m}$ and $Eu^{152}$.

parts of the decay scheme) by Alburger et al.,[4] and by Grodzins and Sunyar.[5] A lower limit of 50 years was placed by both groups on the partial isomeric mean life, representing a retardation in terms of single-proton transitions in excess of $10^{13}$ for $E2$ radiation, thus favoring an $M3$ assignment, which would imply a $0^-$ assignment to $Eu^{152m}$. (2) The shapes of the negatron and positron transitions to the $2^+$ first excited states of $Gd^{152}$ and $Sm^{152}$, respectively, were examined.[4] Though the data obtained were not accurate enough to draw unambiguous conclusions, Alburger at al.[4] find that the assumption of an alpha shape for the positron group to the first excited state of $Sm^{152}$ (expected if the spin of $Eu^{152m}$ is $0^-$) leads to better agreement with the energy expected for the inner positron groups. (3) Cohen et al.[6] have measured the magnetic moment of $Eu^{152m}$. They find that it is smaller than $4\times10^{-3}$ nuclear magneton, thus establishing the strongest evidence for 0 spin. (4) We have investigated the $Eu^{152m}(1.511\text{-kev }\beta^-)\,2^+(344\text{-kev }\gamma)\,0^+$ beta-gamma correlation which should yield a strong, "uniquely" determined, correlation if the spin-parity of $Eu^{152m}$ is $0^-$. We find a strong correlation, thus fixing the parity of $Eu^{152m}$ as odd, and thus corroborating the earlier argument[1] based on the allowed $ft$ value of the $K$-capture transition to the $1^-$ level in $Sm^{152}$. The log$ft$ value[7] of the 1.511-Mev transition is 8.6, which is consistent with first forbidden "unique" systematics. The magnitude of the correlation we observe is compatible with a spin-parity of $0^-$ for $Eu^{152m}$ but does not exclude the possibility of a $1^-$ assignment.

The beta-gamma correlation apparatus was conventional. The fast-slow coincidence circuit had a resolving time $\tau \simeq 10^{-8}$sec. Beta detectors of various diameters and of thicknesses equal to or greater than one cm, both plastic and anthracene, were used. The gamma detector was either an $1\frac{1}{2}$ in.$\times$1 in. or 3 in.$\times$3 in. NaI(Tl) scintillator. Transparent sources, containing approximately 3 micrograms of solid, were prepared by evaporating a drop of $EuCl_3$ solution on scotch tape. The sources were approximately 3 mm in diameter and between 20 and 70 microcuries in strength; the counting rate in the beta crystals was never greater than $10^4$ per second.

The first experiments were done in air using an $1\frac{1}{2}$ in.$\times$1 in. NaI(Tl) gamma detector, 3 in. from the source, and a small anthracene scintillator, 0.5$\times$0.5$\times$1 cm in thickness, whose front face was approximately 0.5 inch from the source. With this geometry the multiple scattering in the air path, as well as the scattering between crystals, was small. A strong correlation, $W(\theta)=1+[0.28\pm0.03]P_2(\cos\theta)$ (background coincidences have been subtracted), was observed between 344-kev gamma rays and beta rays of 1.1 to 1.5 Mev. Unfortunately it was very difficult with this geometry to measure or even estimate the effects of scattering, or to determine the geometry corrections. To circumvent this difficulty we compared the observed correlation with that obtained for the $Pr^{144}(\beta^-)\,2^+(\gamma)\,0^+$ $\beta$-$\gamma$ correlation. The $Pr^{144}$ source was placed in the same geometry as the $Eu^{152m}$. The $Pr^{144}$ decay scheme and beta-gamma correlation have been investigated in some detail by Graham et al.[8] They present strong evidence for the transition being $0^-(2293\text{-kev }\beta^-)\,2^+(691\text{-kev }\gamma)\,0^+$, though their beta-gamma correlation is considerably lower than the theory predicts. If we use the anisotropy observed using $Pr^{144}$ as a standard, we find that the beta-gamma correlation of $Eu^{152m}$, for beta energies $>1.1$ Mev, is $W(\theta)=1+(0.50\pm0.06)P_2(\cos\theta)$. The theoretically predicted value for our experimental $\beta$-ray energy range is $W(\theta)=1+0.472P_2(\cos\theta)$ for the spin sequence $0^-(\beta^-)\,2^+(\gamma)\,0^+$.

Anisotropies were then measured using beta detectors of larger diameter placed farther from the source in order to facilitate the calculation of the geometry correction. With this geometry a strong $\cos\theta$ term manifested itself, even at beta energies $>1$ Mev, arising from scattering of the beta rays from the face of the gamma counter into the beta detector. To obviate this difficulty the source and beta detector were placed inside a cylindrical brass vacuum chamber, 6 in. in diam, 1/8-in. wall, lined with Lucite; the 3 in. $\times$3 in. gamma detector was outside of the vacuum chamber, $5\frac{1}{4}$ in. from the source. In this geometry, no electron scattering could take place which depended on the position of the gamma counter. A 1-in. diam, 1 cm thick, Pilot $B$ crystal, 2 in. from the source, was used as the beta detector. The uncorrected correlation was measured to be $W(\theta)=1+[0.286\pm0.02]P_2(\cos\theta)$. Corrections were made for accidental and gamma-gamma coincidences, as well as for coincidences arising with Compton gamma rays under the 344-kev photopeak. The correlation was attenuated to 88% by the finite detector sizes. The corrected correlation was then found to be $W(\theta)=1+[0.36\pm0.03]P_2(\cos\theta)$. This correlation is about 25% smaller than the predicted correlation

for a first forbidden "unique" $\beta^-$ transition. Several effects can contribute to reduce the predicted anisotropy. The source was perhaps somewhat lumpy and there may have been some attenuation due to backscattering and multiple-scattering in the source. The mean life of the 344-kev state is $\sim 10^{-10}$ sec.[9] This comparatively long lifetime could account for a considerable attenuation as a result of nuclear precession. The observed correlation, by itself, can be fitted by a spin-one assignment. In fact, assuming spin-parity $1^-$, a range of ratios of nuclear matrix elements can yield the observed anisotropy. In the approximation[10] $V = \alpha Z/2\rho \gg W_0$, the correlation can be expressed as a function of

$$Y = \frac{i\,V\,C_V\,\mathfrak{M}(\vec{r}) - C_V\,\mathfrak{M}(\vec{\alpha}) + VC_A\,\mathfrak{M}(\vec{\sigma}\times\vec{r})}{i\,C_A\,\mathfrak{M}(B_{ij})}$$

A range of $Y$ from $+0.3$ to $+2.0$ yields agreement with experiment. (It is in general true that an angular correlation, or a shape measurement, cannot by itself decide between a first forbidden and first forbidden "unique" transition.)

All of the experiments[1,4,6] are compatible with a spin-parity of $0^-$ for $Eu^{152m}$. The work of Cohen et al.[6] is the strongest evidence for spin 0. The beta-gamma correlation presented in this Letter proves that the parity of $Eu^{152m}$ is odd, and is compatible with spin zero for $Eu^{152m}$.

The authors would like to thank M. Goldhaber and J. Weneser for stimulating discussions.

---

†Work performed under the auspices of the U. S. Atomic Energy Commission.

‡Now at Department of Physics, Massachusetts Institute of Technology, Cambridge, Massachusetts.

[1]Goldhaber, Grodzins, and Sunyar, Phys. Rev. 109, 1015 (1958).

[2]M. Goldhaber, 1958 Annual International Conference on High-Energy Physics at CERN, edited by B. Ferretti (CERN, Geneva, 1958). See also I. Marklund and L. Page, Nuclear Phys. 9, 88 (1958).

[3]The spin of $Eu^{152}$ has been measured as 3 [Abraham, Kedzie, and Jeffries, Phys. Rev. 108, 58 (1957)]. The $Eu^{152}$ (1470 kev) $2^+$ (344 kev) $0^+$ $\beta$-$\gamma$ correlation has been measured [L. Grodzins (to be published)] to be $W(\theta) = 1-(0.45 \pm 0.05)\cos^2\theta$, thus establishing the odd parity.

[4]Alburger, Ofer, and Goldhaber, Phys. Rev. 112, 1998 (1958).

[5]L. Grodzins and A. W. Sunyar (unpublished).

[6]Cohen, Schwartz, and Novick, preceding Letter [Phys. Rev. Lett. 2, 305 (1959)].

[7]L. Grodzins and H. Kendall, Bull. Am. Phys. Soc. Ser. II, 1, 163 (1956).

[8]Graham, Geiger, and Eastwood, Can. J. Phys. 36, 1084 (1958).

[9]A. W. Sunyar (unpublished).

[10]M. Morita and R. S. Morita, Phys. Rev. 109, 2048 (1958).

---

## INELASTIC DEUTERON SCATTERING FROM $Cu^{63}$ AND $Cu^{65}$†

J. L. Yntema and B. Zeidman
Argonne National Laboratory,
Lemont, Illinois
(Received February 24, 1959)

A gross structure has been observed in the spectra obtained from inelastic scattering of protons,[1] deuterons,[2] and alpha particles[3,4] by nuclei. Similarly, gross structure has been observed in a number of $(d,p)$ spectra.[5] A number of possible interpretations have been suggested for the appearance of gross structure in inelastic scattering.[6] In the investigation of the elastic scattering of deuterons by separated isotopes of nickel and copper,[7,8] it was found that the spectra of $Cu^{63}$ and $Cu^{65}$ show a group in the neighborhood of 1.3 Mev. The spectra of the two copper isotopes together with the spectrum obtained for $Ni^{58}$, are shown in Fig. 1. The resolution is such that the levels in the copper isotopes could not be well resolved. However, it is clear both from the location and the width of the peak that the peak is due to more than one of the five levels around 1.3 Mev in these isotopes. The angular distribution of the inelastically scattered deuterons of the $2^+$ level at 1.45 Mev in $Ni^{58}$ can be uniquely fitted by $F(\theta)\times[j_2(QR)]^2$, where $F = 1/(Q^2+\alpha^2)^2$, $Q$ is the momentum transfer, and $\alpha$ is a constant. The angular distributions of the inelastic groups in the copper isotopes are shown in Fig. 2 together with the distribution obtained for $Ni^{58}$ (solid line). The three sets of data were

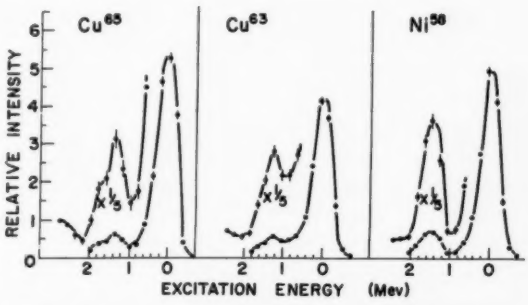


FIG. 1. Deuteron spectra of $Ni^{58}$, $Cu^{63}$, and $Cu^{65}$ at 44° (lab system).

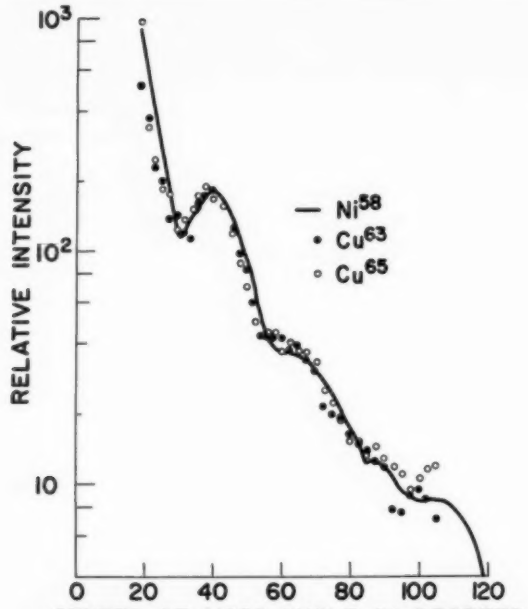


FIG. 2. Angular distribution of the cross section of the 1.45-Mev level in $Ni^{58}$ (solid line) and the groups near 1.3 Mev in $Cu^{63}$ and $Cu^{65}$.

normalized to each other at 40°. The experimental result strongly suggests that the angular distributions from the groups of levels near 1.3 Mev in $Cu^{63}$ and $Cu^{65}$ are due to the same process as that from the $2^+$ level in $Ni^{58}$.

In particular, the experimental result is not inconsistent with the considerations of Lawson and Uretsky.[9] According to their view, the single state at 1.4 Mev in $Ni^{58}$ is due to pair rearrangement in the neutron configuration $(f_{5/2})^2$ and four of the closely-spaced states in each of the Cu isotopes are due to the coupling of the $p_{3/2}$ proton to such an excited neutron state. However, it should be observed that the peaks of the inelastic groups are not at the measured energies of the $2^+$ levels in $Ni^{62}$ and $Ni^{64}$. The measured position of the $2^+$ level in $Ni^{62}$ is 1.17 Mev while the position of the peak for $Cu^{63}$ is closer to 1.3 Mev. Similarly the position of the peak in the $Cu^{65}$ group is somewhat higher than the measured $2^+$ level at 1.34 Mev in $Ni^{64}$. In view of the excellent agreement of our energy calibration with the 1.45-Mev level in $Ni^{58}$, the discrepancy, though slight, appears to be significant. Actually, there are five levels in the excited group in each of the Cu isotopes, and it is reasonable to assume that one of them is due to single-particle excitation of the $p_{3/2}$ protons to the $f_{5/2}$ state. In this case the gross structure can be definitely explained in terms of a $0-2$ excitation by pair rearrangement. It seems very striking that the scattering process is so insensitive to the presence of the extra proton and to the number of neutron pairs apparently involved in the configurations $(f_{5/2})^2$, $(p_{3/2})^4(f_{5/2})^2$, and $(p_{3/2})^4(f_{5/2})^4$.

It does seem plausible that a careful measurement of the angular dependence of the gross structure will result in the unambiguous assignment of an $l$ value in the inelastic scattering process, at least in a number of cases. It also appears likely that in many cases pair-rearrangement excitation will provide a satisfactory explanation of the effect.

We wish to acknowledge helpful discussions with Dr. D. R. Inglis, Dr. D. Kurath, and Dr. J. B. Raz and the cooperation of W. Ramler and the cyclotron group.

---

†Work performed under the auspices of the U. S. Atomic Energy Commission.

[1]B. L. Cohen, Phys. Rev. 105, 1549 (1957); B. L. Cohen and A. G. Rubin, Phys. Rev. 111, 1568 (1958).

[2]J. L. Yntema and B. Zeidman, Phys. Rev. (to be published).

[3]D. R. Sweetman and N. S. Wall (unpublished).

[4]J. L. Yntema and B. Zeidman (unpublished).

[5]Schiffer, Lee, Yntema, and Zeidman, Phys. Rev. 110, 1216 (1958).

[6]A. Tomasini, Nuovo cimento 6, 927 (1957); A. M. Lane and E. P. Pendlebury (private communication to J. P. Schiffer); T. Tamura and D. C. Choudhury, Phys. Rev. (to be published).

[7]J. L. Yntema, Phys. Rev. (to be published).

[8]The targets were obtained from the Atomic Energy Research Establishment, Harwell, England.

[9]R. D. Lawson and J. L. Uretsky, Phys. Rev. 108, 1300 (1957).

---

## *p-p* TRIPLE SCATTERING AT 143 Mev*

C. F. Hwang,† T. R. Ophel, E. H. Thorndike,‡ Richard Wilson, and N. F. Ramsey
Cyclotron Laboratory, Harvard University, Cambridge, Massachusetts
(Received March 11, 1959)

The depolarization parameter $D$ as defined by Wolfenstein[1] for proton-proton scattering at an energy near 150 Mev was first measured by

Taylor and Wood.[2] Another measurement of this parameter has been made at the Harvard Cyclotron Laboratory using a polarized proton beam of $P_1 = 0.67$, $E_{\text{mean}} = 147$ Mev, and an energy spread of ±2 Mev.

Our apparatus and experimental procedure followed essentially that of Chamberlain et al.[3] The beam was scattered off liquid hydrogen at an angle $\theta_2$ and analyzed by carbon scattering at an angle $\theta_3$. $D$ was measured at 5° intervals from 20° to 40° lab. The angular resolution of the second scattering ($\theta_2$) is determined by the intersection of the $1\frac{1}{4}$ in. wide beam with the 4-in. diameter hydrogen target, and the 1-in. wide defining counter located 46 in. from the center of the hydrogen target. It varies from ±2.3° at 20° lab to 3.0° at 40° lab.

At each angle we observed a counting rate of about 20 counts/min of triply scattered protons. Random coincidences (1%) and background (2%) were separately determined and corrected for. The analyzing power $P_1P_3$ was measured at the mean third scattering energy corresponding to each $\theta_2$. The measurement of $D$ depends critically upon the alignment of $\theta_3$. We align at each $\theta_3$ by sweeping a profile of the twice scattered beam at small angles of $\theta_3$, checking after the asymmetry measurement.

The directions of the second and third scatterings are represented by further subscripts $N$ and $S$. Thus $\theta_{3S}$ and $\theta_{3N}$ represent scatterings in the same and opposite directions, respectively, as the first scattering inside the cyclotron, and $I(\theta_{2N}, \theta_{3N})$ is the corrected, normalized, counting rate at the angles $(\theta_{2N}, \theta_{3N})$. Then

$$e_{3n}(\theta_2) = \frac{I(\theta_2, \theta_{3S}) - I(\theta_2, \theta_{3N})}{I(\theta_2, \theta_{3S}) + I(\theta_2, \theta_{3N})}, \tag{1}$$

$$D(\theta_2) = \frac{1}{2P_1P_3}[(1 + P_1P_2)e_{3n}(\theta_{2S}) + (1 - P_1P_2)e_{3n}(\theta_{2N})], \tag{2}$$

$$P_2'(\theta_2) = \frac{1}{2P_3}[(1 + P_1P_2)e_{3n}(\theta_{2S}) - (1 - P_1P_2)e_{3n}(\theta_{2N})], \tag{3}$$

$$P_2(\theta_2) = \frac{1}{P_1}\left(\frac{I(S) - I(N)}{I(S) + I(N)}\right),$$

where

$$I(S) = I(\theta_{2S}, \theta_{3S}) + I(\theta_{2S}, \theta_{3N}),$$

$$I(N) = I(\theta_{2N}, \theta_{3S}) + I(\theta_{2N}, \theta_{3N}).$$

Our values of $D$ and those of Taylor and Wood along with the theoretical predictions of Gammel and Thaler[4] and Signell and Marshak,[5] are given in Fig. 1. Our values of $P_2$ and $P_2'$ are compared with the $P_2$ results of Palmieri et al.[6] in Fig. 2. Note that $P_2 = P_2'$ if time reversal is valid for the $p$-$p$ interaction.

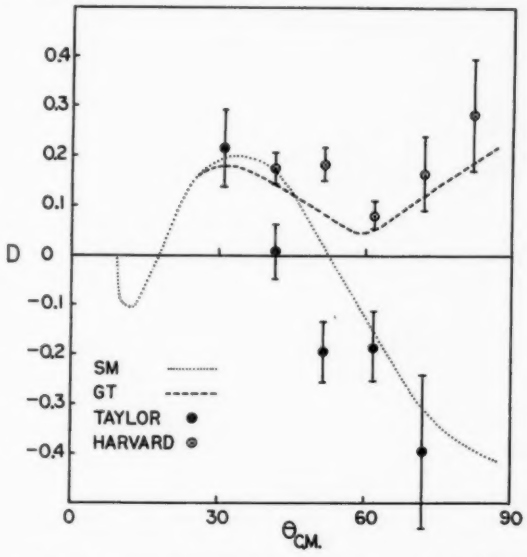


FIG. 1. Experimental measurement and theoretical predictions of the triple scattering parameter $D(\theta)$.

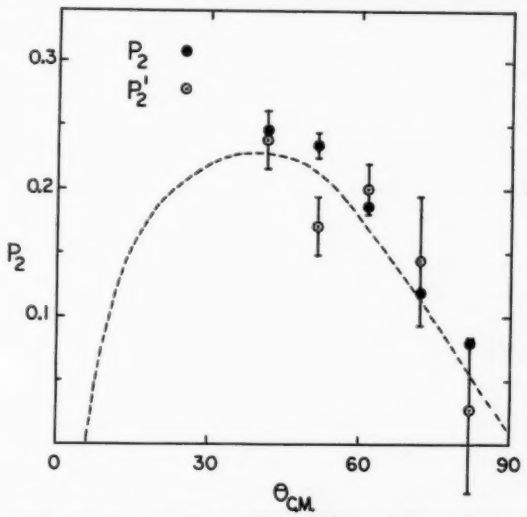


FIG. 2. Comparison of $P_2$ and $P_2'$ with $p$-$p$ polarization data (corrected for a small difference of incident proton energy) of Palmieri et al. (The latter data are represented by the dashed curve.)

$D$ has been measured at 635 Mev by Kumekin, Mescheryakov, Nuruschev, and Stolotov,[7] and at 315 Mev by Chamberlain et al.[3] The angular dependence of their results is similar to ours. Gammel and Thaler[4,8] try to fit data with a static potential plus a term linear in momentum ($\vec{L}\cdot\vec{S}$ term). They always find that the curves for $D$ at various energies are parallel to each other. To reconcile the results of Taylor and Wood with those at higher energies, they would have to include a term of higher order in momentum.

*Supported by the joint program of the Office of Naval Research and the U. S. Atomic Energy Commission.

†Corning Glass Works Foundation Predoctoral Fellow.

‡National Science Foundation Predoctoral Fellow.

[1]L. Wolfenstein, Annual Review of Nuclear Science (Annual Reviews, Inc., Palo Alto, 1956), Vol. 6, p. 65.

[2]1958 Annual International Conference on High-Energy Physics at CERN, edited by B. Ferretti (CERN, Geneva, 1958), p. 56. A. E. Taylor (private communication).

[3]Chamberlain, Segrè, Tripp, Wiegand, and Ypsilantis, Phys. Rev. 105, 288 (1957).

[4]J. L. Gammel and R. M. Thaler, Phys. Rev. 108, 163 (1957).

[5]Signell, Zinn, and Marshak, Phys. Rev. Lett. 1, 416 (1958).

[6]Palmieri, Cormack, Ramsey, and Wilson, Ann. Phys. 5, 299 (1958).

[7]1958 Annual International Conference on High-Energy Physics at CERN, edited by B. Ferretti (CERN, Geneva, 1958), p. 57. V. P. Dzhelepov (private communication).

[8]J. L. Gammel and R. M. Thaler (private communication).

## $K^-$-HYDROGEN CHARGE-EXCHANGE SCATTERING*

Philippe Eberhard,† Arthur H. Rosenfeld, Frank T. Solmitz, Robert D. Tripp, and Mason B. Watson

Lawrence Radiation Laboratory, University of California, Berkeley, California

(Received March 13, 1959)

In the course of a bubble chamber investigation of the interaction of low-energy $K^-$ mesons in hydrogen, we have observed forty-five reactions of the type $K^- + p \rightarrow \overline{K}^0 + n$ followed by the observable decay $K_1 \rightarrow \pi^+ + \pi^-$.[1]

The only other type of event which could be confused with the observed type is the much more frequent sequence $K^- + p \rightarrow \Lambda + \pi^0$, $\Lambda \rightarrow p + \pi^-$. However, in $\Lambda$ decay, the proton usually stops, but if it does not, its greater ionization generally permits identification. In order to certify the identification, all $V$'s in which the positive decay product did not stop in the chamber were measured and fitted to both the $\Lambda$ and $K_1$ interpretations. All events fitted one or the other—there were no ambiguities.

The calculated momentum of the $K^-$ at the point of interaction $P_{K^-}$ depends sensitively on the $\overline{K}^0$-$K^-$ mass excess, which has been measured in this and other experiments to be $3.9 \pm 0.6$ Mev.[2] The threshold for charge exchange is then $89 \pm 5$ Mev/$c$.

For each event, $P_{K^-}$ was adjusted to give a simultaneous best fit to the production kinematics, by the use of the momentum of the $K^-$ (computed from its decay kinematics), the curvature of the $K^-$, and the known momentum distribution of the $K^-$ beam. The cross section below 300 Mev/$c$ was then obtained by constructing an ideogram which gave the fraction of events in each of the four momentum intervals below 300 Mev/$c$ shown in Fig. 1.

Data were also taken with the beam momentum adjusted for $310 \pm 22$ Mev/$c$ and $410 \pm 15$ Mev/$c$. Even at these higher momenta the $K^-$ velocity is low enough that ionization can be used to distinguish $K^-$ from $\mu^-$ and $\pi^-$ contamination in the beam.

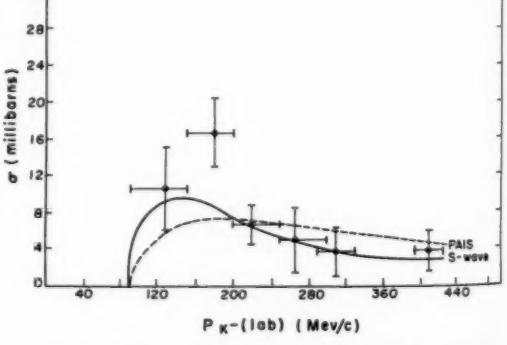


FIG. 1. $K^-$-hydrogen charge-exchange cross section vs $K^-$ laboratory momentum. The solid curve is the prediction of the $S$-wave zero-effective-range theory. The dashed curve (arbitrary ordinate) is the prediction of the Pais theory with $\lambda = -1$.

The fraction of $K^0$ decaying by the $\pi^+ + \pi^-$ mode was taken to be $0.34 \pm 0.02$.[3]

The $K_1^0$ mean life obtained from these events is $(0.87 \pm 0.13) \times 10^{-10}$ sec, in agreement with other experiments.[4]

Figure 1 shows the cross section as a function of $K^-$ laboratory momentum. The solid curve represents the charge-exchange cross section as evaluated from the $S$-wave, zero-effective-range approximation,[5] which fits the data satisfactorily. The dashed curve is the charge-exchange cross section (with arbitrary ordinate) predicted by Pais[6] in his theory embodying opposite parities for charged and neutral $K$'s. There is in this theory a free parameter $\lambda$ which can range from -1 (the prediction of perturbation theory) to +1. We have plotted $\lambda = -1$ as being the theoretically simplest choice (it also fits the data best). It can be seen that our data are inadequate to distinguish between the two curves. Both curves have been modified to take into account the mass differences. For the effective-range theory this was done simply by the introduction of a factor $p_{\text{final}}/v_{\text{initial}}$ into the cross sections. These effects dominate near threshold and tend to obscure the swift $p^2$ rise which would otherwise be characteristic of the Pais theory.

Figure 2 shows the angular distribution as a function of momentum. The $S$-wave effective-range theory predicts, of course, isotropy. The dashed curve is the Pais prediction from $\lambda = -1$, $P_K = 180$ Mev/$c$. Chi-squared tests on the experimental angular distribution show a probability of about 5% associated with either the isotropic or Pais hypotheses.

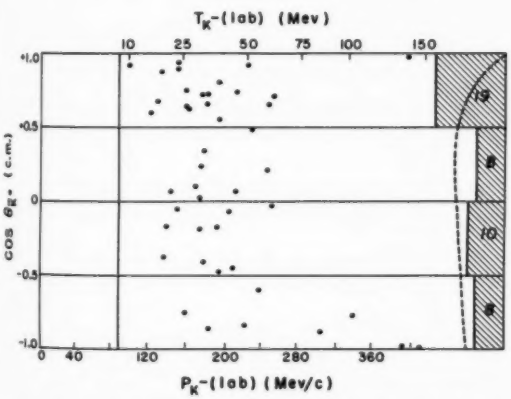


FIG. 2. Angular distribution of $K^-$-hydrogen charge-exchange scattering vs $K^-$ laboratory momentum. Each dot represents an event. A histogram appears at the right. The curve represents the prediction of the Pais theory for $\lambda = -1$ at a momentum of 180 Mev/$c$.

We wish to thank Professor R. Dalitz, Professor A. Pais, and Professor J. D. Jackson for illuminating discussions, and Professor Luis Alvarez and other members of the hydrogen bubble chamber group for their interest and cooperation.

---

*This work was done under the auspices of the U. S. Atomic Energy Commission.

†On leave from the Centre National de la Recherche Scientifique, Paris, France.

[1]Preliminary cross sections for elastic scattering and hyperon production channels are given in the report of the 1958 Annual International Conference on High-Energy Physics at CERN, edited by B. Ferretti (CERN, Geneva, 1958), and in Bull. Am. Phys. Soc. Ser. II, 3, 336 and 363 (1958); 4, 24 (1959); data analysis is continuing. The electrostatically separated beam is described by Horwitz, Murray, Ross, and Tripp, University of California Radiation Laboratory Report UCRL-8629, June 1958 (unpublished).

[2]Rosenfeld, Solmitz, and Tripp, Phys. Rev. Lett. 2, 110 (1959); Crawford, Cresti, Good, Stevenson, and Ticho, Phys. Rev. Lett. 2, 112 (1959).

[3]Crawford, Cresti, Douglass, Good, Kalbfleisch, Stevenson, and Ticho, Phys. Rev. Lett. 2, 266 (1959).

[4]D. Glaser, 1958 Annual International Conference on High-Energy Physics at CERN, edited by B. Ferretti (CERN, Geneva, 1958), p. 272.

[5]Jackson, Ravenhall, and Wyld, Nuovo Cimento 10, 834 (1958). At the 1958 Geneva Conference, Dalitz[1] used this approximation to make an experimental fit, largely based on our very preliminary data. We have still not completed the analysis of all our data, but at present it appears that the cross sections for elastic scattering and charged $\Sigma$ production are larger by about 25% and 15%, respectively, than the values used by Dalitz.

[6]A. Pais, Phys. Rev. 112, 624 (1958).

---

## NUCLEAR INTERACTION OF A PROTON OF ABOUT $10^{15}$ ev PRODUCING AN ELECTRON-PHOTON CASCADE OF $2.4 \times 10^{13}$ ev*

M. W. Teucher, E. Lohrmann, D. M. Haskin, and Marcel Schein
University of Chicago, Chicago, Illinois
(Received March 16, 1959)

In a stack of 22 liters of Ilford $G5$ emulsion flown by a Skyhook balloon for 13 hours above 110 000 feet from Brownwood, Texas, a nuclear interaction initiated by a proton of type $6+16_p$ was found. The angular distribution of the 16

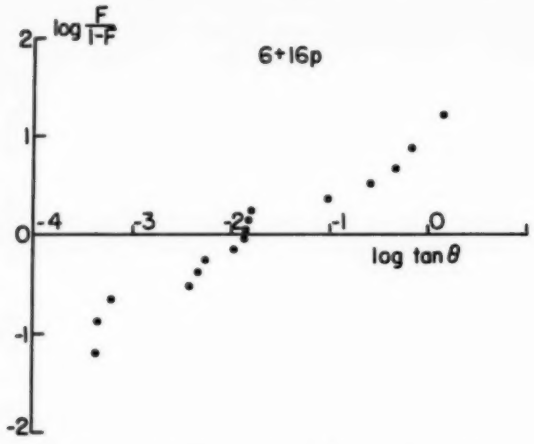


FIG. 1. Angular distribution of shower particles for primary event $6+16p$. $F$ is the fraction of particles in the laboratory system found in a cone of half opening angle $\theta$.

shower particles is shown in Fig. 1. It indicates that the primary energy is probably between $10^{14}$ and $10^{15}$ ev. Between the three innermost tracks of the forward cone, at a distance of about 4 mm from the origin, an unusually energetic electron-photon cascade is initiated which could be followed for 22.6 cm [=7.8 c.u. (cascade units)] in the stack. The longitudinal and the lateral development were investigated by drawing target diagrams of the electrons after 4, 5.6, and 7.1 c.u. The results are shown in Table I. The density $\Pi(r)$ of the electron tracks could be measured down to very small distances from the cascade axis ($\approx 10^{-5}$ radian). No evidence of a double or multiple core structure could be found. It may, therefore, be assumed that this cascade was started by one single high-energy $\pi^0$ decaying into $\gamma$-rays. This conclusion is further supported by the low meson multiplicity in the primary event which makes the probability of finding two high-energy $\pi^0$ mesons within the solid angle of $10^{-5}$ radian fairly small. Only one small secondary nuclear interaction of the shower particles was found. Its influence on the cascade is negligible. The cascade can, therefore, be regarded to be purely electromagnetic in nature. Hence a comparison with electromagnetic theory can be attempted. The longitudinal development was compared with approximation $A$ of Rossi and Greisen.[1] The lowest energy $E$ of the cascade electrons counted in this experiment was determined by multiple-scattering measurements. The extrapolation of the electron density distribution beyond the largest distances $R$ quoted in Table I was carried out and corrected after Pinkau[2] and Eyges and Fernbach.[3] The longitudinal development is in good agreement with approximation $A$ for a primary energy of $2.5\times 10^{13}$ ev for the $\pi^0$ which does not depend critically on the way the energy is shared by the four electrons. In Fig. 2 the integral number of electrons at 7.1 c.u. from the origin is plotted against the distance $r$ from the cascade axis. Using the theoretical computation developed by Nishimura and Kamata[4] and calculations by Pinkau,[5] one obtains an energy of $2.4\times 10^{13}$ ev from Fig. 2 which is in satisfactory agreement with the estimate based on the longitudinal development mentioned previously.

Table I. Development of electron-photon cascade. $t$ = distance from primary event in cascade units. $N$ = number of tracks within distance $R$ in microns from the axis of the cascade. $\gamma$ = quantity defined by Eq. (1).

| $t$ | $N$ | $R$ | $\gamma$ |
|---|---|---|---|
| 4.0 | 1050 | 350 | 1.36±0.1 |
| 5.6 | 3560 | 550 | 1.29±0.1 |
| 7.1 | 6730 | 770 | 1.24±0.1 |

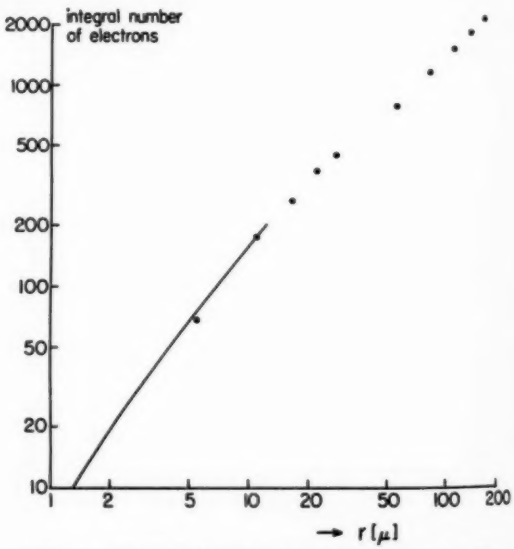


FIG. 2. Lateral distribution of electrons at a distance of 7.1 c.u. from the primary event. $r$ = distance from cascade axis. ● = experimental results. Solid curve = distribution function calculated by Pinkau.[5]

The radial density distribution of electrons at $t=4$, 5.6, and 7.1 c.u. was measured between $r=10\mu$ ($3.5\times10^{-4}$ c.u.) and the value $R$ quoted in Table I. For each value of $t$ the density distribution can be fitted by a power law:

$$\Pi(r)\propto r^{-\gamma}, \tag{1}$$

where $\gamma$ is slowly increasing with $r$. The average exponent $\gamma$ in the indicated interval is given in Table I. The measured values of $\gamma$ are in agreement with the distribution functions close to the shower axis as calculated by Nishimura and Kamata,[4]

$$\Pi(E_0, r, t)\propto r^{s-2}, \tag{2}$$

with $s$ defined by

$$\lambda_1'(s)t+\ln(E_0r/K)=0, \tag{3}$$

in the notation of Rossi and Greisen. Our measurements do not show any significant deviations from electromagnetic cascade theory at a primary energy of $2.5\times10^{13}$ ev. Pomeranchuk[6] and Migdal[7] also obtained Eq. (2) from their theory. Their value of $s$ is defined by

$$\lambda_1'(s)t+\ln(E_0/E)=0. \tag{4}$$

Our observations, however, are not in agreement with these results.[8]

One of the three innermost tracks in the forward cone undergoes a secondary interaction of type $4+29_p$ after 7.5 cm. Its energy can be estimated[9] from the angular distribution of the 29 shower particles to be $5\times10^{11}$ ev using

$$\ln\gamma_C=-\frac{1}{n}\sum_{i=1}^{n}\ln\tan\theta_i+\ln C, \tag{5}$$

with $C=0.7$ as determined experimentally and discussed elsewhere.[10] Within a cone of half opening angle $1.7\times10^{-3}$ rad from the axis, we found four high-energy electron pairs originating at distances less than 1 c.u. from the primary event. They are attributed to two $\pi^0$ mesons. Their energies can be estimated both from Pinkau's[5] method and from the angular separation of the pairs. One obtains for the $\pi^0$ mesons energies between 100 and 500 Bev. The energy of these $\pi^0$'s and the secondary interaction are smaller by a factor of 50 to 100 compared with the $\pi^0$ starting the main cascade.

Assuming a primary energy of $5\times10^{14}$ ev ($\gamma_C=500$), we would obtain for the high-energy $\pi^0$ meson in the center-of-mass system an energy of at least 25 Bev which is unusually high. Lowering the primary energy would even increase this value. An alternative explanation of the event would be a reaction of the kind.

$$p+\mathfrak{N}\rightarrow K+\Sigma^0+\mathfrak{N}+\pi+\pi+\ldots,$$

$$\Sigma^0\rightarrow\gamma+\Lambda^0,$$

where the primary proton emerges after the collision as a $\Sigma^0$ of very high energy. A lower limit for the primary energy under this assumption is $2\times10^{14}$ ev. This explanation would avoid the very high energy of the $\pi^0$ meson in the center-of-mass system. Due to the very short lifetime of the $\Sigma^0$, it also offers a somewhat better explanation for the short distance between the primary event and the origin of the cascade.

This event seems to be the highest energy proton collision in nuclear emulsion which has been described so far, since all the other events known to us with energies greater than $10^{14}$ ev per nucleon were produced by $\alpha$-particles.[11-13] It shows that the primary proton spectrum certainly extends to these very high energies.

*Supported in part by a joint program of the Office of Naval Research and the U. S. Atomic Energy Commission, and by the National Science Foundation.

[1]B. Rossi and K. Greisen, Revs. Modern Phys. 13, 240 (1940).

[2]K. Pinkau, Nuovo cimento 3, 1285 (1956).

[3]L. L. Eyges and S. Fernbach, Phys. Rev. 82, 23 (1951).

[4]J. Nishimura and K. Kamata, Prog. Theor. Phys. Japan 7, 185 (1952); 5, 889 (1950).

[5]K. Pinkau, Phil. Mag. 2, 1389 (1957).

[6]I. Pomeranchuk, J. Phys. U.S.S.R. 8, 17 (1944).

[7]A. Migdal, J. Phys. U.S.S.R. 9, 183 (1945).

[8]For a possible explanation see Nishimura and Kamata.[4]

[9]Castagnoli, Cortini, Franzinetti, Manfredini, and Moreno, Nuovo cimento 10, 1539 (1953).

[10]Jain, Lohrmann, and Teucher (in press).

[11]Fowler, Freier, Lattes, and Ney, Suppl. Nuovo cimento 8, 725 (1958).

[12]Ciok, Danysz, Gierula, Jurak, Miesowicz, and Wolter, Nuovo cimento 6, 1409 (1957).

[13]E. Lohrmann and M. W. Teucher, Phys. Rev. 112, 587 (1958).

## REMARK ON STRONG INTERACTIONS

Saul Barshay
Institute for Theoretical Physics,
University of Copenhagen,
Copenhagen, Denmark
(Received December 29, 1958)

In a recent note of Pais,[1] the question has been raised as to the conservation of parity, $P$, in

certain of the strong interactions. The framework for the discussion was the doublet approximation, (DA),[2] a rather high group of symmetries invoked for two classes of Yukawa-type meson-baryon interactions, the pion (nonstrange meson)-baryon interactions and the $K$ meson (strange meson)-baryon interactions. These symmetries provide selection rules inhibiting, among other things, the following reactions:

$$K^- + p \to \Sigma^+ + \pi^-,$$
$$\pi^+ + p \to \Sigma^+ + \pi^+,$$
$$K^+ + n \to K^0 + p. \qquad (1)$$

Now these processes are observed to occur and we shall comment further on this in a moment. In order to overcome the selection rules, Pais[3,4] has first discussed at length the possibility of a perturbation to the DA, called the DP, which conserves $P$ but violates charge independence and charge symmetry, as well as the invariances leading to the selection rules mentioned above. Pais has given reasonable arguments that the specific interaction introduced for the DP (which involves the assumption that the charged and neutral $K$ mesons have opposite intrinsic parity) may exhibit itself in $K$-meson physics as a development in powers of $f^2(m_K/m_\pi)^2$, and in $\pi$-meson physics as a development in powers of $f^2$, where $f^2$ is of the order of the fine structure constant, and $(m_K/m_\pi)$ is the ratio of the $K$-meson mass to the pion mass. One might then expect deviations from charge independence in, for example, the absorption of $K^-$ on deuterium.[3] In the most recent note,[1] however, an alternative viewpoint is discussed, to the effect that the DP conserves isotopic spin but not parity. Strong four-fermion interactions are mentioned in this connection, although, if the charged and neutral $K$ mesons are indeed a doublet, one may have to worry about the possible existence of the old, charge-independent $KK\pi$ interaction suggested some time ago by Goldhaber,[5] the present author,[6] and Schwinger[7] (this interaction implies parity-doublets only if the strong interactions are rigorously invariant under DP). The point that Pais[1] makes is that the effects of parity-nonconservation in the DP would be more markedly evident in the "inhibited" processes, (1), than in the following "allowed" processes which proceed through the DA (as well as the DP):

$$\pi^- + p \to \Sigma^- + K^+ \text{ or } \Lambda^0 + K^0,$$
$$K^- + p \to \Sigma^- + \pi^+ \text{ or } \Sigma^0 + \pi^0. \qquad (2)$$

In this note we would like to raise and discuss the following question: Is it really a reasonable approximation to discuss possible parity-nonconserving effects in connection with reactions (1), induced by the DP, when experiment tells us that these "inhibited" reactions occur with as great, if not greater, cross sections[8] than the "allowed" reactions (2), induced by the combined DA and DP? Indeed, it may quite reasonably be asked whether it is a reasonable approximation to talk about a perturbation to a system of very high symmetries when the so-called perturbation so completely erases the simplest experimental manifestations of the hypothesized symmetries. The analogy usually made here with the distortion of charge independence in the pion-nucleon system by electromagnetism would seem to be open to the remark that, contrary to this situation, the rudiments of charge independence are amply evident in the experiments.[9]

Suppose we consider a somewhat different division of the eight Yukawa-type interactions from that usually considered,[10] that is, the division into pion and $K$-meson interactions, respectively, with all suitable combinations of strange and nonstrange baryons. Consider a division into the interactions of the nonstrange baryons with both pions and $K$ mesons, and the interactions of the strange baryons among themselves, with both pions and $K$ mesons. Symbolically, we have for the two groups of interactions, designated hereafter by (I) and (II), the following[11]:

$$\text{(I)} \begin{cases} \bar{N}\gamma_5 N\pi \\ \bar{N}\Gamma_1 \Sigma K \\ \bar{N}\Gamma_2 \Lambda K \end{cases} \qquad \text{(II)} \begin{cases} \bar{\Xi}\gamma_5 \Xi\pi;\ \bar{\Sigma}\gamma_5 \Sigma\pi \\ \bar{\Sigma}\Gamma_3 \Lambda\pi;\ \bar{\Xi}\Gamma_4 \Sigma\bar{K} \\ \bar{\Xi}\Gamma_5 \Lambda\bar{K}. \end{cases} \qquad (3)$$

We assume the conventional isotopic spin multiplet assignments and the conservation of isotopic spin. The $\Gamma_i$, with $i = 1 \ldots 5$, are either the unit matrix or $\gamma_5$, depending upon the intrinsic parities of the strange particles involved in the coupling.

It would appear that at present our most direct experimental contact is with the couplings in (I). Analyses of pion-nucleon and $K$-meson–nucleon elastic scattering experiments with the tool of the forward-angle dispersion relations

come fairly directly to the three renormalized coupling strengths and the two (unknown) relative parities involved in (I),[12] although the determination of all of these quantities by this method may not be unambiguous and recourse to specific experiments may be necessary. Similarly, photoproduction of pions and of $\Lambda$ and $\Sigma$ particles with $K$ mesons may be analyzed to yield information concerning the primary Yukawa-type processes in (I).[13] The renormalized coupling strengths associated with the interactions in (II) are presently somewhat more difficult to relate to experimental results.[14] We do not know whether they are all necessarily primary (since several are either induced by others together with the interactions in (I) or are induced by the latter interactions alone) or whether they are very strong or even moderately strong, as the interactions in (I) appear to be. Some of these interactions may indeed be weaker.[15] Models in which the primary pion-hyperon couplings are taken to be quite strong have been widely discussed, especially with reference to calculations of the forces giving rise to hyperfragments.[16,17] It is difficult to see how any firm conclusions can be reached from these calculations as to the primary nature or strength of the pion-hyperon interactions, since an infinitely repulsive core is usually placed at about the range of the force mediated by the exchange of a single $K$ meson and since, in the case of $\Lambda$ binding, the exchange of at least two pions is involved (this process is not only related to primary and effective pion-hyperon couplings, but also to pion-nucleon scattering through the $K$-meson cloud of the hyperon). The experimental data on the associated production of $\Lambda$ and $\Sigma$ particles in pion-nucleon collisions and on $K^-$ absorption by protons,[18] as well as that on $K$-meson–nucleon scattering, is not inconsistent with the possibility that these processes are induced largely by the interactions in (I) in two possible situations: (1) The relative $\Sigma$-$\Lambda$ parity is even, but the coupling strengths of $\Lambda$ and $\Sigma$ particles to $K$ mesons and nucleons differ (in order to avoid the selection rules of the DA). (2) The relative $\Sigma$-$\Lambda$ parity is odd (in this case the above coupling strengths are also likely to differ).[19,20] The presently indicated degree of parity conservation in associated production and $K^-$ absorption[21,22] would seem to preclude the existence of comparably strong interactions in (II) which, taken together with the interactions in (I), did not conserve parity. However, terms in (II) with coupling constants an order of magnitude or more smaller than the pion-nucleon coupling are not necessarily precluded. For example, in the case of even relative $\Sigma$-$\Lambda$ parity, a scalar coupling of $\Lambda$ to $\Sigma$ and $\pi$ would give rise to parity-nonconserving effects in interference with the interactions in (I). Since in certain processes such relatively weak couplings might interfere more effectively with the effects induced by the interactions in (I), it would seem useful to consider experimentally a variety of further processes involving strange particles in discussing the possibility of parity-nonconserving effects. Such processes as the following might further probe the interactions in (II):

$$\Sigma^- + p \to \Lambda + n, \qquad \Xi^- + p \to \Lambda + \Lambda,$$
$$\Sigma^- + p \to \Sigma^- + p, \qquad K^- + p \to \Xi^- + K^+,$$
$$\Xi^- + p \to \Xi^- + p. \tag{4}$$

The elastic and inelastic hyperon-nucleon interactions with small momentum transfer may be particularly sensitive to the single pion exchange and thus to the nature of the pion-hyperon couplings.[14] Without the introduction of quadrilinear interactions of various sorts, whose purpose is to distort the hypothesized very high symmetry of the Yukawa-type meson-baryon interactions (for which there is, at present, no experimental support), there is yet much room within the limits of our very scant knowledge of the Yukawa-type interactions, in group (II) in particular, for possible small effects of parity nonconservation. If the conservation of parity in the strong interactions is indeed a rigorous invariance, it may not be necessary to "explain" it in terms of other specially constructed symmetries of the Hamiltonian, unless experiments give indication of the presence of these latter symmetries in at least as convincing a manner as they indicate the charge independence of the pion-nucleon system in the absence of electromagnetic effects.

I would like to thank Dr. S. Glashow for helpful discussions. I would also like to thank Professor Ben Mottelson and Professor E. Henley for several conversations. I am indebted to Professor N. Bohr and Professor A. Bohr for the kind hospitality of the Institute for Theoretical Physics and to the National Science Foundation for Fellowship support.

[1]A. Pais, Phys. Rev. Lett. 1, 418 (1958).
[2]A. Pais, Phys. Rev. 110, 574 (1958).

[3]A. Pais, Phys. Rev. 112, 624 (1958).
[4]A. Pais, "Notes on the Dynamics for Odd ($K^+$, $K^0$)-parity" (to be published).
[5]M. Goldhaber, Phys. Rev. 101, 433 (1956).
[6]S. Barshay, Phys. Rev. 104, 851 (1956).
[7]J. Schwinger, Phys. Rev. 104, 1164 (1956).
[8]For example, in $K^-$-$p$ interactions at about 300 Mev/$c$, the cross section for $\Sigma^+ - \pi^-$ production is about 1.5 times that for $\Sigma^- - \pi^+$ production. Both this process and $K^+$ charge exchange scattering seem to occur more frequently as the available energy increases. However, neglect of the $\Sigma - \Lambda$ mass difference, basic to the DA, should be a better, rather than a worse approximation, as the available energy increases. I am much indebted to Professor A. Rosenfeld for communication of the preliminary results of the Berkeley bubble chamber groups.
[9]This question may also be raised with reference to a recent work of G. Feinberg and F. Gürsey [Phys. Rev. (to be published)] in which a highly symmetric DA and a DP are chosen such that $CP$ invariance implies $C$ and $P$ invariance separately, and it is then argued that this is the interaction realized in nature, thereby giving an a posteriori reason for parity conservation in strong interactions.
[10]M. Gell-Mann, Phys. Rev. 106, 1296 (1957).
[11]The standard particle symbols are used for the field operators and the isotopic spin operators and indices are suppressed.
[12]For a summary and references to original work, see the report of R. H. Dalitz, 1958 Annual International Conference on High-Energy Physics at CERN, edited by B. Ferretti (CERN, Geneva, 1958), Session 6.
[13]M. Gell-Mann, 1958 Annual International Conference on High-Energy Physics at CERN, edited by B. Ferretti (CERN, Geneva, 1958), Session 5.
[14]See, however, the proposals for determining these coupling strengths recently suggested by S. L. Glashow and the present author, Phys. Rev. Lett. (to be published).
[15]In this connection, it is interesting to refer to the remarks of J. R. Oppenheimer at the end of Session 9 in 1958 Annual International Conference on High-Energy Physics at CERN, edited by B. Ferretti (CERN, Geneva, 1958).
[16]D. B. Lichtenberg and M. Ross, Phys. Rev. 107, 1714 (1957).
[17]F. Ferrari and L. Fonda, Nuovo cimento 5, 842 (1958).
[18]S. Barshay (to be published).
[19]F. Gürsey, Phys. Rev. Lett. 1, 98 (1958).
[20]A conjecture that this situation might hold, based on an elementary analysis of the apparent marked difference between the properties of the two isotopic spin states in low-energy $K^+$-nucleon scattering, is discussed in S. Barshay, Phys. Rev. Lett. 1, 97 (1958).
[21]Crawford, Cresti, Good, Solmitz, and Stevenson, Phys. Rev. Lett. 1, 209 (1958).
[22]Alvarez, Bradner, Falk-Vairant, Gow, Rosenfeld, Solmitz, and Tripp, University of California Radiation Laboratory Report UCRL-3775 (unpublished).

## STRONG-COUPLING THEORY OF THE $S=-1$ HYPERONS: THE $\Lambda^0$ AS A BOUND STATE*

L. F. Landovitz
Brookhaven National Laboratory,
Upton, New York

and

B. Margolis
Columbia University,
New York, New York

(Received March 5, 1959)

It has always appeared to be an attractive idea to eliminate some of the hyperons by considering them to be bound states.[1] We have tried a variant of this idea: suppose that the strangeness-producing interaction (perhaps that of the $K$ mesons with nucleons) were to produce different core particles and that the pion interactions produced whatever additional multiplicity were present within the different strangeness subspaces.

Thus, restricting ourselves to linear charge-independent pion interactions, for the $S=-1$ case, we consider the interaction of pseudoscalar pions with an isotopic spin-one baryon core in the static approximation (a $T=0$ core would require a quadratic interaction with pions); we shall treat this system in the strong-coupling approximation which has been recently extended to treat cases of this type.[2] Further, we assume that the parameters to be used are the same as those used in the nucleon case: this may be viewed as an extension of global symmetry.

The interaction Hamiltonian is taken to be

$$H_1 = \frac{2g}{\kappa}(2\pi)^{\frac{1}{2}} \int d^3x \; T_\alpha \phi_\alpha \; \vec{\sigma}\cdot\vec{\nabla} U,$$

where $\kappa$ is the $\pi$ mass, $T_\alpha$ the $3\times 3$ spin-one matrices (the factor of two is necessary to achieve correspondence with the nucleon case since $\tau_\alpha$ is used rather than $\tau_\alpha/2$, the nucleon isotopic spin). We then find a band structure as in the nucleon case: for the $y=\frac{1}{2}$ band with $\vec{Y}=\vec{T}+\vec{J}$ (the vector sum of the isotopic spin and total angular momentum), the levels above the ground state are given by

$$E_{jt} = \frac{27}{64}\left(\frac{j(j+1)+t(t+1)-\frac{3}{4}}{g^2/\kappa a}\right)\kappa,$$

and $|(j-t)| \leq \frac{1}{2} \leq j+t$, $j$ is half-odd integral, $t$ is integral. Thus the ground state is $j=\frac{1}{2}$, $t=0$, the next state $t=1$, $j=\frac{1}{2}$, and the next above that $t=1$,

$j=\frac{1}{2}$. Taking $g^2/\kappa a \approx 2$ as in the nucleon case, we find

$$E_{1,1/2} - E_{0,1/2} \cong 59 \text{ Mev},$$

$$E_{1,3/2} - E_{1,1/2} \cong 89 \text{ Mev}.$$

If we identify the ground state with the $\Lambda^0$, and the next state with the $\Sigma$, then the $\Sigma$-$\Lambda^0$ mass difference is 59 Mev as compared with the experimental value ~75 Mev. It is to be noted that this is a true bound state since the mass difference is less than a pion mass. An obvious consequence of this identification is that the $\Lambda^0$ and $\Sigma$ have the same parity.[3]

Further, the excited state, $\Sigma^*$, cannot decay into a $\Sigma$ but can decay into a $\Lambda^0$ by pion emission. However, if we were to take the experimental $\Sigma$-$\Lambda^0$ mass as determining $g^2/\kappa a$, then $\Sigma^*$ would be 113 Mev above the $\Sigma$ and if the lifetime were sufficiently short, the width of the level would permit it to decay into a $\Sigma$. Thus, it would give rise to a scattering resonance in $\pi$-$\Sigma$ scattering and, as a final state interaction, in $K^- + p$ scattering; i.e., there should be a $t=1$, $j=\frac{3}{2}$ resonance.[4] Unfortunately $m_K + m_p > E_\Sigma$ and thus one would be on the tail of the resonance. Higher resonances corresponding to higher values of $y$ should also be present.

A complete treatment of the problem with further results will be published elsewhere later.

We wish to thank Professor G. C. Wick, Professor R. Serber, Dr. G. Feinberg, and Dr. R. Behrends for many helpful discussions.

---

*Work supported in part by the U. S. Atomic Energy Commission.

[1]See, for example, S. Sakata, Progr. Theoret. Phys. (Kyoto) 16, 686 (1956).

[2]L. Landovitz and B. Margolis, Phys. Rev. Lett. 1, 206 (1958); Ann. Phys. (to be published).

[3]There have been several suggestions that the $\Lambda^0$ and $\Sigma$ have opposite parity; see, e.g., S. Barshay, Phys. Rev. Lett. 1, 97 (1958).

[4]For a discussion of the interpretation of the $K$-$p$ scattering in terms of a phenomenological resonant state, see M. Ross, Phys. Rev. 112, 986 (1958).

# ABSTRACTS

*In this section are printed the abstracts of Articles that have been forwarded to The American Institute of Physics for publication in THE PHYSICAL REVIEW. In quoting information obtained from this section before the appearance of the corresponding Article, reference should be made to "Physical Review (to be published)" rather than to this Journal.*

STUDIES OF LIQUID HELIUM. Ira L. Karp, Boeing Airplane Company, Seattle, Washington (Received March 28, 1958; revised manuscript received December 31, 1958).

A calculation scheme suitable for studying the ground state of many-body Bose quantum systems with strong forces is developed. The calculation scheme is based on the nodeless property of the ground-state wave function and is capable of yielding in some cases upper and lower bounds on the ground-state energy and corresponding wave functions. From a treatment of liquid helium in the ground state, including a short-range interaction form, it is concluded that the calculation scheme is suitable for problems with involved interactions and is capable of reducing the problem to the mathematical one of calculation of the energy and lattice structure of a classical crystal at absolute zero of temperature.

KINETIC EQUATION FOR A PLASMA WITH UNSTEADY CORRELATIONS. C. M. Tchen, Applied Mathematics Division, National Bureau of Standards, Washington, D. C. (Received July 9, 1958; revised manuscript received December 11, 1958).

As a generalization of the Boltzmann equation, the kinetic equation for a plasma is derived in the form of a generalized Fokker-Planck equation, by considering unsteady correlations, including non-Markovian and nonlinear behavior. Both the binary and ternary correlations are used for many kinds of particles with different temperatures. The coefficients of the kinetic equation depend on the law of interaction for a pair of particles and are influenced by relaxation. The effective potential of friction consists of two parts: the static part corresponds to the Debye potential and is isotropic; the dynamical part is axially symmetrical about the direction of motion, and causes a dynamical friction. The results show that the friction is proportional to velocity for slow particles, and inversely proportional to the square of velocity for fast particles. This tendency of the fast particles to overcome repulsion is a property connected with the "run-away" of electrons. A criterion for maximum friction is derived. The nonlinear interaction, which mainly affects the shielding phenomena, assures the convergence of the coefficients in case of distant interaction. On the other hand, the disturbances associated with the correlation function provide cooperative phenomena of such a type as to assure convergence at close interaction. Since the length scales of interaction are well determined in this way, the kinetic equation can be expected to be valid over a longer range than does the Boltzmann equation. The large scale agrees with the Debye radius, when the shielding term is linearized, as should be expected; the small scale differs from the Landau parameter, and depends on the local distribution function. When time relaxation is left aside and linearization is made, the kinetic equation degenerates to the classical Fokker-Planck equation with convergent coefficients.

SELF-CONSISTENT FIELD OF SINGLE-TYPE ELECTRONS IN A UNIFORM MAGNETIC FIELD. Lewi Tonks, Radiation Laboratory, University of California, Livermore, California (Received November 10, 1958; revised manuscript received December 22, 1958).

A problem which has been brought to the fore by Christofilos' proposed thermonuclear machine, "Astron," is that of electrons rotating in a uniform impressed magnetic field in such a way as to form a cylinder in space--a disembodied current-carrying helix. In the present paper the self-consistent magnetic field for such a "helix," infinitely long and made up of relativistic electrons of identical mass, axial velocity, and canonical angular momentum, has been calculated for the interesting range of the two pertinent parameters. The first is the ratio, denoted by $g_2$, of apogee radius to the radius of gyration in the impressed field. The second is the quotient of the number of electrons per classical-electron diameter along the axis and the ratio of relativistic to rest mass. It is denoted by $(2r_e/\gamma)N$ and is called the "strength" of the layer.

When $g_2$ is less than 2, the trajectories of the electrons, when they are few in number, are approximately circles which include the axis. As the layer strength is increased, these trajectories stay closer and closer to the locus of apogees.

The interior field never reverses and approaches $2/g_2 - 1$ as the strength reaches $2(g_2 - 1)$, the largest value possible for a given $g_2$.

When $g_2$ is greater than 2, the trajectories in a weak layer are approximately circles which do not include the axis, but with increasing strength the perigees approach, cross, and then recede from the axis. As they cross, the interior field decreases discontinuously even to the point of partial reversal. The approach to this discontinuity is attended by an enhancement of the interior field.

When $g_2$ is greater than approximately 4, the layer strength peaks at a value in excess of $2(g_2 - 1)$ at the axis crossing, and as the perigee locus then moves outward, the strength decreases toward $2(g_2 - 1)$. Thus there can be two configurations of the layer which have the same strength, one consistent with enhancement of the interior field, the other consistent with reversal.

LANDAU'S MODEL OF LIQUID $He^3$. Tunemaru Usui,* Argonne National Laboratory, Lemont, Illinois (Received October 8, 1958).

Landau's Fermi-liquid model of liquid $He^3$ is studied with regard to its lowest temperature properties. Primary stress is laid on the coefficient of thermal expansion. The spectra used by Abrikosov and Khalatnikov, the perfect-gas type and the "bubble" type, are shown to give a positive coefficient of thermal expansion, in contradiction with experiment. An alternative simple spectrum is suggested which can give a negative coefficient of thermal expansion, namely $\Delta + p^2/2m^*$. In addition, the existence of a negative coefficient of thermal expansion is shown to imply a strong temperature dependence of the energy spectrum, which may cause a sharp deviation of the heat capacity curve from the perfect gas type, similar to the deviations observed in liquid $He^3$.

*Present address: Institute of Physics, College of General Education, University of Tokyo, Komaba, Meguro-ku, Tokyo, Japan.

IMPURITY SCATTERING IN SUPERCONDUCTORS. H. Suhl and B. T. Matthias, Bell Telephone Laboratories, Murray Hill, New Jersey (Received November 20, 1958).

With the Bardeen-Cooper-Schrieffer (B.C.S.) theory as a starting point, perturbation theory is used to determine the reduction in superconducting transition temperature due to scattering by impurities in the superconductor. Two cases are discussed: scattering due to a localized exchange interaction between the spins of the conduction electrons and impurity spins, and purely orbital scattering by nonmagnetic impurities. In the former case good quantitative agreement with observations is obtained. In the latter case numerical agreement is less good, but the qualitative feature that the initial reduction in $T_C$ is a universal function of residual resistivity is made evident. It is further shown that indiscriminate application of perturbation theory of B.C.S. states leads to the wrong result in predicting the transition temperature, if the transition is of second order.

DEDUCTION OF THE VOLUME DEPENDENCE OF THE COHESIVE ENERGY OF SOLIDS FROM SHOCK-WAVE COMPRESSION MEASUREMENTS. G. B. Benedek, Division of Engineering and Applied Physics, Harvard University, Cambridge, Massachusetts (Received November 19, 1958).

By applying the Mie-Grüneisen equation of state to measurements of the compression of solids by strong shock waves, it is possible to determine the volume dependence of the cohesive energy. The method for carrying out this deduction is presented along with a detailed exposition of the underlying assumptions. The method is applied to six metals, Be, Al, Co, Ni, Cu, and Ag, for which the experimental data are most extensive. The volume dependence of the cohesive energy for these six metals is presented in both analytical and graphical form.

OPTICAL PROPERTIES OF NICKEL AND TUNGSTEN AND THEIR INTERPRETATION ACCORDING TO DRUDE'S FORMULA. S. Roberts, General Electric Research Laboratory, Schenectady, New York (Received August 22, 1958).

New optical data are reported for nickel at 88°, 298° and 473°K and for tungsten at 298°, 1100° and 1600°K in the wavelength range 0.365 to 2.65 microns. These data are shown to depend on wavelength in a way which is in good quantitative agreement with a formula initially proposed by Drude. By attributing different terms in Drude's equation to the motion of different classes of free and bound electrons, one may conclude that several

classes of each are present in both metals. Each class of free electrons accounts for a portion of the dc conductivity and has its own characteristic relaxation time or wavelength. From this analysis it appears that most of the dc conductivity may be attributed to one class of free electrons, although optical properties are strongly influenced by other classes as well. In both metals the characteristic wavelength $\lambda_{\gamma_1}$ of the first class of free electrons proves to be proportional to the corresponding conductivity $\sigma_1$ at different temperatures. In nickel the constant ratio $\sigma_1/\lambda_{\gamma_1}$ accounts for the low temperature coefficient of optical properties throughout the visible and near infrared range. In tungsten this constant ratio contributes to the existence of the $x$-point or crossover wavelength in the spectral emissivity. It is shown that the anomalous skin effect should not be a significant factor in the measured optical properties of a metal like nickel in the range of wavelength where these properties have only a small temperature coefficient.

STIMULATED INFRARED EMISSION FROM Sm CENTERS IN SrS PHOSPHORS. Seymour P. Keller, Research Laboratory, International Business Machines Corporation, Poughkeepsie, New York (Received October 23, 1958).

Previous investigations of the two phosphor systems SrS:Ce,Sm and SrS:Eu,Sm indicated that two energy levels within the energy gap were associated with the Sm site. Under certain conditions one expected that a transition between these two levels of the same center would result in an infrared emission. This emission was not seen at room temperature but it has recently been observed at 77°K under dynamic conditions of simultaneous irradiation by ultraviolet and visible light. Correlation is made between the observed predicted emission and the simplified band-theory model proposed earlier.

LATTICE SPECIFIC HEATS NEAR 0°K WITH AN APPLICATION TO GERMANIUM. Paul M. Marcus and Anthony J. Kennedy, Carnegie Institute of Technology, Pittsburgh, Pennsylvania (Received November 17, 1958).

Formulas for the low-temperature lattice specific heat are developed on the basis of the general adiabatic and harmonic assumptions, independently of special models or numerical procedures. Explicit simple formulas are obtained for $\theta_D(0)$, the equivalent Debye temperature at 0°K, and for the curvature of $\theta_D(T)$ at 0°K. Discussions are given of the resulting dependence of $\theta_D(0)$ on physical parameters and the significance of the formula for $\theta_D(0)$ as a check on the basic assumptions, of the absence of a linear term in $\theta_D(T)$, and of the dependence of the curvature on the dispersion of elastic waves. $\theta_D(0)$ is calculated for Ge as 374.0°K; an error of ±2°K is estimated as due to errors in the elastic constants whereas the computational error is negligible. $\theta_D(T)$ is calculated for Ge for $[T/\theta_D(0)] < 0.11$ using two models. The first is a simple model of the frequency spectrum which gives results like typical force-constant models, and disagrees with measurement. The second is a model of the frequency spectrum based on the direct measurements by inelastic neutron scattering; this model shows much greater dispersion, and gives much better agreement of $\theta_D(T)$ with measurement.

SLOW CAPTURE OF HOLES AND ELECTRONS BY SURFACE STATES ON GERMANIUM AND SILICON AT LOW TEMPERATURES. S. Roy Morrison, Honeywell Research Center, Hopkins, Minnesota (Received April 22, 1957; revised manuscript received December 8, 1958).

Field-effect decay curves at temperatures the order of liquid nitrogen are presented for $n$- and $p$-type germanium and for $p$-type silicon. A strongly asymmetric decay is observed, depending upon whether the induced charge is positive or negative. The decay is strongly influenced by illumination, temperature, and magnitude and sign of the field. Injected minority carriers also affect the decay rate. It is suggested that the trapping centers involved are the fast states, or recombination centers at the surface. After a disturbance of the charge in these states the approach to steady state is slow due to the limited supply of minority carriers arriving at the surface. The results observed are compared with a model which takes surface barrier effects into consideration and are found in reasonably quantitative agreement.

CROSS-RELAXATION IN SPIN SYSTEMS. N. Bloembergen, S. Shapiro, P. S. Pershan, and J. O. Artman,* Gordon McKay Laboratory, Har-

vard University, Cambridge, Massachusetts (Received November 20, 1958).

The energy transfer between adjacent resonances in nuclear and electron spin systems is analyzed in terms of the overlap of line-shape functions. The procedure is an enlargement on the original proposal of Kronig and Bouwkamp, and consists of taking partial account of off-diagonal elements in the spin-spin interaction, which are omitted in Van Vleck's truncated Hamiltonian. If the frequency of these off-diagonal elements is sufficiently small, they give rise to an additional kind of spin-spin relaxation, observed by Gorter and co-workers. They are also responsible for cross-saturation effects in paramagnetic salts of the type observed by Townes and co-workers. A crucial experiment is described which can be explained by spin-spin interactions, but not by the assumption of a hot phonon region. Implications of the cross-relaxation for the operation of solid state masers are discussed. Special consideration is given to magnetically dilute substances and inhomogeneously broadened lines. Paradoxically, the latter will usually still undergo a homogeneous steady-state saturation.

*Now at Applied Physics Laboratory, Johns Hopkins University.

MULTIPLE QUANTUM TRANSITIONS IN NUCLEAR MAGNETIC RESONANCE. Shaul Yatsiv, Stanford University, Stanford, California (Received April 24, 1958).

The theory of Bloch and Wangsness for nuclear magnetic resonance (nmr) signals is applied to multiple quantum transitions. In most of the nmr experiments, the energy level schemes are only slightly different from an equally spaced Zeeman pattern, so that a simultaneous absorption of several radiation quanta with the same frequency can take place. It is found that the multiplicity, or the number of quanta absorbed in the transition, is most easily determined through the specific dependence of the multiple-quantum signals on the rf field amplitude. The dependence of the signals on various relaxation parameters is developed and is found to provide information about relaxation processes which is not derivable from ordinary single-quantum transitions.

A method of enhancing multiple transitions by audio-modulation of the radiofrequency field is described. This is helpful in cases where the frequency deviations from an equally spaced Zeeman pattern are so large that a direct multiple transition is too weak to be observed.

EFFECT OF IMPURITIES ON ANGULAR CORRELATION OF POSITRON ANNIHILATION RADIATION. R. L. deZafra,* Physics Department, University of Maryland, College Park, Maryland (Received September 22, 1958).

Angular distribution measurements on two-quantum annihilation radiation from positrons stopping in liquid targets have been made as a function of concentration of certain impurities in the target materials. The impurities tested were $Mn^{++}$ and $Co^{++}$ ions (dissolved from their chloride salts) and $NO_2^-$ and $NO_3^-$ ions (dissolved from their sodium salts) in water, and chloroform and the free radical diphenyl-picryl-hydrazyl in benzene. The paramagnetic ions are found to produce a strong enhancement of the narrow-distribution component, ascribed to exchange conversion between triplet and singlet positronium. Conversion cross sections of a few times $10^{-19}cm^2$ are obtained assuming a positronium velocity about 5 times thermal velocity at conversion. These are in fair agreement with recent determinations made from lifetime studies. The nitrate and nitrite ions may cause a further broadening of the broad component, which appears to be associated with the chemical binding of positrons to the ions. It is also found that positrons are chemically bound to the chloroform molecule. Some evidence is presented to show that the free radical (diphenyl-picryl-hydrazyl) may not, as previously supposed, act to convert triplet to singlet positronium, but may in fact give rise to chemical binding of positronium to the free radical.

*Now at the Physics Department, University of Pennsylvania, Philadelphia, Pennsylvania.

THRESHOLD PROPERTIES OF SCATTERING AND REACTION CROSS SECTIONS. Roger G. Newton, Indiana University, Bloomington, Indiana (Received November 17, 1958).

The detailed behavior of elastic and inelastic scattering cross sections as functions of the en-

ergy at the threshold of a new reaction is derived from general principles. The results lend themselves in certain cases to the experimental determination of spins and parities of reaction products, as well as of not directly observable scattering amplitudes and inelastic cross sections. A number of special cases are treated in detail.

NUCLEAR SPECTROSCOPY OF ODD-MASS (161-173) NUCLIDES PRODUCED BY PROTON IRRADIATION OF Er AND Yb. B. Harmatz and T. H. Handley, Oak Ridge National Laboratory, Oak Ridge, Tennessee, and J. W. Mihelich, University of Notre Dame, Notre Dame, Indiana (Received November 17, 1958).

To study the isotope effect on nuclear levels of odd-mass rare-earth isotopes, enriched isotopes of Er and Yb were irradiated with protons in the ORNL 86-inch cyclotron. After chemical separation, the decay chains leading to stable isotopes were analyzed with internal-conversion, photographic-recording, permanent-magnet spectrographs. Precise energy values as well as photometrically measured intensities of conversion lines of 8 to 1600 kev energy were obtained. Very light isotopes of Lu and Tm, each eight mass units from the mass stability line, were produced. The following activities were studied: $Tm^{161}$ (~30 min), $Ho^{161m}$ ($E3$, 211 kev), $Tm^{163}$ (2 hr), and $Lu^{167}$ (54 min), all previously unreported, as well as $Tb^{161}$, $Ho^{161}$, $Tm^{165,167}$, $Yb^{167}$, $Lu^{169,171,173}$, $Hf^{173}$, and possibly $Yb^{169m}$. Genetic relationships and partial level schemes for decay chains of masses 151 to 173 are shown. Where comparison is possible, excellent agreement with the predictions of the Copenhagen unified model is obtained, particularly for the case of the various isotopes of Tb ($Z=65$), Ho ($Z=67$), and Tm ($Z=69$), where striking similarities in the level structure are observed.

515-kev AND 679-kev RESONANCES IN THE REACTION $Na^{23}(p,\gamma)Mg^{24}$. Lennart Simons, Institute of Physics, University of Helsinki, Helsinki, Finland (Received November 18, 1958).

The 515-kev and 679-kev resonance levels have previously been assigned $J=1^+$ and $J=3^+$, respectively, the latter being formed by $LS$ coupling. An alternative assignment is presented in this paper, according to which the 515-kev level has $J=2^-$ formed by $jj$ coupling with $j_p=1/2^-$ or $j_p=3/2^-$. $J=3^+$ is confirmed for the 679-kev resonance level, assuming $jj$ coupling with $j_p=3/2^+$.

LIFETIME OF THE 186-kev LEVEL OF THORIUM-231. D. Strominger, Radiation Laboratory and Department of Chemistry, University of California, Berkeley, California (Received November 19, 1958).

The lifetime of the 186-kev level of $Th^{231}$ has been studied following $U^{235}$ alpha decay. The half-life value of this level is $0.77\pm0.12$ m$\mu$sec.

POLARIZATION OF NEUTRONS FROM $Li^7(p,n)Be^7$ AND FROM $n$-$d$ SCATTERING. L. Cranberg, University of California, Los Alamos Scientific Laboratory, Los Alamos, New Mexico (Received November 24, 1958).

The polarization of neutrons produced in the reaction $Li^7(p,n)Be^7$ has been examined using $n$-$He^4$ scattering as an analyzer and the pulsed-beam time-of-flight technique as a neutron spectrometer. Results are reported up to 4.95 Mev proton energy. The data include results on the neutron groups corresponding to beryllium-7 being left in its ground state and first excited state. Using neutrons of 2.1 Mev which are polarized 38%, the polarization for $n$-$d$ scattering at several angles has been found to be less than 0.07, which is consistent with a prediction by Christian and Gammel of negligible polarization.

PROTON-PROTON SCATTERING FROM 1.4 TO 2.4 Mev. David J. Knecht, S. Messelt,* E. D. Berners,† and L. C. Northcliffe,‡ University of Wisconsin, Madison, Wisconsin (Received November 17, 1958).

Differential cross sections for the scattering of protons by protons have been measured at energies of 1.397, 1.855, and 2.425 Mev over an angular range from 12° to 90° in the center-of-mass system. Total uncertainties vary from about ±0.1% at large angles to ±0.3% at the smallest angles. A thorough investigation of sources of error has yielded cross-section values in disagreement with previously published values. A simple phase-shift analysis has been made. Without the inclusion of vacuum polarization con-

tributions, a satisfactory fit is not obtained with only $S$-wave and effective nuclear $P$-wave phase shifts. With their inclusion, the data are fitted well by pure $S$-wave nuclear scattering. An upper limit on the magnitude of the effective nuclear $P$-wave phase shift is estimated at about 0.02° at these energies.

*On leave from the University of Oslo, Norway.
†Now at Marquette University, Milwaukee, Wisconsin.
‡Now at Yale University, New Haven, Connecticut.

EVIDENCE FOR THREE-BODY VECTOR FORCES IN LIGHT NUCLEI. Arnold M. Feingold, Department of Physics, University of Utah, Salt Lake City, Utah (Received November 18, 1958).

The splittings of the $P$ doublet states of $Li^7$ and $N^{15}$, and the $D$ doublet states of $O^{17}$, are calculated with phenomenological two-body vector forces of both Gaussian and Yukawa shapes with arbitrary ranges and exchange character. It is found to be impossible to fit the experimental data with a two-body force of fixed strength, in agreement with Pearse's calculations based on a relativistic two-body vector force. The splittings are then calculated with a phenomenological three-body vector force of the type expected to arise from higher order effects of the tensor force. The predicted ratio of the $P$ doublet splitting in $N^{15}$ to that in $Li^7$ is found to be quite insensitive to the range or shape of the three-body force, and in excellent agreement with experiment, provided that the exchange character of the force is not chosen close to the Serber mixture. The $O^{17}$ $D$ doublet splitting, while somewhat more sensitive to the choice of range and exchange mixture, can also be fitted simultaneously, with a wide variety of three-body vector potentials. An attempt is then made to derive the parameters of the three-body vector force from the Gammel-Thaler tensor force parameters, but the resultant force has the wrong exchange character, and is also much too weak, to fit the experimental data. This is mainly due to the Serber-like exchange character of the Gammel-Thaler tensor force. A moderate increase in the strength or range of the odd-state tensor force would give a satisfactory three-body vector force. The splitting of the $^3D$ states of $Li^6$ is also examined. Here one-, two-, and three-body vector forces all predict too small a splitting, when the strength of the interaction is normalized to the $Li^7$ $P$ doublet splitting. For the three-body vector force, however, there exists the possibility that the strength parameter is greater for $Li^6$ than for $Li^7$, which would improve the fitting.

HIGHER ORDER CORRECTIONS TO THE ALLOWED BETA DECAY. Masato Morita, Columbia University, New York, New York (Received September 8, 1958; revised manuscript received November 24, 1958).

The shape of the allowed beta spectrum and the directional correlations of the allowed beta ray and gamma or alpha ray have been investigated theoretically with an assumption of $VA$. We take into account the Coulomb field due to the daughter nucleus, the finite de Broglie wavelength effect, and the contribution of the second forbidden matrix elements, $\mathfrak{M}(r^2)$, $\mathfrak{M}(\vec{\alpha}\cdot\vec{r})$, $\mathfrak{M}(\vec{\sigma}r^2)$, $\mathfrak{M}((\vec{\sigma}\cdot\vec{r})\vec{r})$, $\mathfrak{M}(\gamma_5\vec{r})$, and $\mathfrak{M}(\vec{\alpha}\times\vec{r})$, simultaneously. Relations between coordinate-type and momentum-type matrix elements are given in the nonrelativistic approximation. In this case, $\mathfrak{M}(\vec{\alpha}\times\vec{r})/\mathfrak{M}(\vec{\sigma})=M^{-1}$. The correction factors for the beta spectra of $B^{12}$ and $N^{12}$ as well as their ratio have almost no energy dependence, since several corrections cancel each other. On the other hand, this ratio varies by 12% over the whole spectrum, if we adopt $\mathfrak{M}(\vec{\alpha}\times\vec{r})/\mathfrak{M}(\vec{\sigma})=M^{-1}(\mu_p-\mu_n)$ given by Gell-Mann. The beta-alpha directional correlation of $Li^8$ is discussed also.

EXCITATION FUNCTIONS OF $U^{235}$ AND $U^{238}$ BOMBARDED WITH HELIUM AND DEUTERIUM IONS. J. Wing, W. J. Ramler, A. L. Harkness, and J. R. Huizenga, Argonne National Laboratory, Lemont, Illinois (Received November 14, 1958).

Cross sections were determined for the reactions $U^{238}(He^4,n)Pu^{241}$ [including $U^{238}(He^4,p)Np^{241}\xrightarrow{\beta^-}Pu^{241}$], $U^{238}(He^4,2n)Pu^{240}$, $U^{238}(He^4,3n)Pu^{239}$, $U^{238}(He^4,4n)Pu^{238}$, $U^{238}(He^4,\text{fission})$, $U^{235}(He^4,n)Pu^{238}$, and $U^{235}(He^4,3n)Pu^{236}$ induced by helium ions of energies from 18.0 to 43.0 Mev. The yields of $Pu^{239}$, $Pu^{240}$, and $Pu^{241}$ were determined by a mass spectrometric technique. Cross sections were measured for the reactions $U^{238}(d,p)U^{239}$, $U^{238}(d,2n)Np^{238}$, $U^{238}(d,4n)Np^{236}$ (22 hr), $U^{238}(d,t;d,p2n)U^{237}$, $U^{235}(d,n)Np^{236}$ (22 hr), $U^{235}(d,2n)Np^{235}$, and $U^{235}(d,3n)Np^{234}$ induced by deuterons of energies from 5.8 to 21.5 Mev. The above excitation functions are compared with similar excitation functions of nonfissile nuclei to show

the effect of fissionability on spallation cross sections. Mean values of $\Gamma_n/\Gamma_f$ are derived for several heavy nuclides by fitting the experimental excitation functions with theoretical cross sections calculated from the Jackson model modified for fission. In addition to the discussion on the compound nucleus formation mechanism, some discussion of the experimental evidence for direct interactions is given.

RATIOS OF ABUNDANCES, MAGNETIC MOMENTS, AND CAPTURE CROSS SECTIONS OF GADOLINIUM ISOTOPES FROM PARAMAGNETIC RESONANCE. W. Low, Department of Physics, Hebrew University, Jerusalem, Israel, and D. Shaltiel, Department of Physics, Israel Institute of Technology, Haifa, Israel (Received November 20, 1958).

Precision measurements on the hyperfine structure of the transitions corresponding to $\Delta M = 4$ of the cubic-field paramagnetic resonance spectrum of gadolinium in single crystals of thorium oxide yield the following values: Isotopic abundance: even isotopes, 69.45%; $Gd^{155}$, 15.05 $\pm 0.2\%$; $Gd^{157}$, $15.5 \pm 0.2\%$. Ratio of magnetic moments: $\mu^{155}/\mu^{157} = 0.7495 \pm 0.0045$.

Irradiation of crystals at the Harwell pile with a thermal neutron flux of $1.2 \times 10^{12}$ $n/cm^2$ sec, and a fast flux of $2.3 \times 10^{11}$ $n/cm^2$ sec, yields the ratio of nuclear capture cross sections $\sigma^{157}/\sigma^{155} = 2.82$, using the above abundance values.

No $F$-center spectrum was detected in crystals irradiated with a total neutron flux of about $10^{18}$ $n/cm^2$. The paramagnetic resonance spectrum of gadolinium in irradiated crystals is unchanged, indicating negligible radiation damage in the neighborhood of the paramagnetic ions.

EVIDENCE FOR DIRECT INTERACTIONS AT LOW ENERGY. H. A. Lackner,* G. F. Dell, and H. J. Hausman, Department of Physics, The Ohio State University, Columbus, Ohio (Received November 19, 1958).

The angular distributions of protons corresponding to the first excited state transition in the reaction $Mg^{24}(p,p')_{1.38\ Mev}$ have been measured for bombarding energies between 5.0 and 6.2 Mev. The angular correlations between the gamma rays emitted from the first excited state of $Mg^{24}$ and the inelastically scattered protons have been measured at two different bombarding energies and for three proton detection directions. The angular correlation data are fitted to curves of the form $A+B\sin^2[2(\theta-\theta_q)]$, where $\theta_q$ is the momentum transfer direction for the reaction. The angular correlation data are consistent with predictions of the direct-interaction theory.

*Now at the University of California Radiation Laboratory, Livermore, California.

ANGULAR DISTRIBUTIONS OF PHOTOPIONS FROM HYDROGEN. Edward A. Knapp, Robert W. Kenney, and Victor Perez-Mendez, Radiation Laboratory, University of California, Berkeley, California (Received November 19, 1958).

An accurate measurement of the differential cross section for the photoproduction of positive pions from protons has been made at the Berkeley synchrotron for photon energies of 260 and 290 Mev. The mesons were produced in a thin-walled liquid-hydrogen target, and the meson-detection apparatus utilized the characteristic decay of the pion. The measurements were done in two steps, from 0° to 50° with equipment specifically designed to reduce a very high forward-angle positron background, and from 30° to 160° with equipment whose efficiency and solid angle could be accurately determined.

The abrupt flattening of the observed cross section in the region forward of 40° is due to "photoelectric ejection" of pions from the cloud surrounding the nucleon. The results are compared to the theory of photoproduction derived from the dispersion relations, and the agreement is satisfactory within the limitations of the theory.

ANALYSIS OF THE $\Lambda$-HYPERNUCLEAR THREE-BODY SYSTEMS. B. W. Downs, Laboratory of Nuclear Studies, Cornell University, and R. H. Dalitz, Enrico Fermi Institute for Nuclear Studies, and Physics Department, University of Chicago, Chicago, Illinois (Received November 17, 1958).

An analysis of the $\Lambda$-hypernuclear three-body systems is made by a variational method with a six-parameter trial function. An upper bound for the strength of the $\Lambda$-nucleon interaction required to account for the observed binding of the $T=0$ hypertriton ${}_{\Lambda}H^3$ is obtained. This upper bound is 10-20% (depending upon the value taken for the

binding energy) lower than the previous estimate by the same authors. An improved quantitative estimate of the spin dependence of the Λ-nucleon interaction (neglecting the possible influence of three-body forces) is obtained from the results of this analysis and those of a previous analysis of ${}_{\Lambda}He^{5}$; from this estimate it follows that the existence of a bound Λ-nucleon system is strongly excluded. The analysis of the $T=1$ triplet ${}_{\Lambda}He^{3}$, ${}_{\Lambda}H^{3}$, ${}_{\Lambda}n^{3}$ indicates that these systems are not expected to form bound states. It appears that the essential conclusions of this work would not be seriously affected if there exist moderately-strong three-body forces arising from pion exchange processes.

COULOMB EFFECTS IN BOSON EMISSION. Michael J. Moravcsik, University of California Radiation Laboratory, Livermore, California (Received November 17, 1958).

The corrections in boson emission processes due to Coulomb forces between the two particles are considered. The usual "Coulomb penetration factor" is modified by relativistic and finite-size effects. Numerical results are given for the emission by a nucleon of pions and $K$-mesons in $S$ and $P$ states. It is emphasized, however, that in the absence of precise knowledge about the mechanism of emission the present numerical results should be considered only approximate.

## ERRATUM

LIFETIMES OF THE FIRST EXCITED $0^{+}$ STATES OF $Ca^{40}$ AND $Zr^{90}$. Robert M. Kloepper, Robert B. Day, and David A. Lind [Phys. Rev. Lett. 2, 240 (1959)].

The second last sentence of the Abstract should have read: "Mean lives for the first excited states of $Ca^{40}$ and $Zr^{90}$ were found to be $(3.4\pm0.2)\times10^{-9}$ sec and $(90\pm6)\times10^{-9}$ sec, respectively."